OPEN ACCESS
IOP Publishing | Dongguan Institute of Materials Science and Technology, CAS
MATERIALS FUTURES
Mater. Futures 5 (2026) 033001 (59pp)
https://doi.org/10.1088/2752-5724/ae5120

Roadmap

# 2026 roadmap on next-generation solid electrolytes for battery applications

**Florian Strauss[1,*], Torsten Brezesinski[1,*], Saneyuki Ohno[2,3], Yi Huang[2], Peng Song[2], Xabier Martinez de Irujo-Labalde[4], Wolfgang G Zeier[4,5], Jelena Popovic-Neuber[6], Hugo Braun[7,8], Arndt Remhof[7,8], Corsin Battaglia[7,9,10], Theodosios Famprikis[11,20], Marnix Wagemaker[11], Ke Huang[12], Yan Zeng[12], Bin Ouyang[12], Juhyoun Park[13], Yoon Seok Jung[13,14], Jingui Yang[1], Siyuan Guo[1], Shuo Wang[15], Shu-Bo Wang[15], Eric McCalla[16], Benjamin Mercier-Guyon[17], Ove Korjus[17], Patrice Perrenot[17], Claire Villevieille[17], H Martin R Wilkening[18], Kerstin Wissel[19] and Oliver Clemens[19]**

[1] Institute of Nanotechnology, Karlsruhe Institute of Technology (KIT), Kaiserstr. 12, 76131 Karlsruhe, Germany
[2] Institute of Multidisciplinary Research for Advanced Materials, Tohoku University, Miyagi 980-8577, Japan
[3] Department of Frontier Sciences for Advanced Environment, Graduate School of Environmental Studies, Tohoku University, Miyagi 980-8572, Japan
[4] Institute of Inorganic and Analytical Chemistry, University of Münster, Corrensstr. 28/30, 48149 Münster, Germany
[5] Institute of Energy Materials and Devices (IMD), IMD-4: Helmholtz Institute Münster, Forschungszentrum Jülich GmbH, 48149 Münster, Germany
[6] Department of Energy and Petroleum Engineering, University of Stavanger, Stavanger, Norway
[7] Empa—Swiss Federal Laboratories for Materials Science and Technology, Duebendorf, Switzerland
[8] Institute for Inorganic and Analytical Chemistry, University of Freiburg, Freiburg, Germany
[9] Department of Information Technology and Electrical Engineering, ETH Zurich, Zurich, Switzerland
[10] Institute of Materials, School of Engineering, EPFL, Lausanne, Switzerland
[11] Radiation Science and Technology, Faculty of Applied Sciences, Delft University of Technology, Delft, The Netherlands
[12] Department of Chemistry & Biochemistry, Florida State University, Tallahassee, FL 32306, United States of America
[13] Department of Chemical and Biomolecular Engineering, Yonsei University, Seoul 03722, Republic of Korea
[14] Department of Battery Engineering, Yonsei University, Seoul 03722, Republic of Korea
[15] School of Materials Science and Engineering, Wuhan University of Technology, Wuhan 430070, People's Republic of China
[16] Department of Chemistry, McGill University, Montreal, Canada
[17] Université Grenoble Alpes, Université Savoie Mont Blanc, CNRS, Grenoble INP, LEPMI, 38000 Grenoble, France

[*] Authors to whom any correspondence should be addressed.

[18] Institute of Chemistry and Technology of Materials, Stremayrgasse 9, Graz University of Technology, 8010 Graz, Austria
[19] University of Stuttgart, Institute for Materials Science, Heisenbergstr. 3, 70569 Stuttgart, Germany
[20] Current address: Inorganic Chemistry Laboratory, Department of Chemistry, University of Oxford, Oxford, United Kingdom.

E-mail: florian.strauss@kit.edu and torsten.brezesinski@kit.edu

Received 4 November 2025, revised 20 January 2026
Accepted for publication 10 February 2026
Published 4 May 2026


**Abstract**

The global transition to sustainable energy systems requires breakthroughs in electrochemical storage technologies that are not only safe but also resource efficient. Solid-state batteries (SSBs), which use superionic solid electrolytes (SEs) instead of flammable liquid electrolytes, are at the forefront of this transformation. In general, SEs promise increased safety, access to high-voltage cathode and metal anode chemistries, and new avenues for circular design and recyclability. However, to reach their full potential, intertwined challenges related to ion transport, (electro)chemical stability, manufacturing, processing, and cost must be overcome. This 2026 roadmap on next-generation SEs for battery applications outlines new directions that will contribute to research in the field of SSBs over the next decade. It provides an overview of the current state of the art in sulfide- and halide-based SEs for Li and Na systems, examines post-Li/Na chemistries (K, Mg, and others), and highlights advances in hydroborate, fully reduced (irreducible), and compositionally complex (high-entropy) electrolytes, as well as glass-ceramic electrolytes. Beyond material innovation, the paper emphasizes the critical role of redox activity in SEs, scalable processing, high-throughput synthesis, and machine learning, as well as *operando* analytics and nuclear magnetic resonance spectroscopy to accelerate discoveries and gain a better understanding of structure–property relationships. Finally, the growing importance of recycling and circular design for ensuring sustainability is highlighted. By combining insights from chemistry, materials science, data (computational) science, and manufacturing, this article assumes that future SEs will progressively evolve from passive components to active design elements in high-energy-density electrochemical systems. The integration of multidisciplinary innovations will be crucial to realizing the potential of SSBs in practical technologies that power a decarbonized world.

Supplementary material for this article is available online

Keywords: electrochemical energy storage, solid-state batteries, superionic conductors, synthesis, characterization, recycling

## Contents

## 1. Introduction

*Florian Strauss* and Torsten Brezesinski**

Institute of Nanotechnology, Karlsruhe Institute of Technology (KIT), Kaiserstr. 12, 76131 Karlsruhe, Germany

*E-mail: florian.strauss@kit.edu
and torsten.brezesinski@kit.edu

As the world moves toward electrification and the integration of renewable energies, the need for storage technologies that are intrinsically safe, energy dense, and sustainable is more urgent than ever. One of the most groundbreaking developments in this area is solid-state batteries (SSBs), in which the liquid electrolyte is replaced by an ionically conductive solid, i.e. a superionic solid electrolyte (SE). This paradigm shift promises not only a significant increase in performance but also a fundamental rethinking of the design, manufacture, and recycling of electrochemical energy storage devices. In particular, inorganic SEs appear to be capable of unlocking the potential of high-capacity anodes and high-voltage cathodes, which are currently limited by their incompatibility with conventional liquid electrolytes [1–3]. In the last decade, a wide variety of SEs have been developed using Li-, Na-, and K-ion conductors and alternative ion systems (figure 1(a)), including sulfides, halides, oxides, hydroborates, and other material classes (figure 1(b)), each with unique advantages and challenges [4, 5]. The research field has evolved from (isolated) seminal discoveries such as the high room-temperature ionic conductivity of $Li_{10}GeP_2S_{12}$ (LGPS) (which is similar to that of leading liquid electrolytes [6]) to an increasingly differentiated understanding of structure–property relationships, defect chemistry, migration mechanisms, and interfacial phenomena.

However, the community is now at a critical turning point. The next phase of SE research must move beyond the search for superionic conductivity alone and focus on integrated solutions that balance (electro)chemical stability, mechanical resilience, manufacturability, and recyclability. The focus is shifting slowly from 'What works in the laboratory?' to 'What can be scaled up in practice?' This change requires not only material innovations but also a system-level perspective that combines design at the atomic scale with implementation on an industrial scale.

In this article, we outline the new frontiers that will define the next generation of inorganic SEs and their use in practical battery environments. We begin with sulfide-based systems, which continue to set the standard for high room-temperature ionic conductivity in both lithium and sodium SEs. Halide electrolytes have recently attracted attention due to their high electrochemical (anodic) stability and mechanical softness. Post-Li/Na chemistries, such as potassium, magnesium, and other multivalent systems, offer sustainable (abundant) alternatives for solid-state electrochemical energy storage. In addition to these families, hydroborates and fully reduced electrolytes expand the design space with unique transport properties and improved electrochemical stability. Amorphous ion conductors introduce disorder, thus increasing mobility and structural robustness. Glass-ceramic electrolytes combine the high ion conductivity of the crystalline phase(s) with the flexibility provided by the amorphous matrix, thus improving processability and chemo-mechanical behavior. Redox-active SEs blur the boundary between the electrolyte and the electrode active material, thereby enabling an increase in cell capacity and facilitating redox mediation in the solid state.

Beyond the discovery of new materials and their tailoring, progress will depend on systems that are easily scalable and can be used in cost-effective processing techniques (compatible with industrial manufacturing). Furthermore, high-throughput experimentation, modeling/simulation, and machine learning (ML) will likely make SE design a predictive and automated process. *In situ* and *operando* characterization techniques and advanced nuclear magnetic resonance (NMR) spectroscopy further enable real-time observation of interfacial dynamics and degradation processes. Finally, recycling strategies are emerging to ensure sustainable life cycles and the recovery of materials within SSB ecosystems.

As the field of SE research for batteries enters a phase of rapid growth, the convergence of materials science, data science, and manufacturing technology will drive the development of advanced SSBs. The roadmap for 2026 envisions a future in which the SE is no longer passive but active, enabling transformative electrochemical systems that are developed at the atomic level, integrated across multiple scales, and embedded in a circular, sustainable energy economy. The breakthroughs of the next decade will likely emerge from interdisciplinary collaboration, bringing together insights from crystallography, computer science, interfacial chemistry, and industrial engineering to push the boundaries of what is possible in solid-state electrochemical energy storage.

The potential commercialization of advanced SEs depends crucially on the development of cost-effective manufacturing processes, including the availability of low-cost precursors and low-temperature synthesis routes. Currently, only a few sulfide-, oxide-, and halide-based materials are commercially available for research and development purposes (in kilogram quantities) at relatively high prices. However, if SSBs are to become a widespread technology, production costs must be drastically reduced. Although the development of new synthesis routes (or the use of existing ones) may well be feasible, the price of certain precursors can be a serious obstacle, e.g. in the case of hydroborate or sulfide solid electrolytes (SSEs). For the latter, the price of battery-grade $Li_2S$ remains high, as it is produced mainly from $Li_2SO_4$ using an energy-intensive carbothermal reduction process [7]. Furthermore, it remains questionable whether the materials currently synthesized using mechanochemical processes can be scaled up to have a far-reaching impact on future SSB technologies or

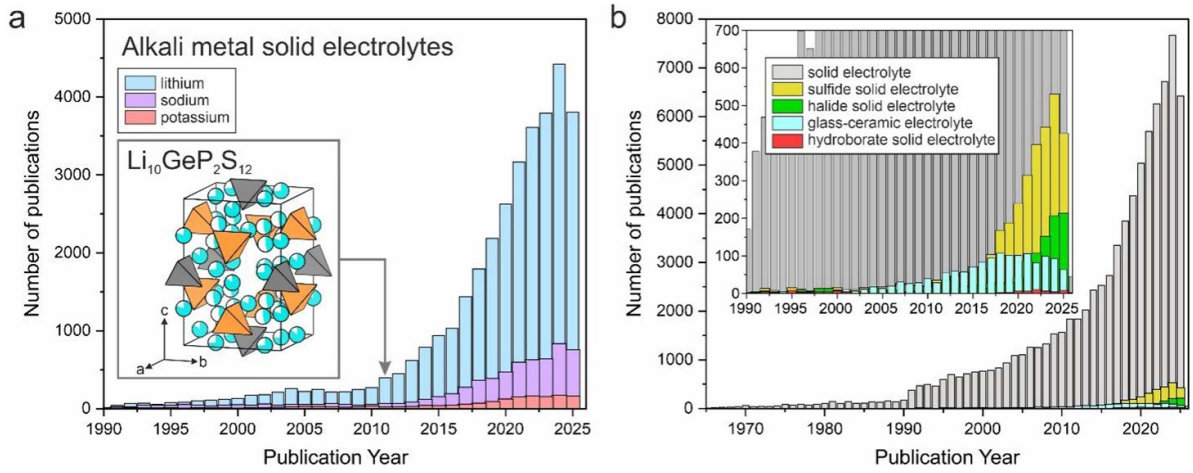


**Figure 1.** Number of publications per year for (a) alkali metal SEs and (b) various classes of SEs based on the keywords indicated in the inset. The data contained herein is sourced from the Web of Science™, Copyright (2025), Clarivate.

whether they are more suited to niche market applications where cost is not a primary consideration. Since this roadmap focuses on SEs that are just emerging from academic research and are of more fundamental interest, commercial and industrial considerations would be highly speculative and are therefore not the focus.

Overall, this article serves both as a snapshot of the current state of knowledge and as a strategic compass for future research by highlighting the challenges and opportunities that lie ahead. The vision is clear: by leveraging the full diversity of the chemical space, utilizing computational and analytical methods, and considering sustainability from design to disposal, the next generation of superionic SEs can redefine the future of batteries and, therefore, also the energy systems that will power our world.

## Acknowledgment

F S is grateful to the German Federal Ministry of Research, Technology and Space (BMFTR) for funding within the project MELLi (03XP0447).

## Conflict of interest

The authors declare no conflict of interest.

## 2. Sulfide SEs: materials-to-devices perspectives

*Saneyuki Ohno*[1,2,*], *Yi Huang*[1] *and Peng Song*[1]

[1]Institute of Multidisciplinary Research for Advanced Materials, Tohoku University, Miyagi 980-8577, Japan
[2]Department of Frontier Sciences for Advanced Environment, Graduate School of Environmental Studies, Tohoku University, Miyagi 980-8572, Japan

[*]E-mail: saneyuki.ohno.c8@tohoku.ac.jp

### Status

Sulfide-based SEs, alongside oxides, represent one of the most historically established and practically relevant classes of solid-state ionic conductors. The prominence of sulfide-based electrolytes stems from two intrinsic advantages: the exceptionally high ionic conductivity enabled by the high polarizability of sulfide anions, and their mechanical softness, which allows the formation of percolating ion-conduction pathways under simple cold pressing at room temperature [8]. Among them, thiophosphate-based glasses and crystalline electrolytes, such as LGPS [6] and argyrodites ($Li_6PS_5X$, X = Cl, Br, I) [9], have been regarded as particularly promising, attracting intensive research from fundamental studies of transport mechanisms to applied demonstrations in SSBs.

The research trajectory of sulfide electrolytes can be traced back to glassy systems. Building upon work on $Ag^+$ and $Cu^+$ conductors in the 1970s, studies in the 1980s on $Li_2S$-$P_2S_5$ glasses [10], thio-silicates [11], and halogen-substituted systems [12] ignited the field of lithium-ion-conducting sulfide electrolytes. The exploration of crystalline phases expanded in the 2000s with the report of lithium superionic conductor (LISICON)-type $Li_4SiS_4$, followed by the discovery of lithium superionic argyrodites in 2008 and $Li_7P_3S_{11}$ in 2009 [13, 14], both of which were inspired by silver superionic conductors. A major breakthrough came in 2011 with the identification of LGPS [6], a LISICON-derived compound, which triggered a surge of activity in SSB research. Subsequent studies demonstrated the potential of sulfide-based SSBs for high-power operation and thick-electrode designs, marking a turning point in the field [15, 16].

In recent decades, tremendous efforts have been devoted not only to the discovery of new compounds but also to elucidating ion transport mechanisms and establishing rational design principles. Figure 2 summarizes the transport properties of representative crystalline sulfide electrolytes discovered during this period. Notably, several sulfide conductors have been reported with room-temperature ionic conductivities exceeding 10 mS $cm^{-1}$. Looking forward, alongside the development of scalable production techniques for practical applications, continued exploration of new materials and mechanistic insights to fully utilize the developed materials will remain central to advancing the field. In the following section, we focus particularly on the effects of (i) crystallinity, (ii) AI-driven materials discovery, (iii) high-entropy (HE) design, (iv) the reproducibility of functionality, and (v) safety assessments, and discuss the present status and future challenges of sulfide SEs.

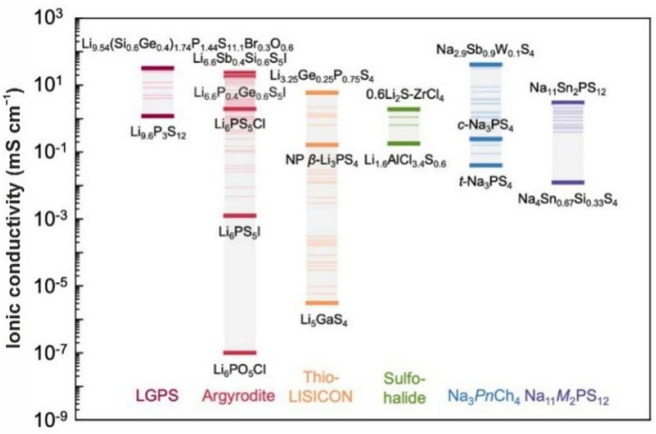


**Figure 2.** Overview of the achieved ionic conductivity for various classes of electrolytes based on Li- and Na-ion conductors. Reproduced from [8]. © IOP Publishing Ltd All rights reserved.

### Current and future challenges

Ionic conductivity is a prerequisite for any material to function as an SE in batteries, yet thermal, chemical, and electrochemical stability are equally critical. Sulfide-based SEs, while offering exceptionally high ionic conductivities, remain challenged by limited thermodynamic stability. As in liquid electrolyte systems, their performance after compositing with active materials and additives and upon cycling is strongly governed by interfacial states. Considerable research has addressed oxidative decomposition near high-voltage cathodes and reductive decomposition near lithium anodes, including gas evolution phenomena. However, we highlight another descriptor that is difficult to formalize in this context, namely crystallinity.

A key advantage of sulfide electrolytes lies in their ability to form metastable phases, including glassy interphases, which nevertheless retain appreciable ionic transport. An intrinsic drawback of such glasses is their inferior thermodynamic stability compared to their crystalline counterparts. On the other hand, glasses possess stress relaxation mechanisms that, through atomic or molecular mobility, mitigate crack formation and enhance mechanical resilience [17]. Given that electro-chemo-mechanical degradation is the dominant failure mode in SSBs, materials development strategies that leverage both the robustness of crystals and the compliance of glasses present a promising pathway.

Several representative studies have highlighted the multifaceted role of crystallinity. Cronau *et al* systematically investigated argyrodites and demonstrated that while highly crystalline electrolytes provide intrinsically higher ionic conductivity, they require substantial stacking pressure to maintain contact and reliable transport [18]. In contrast, their glass-ceramic counterparts, with lower crystallinity, can sustain conductivity even under reduced stack pressure. Wang *et al* compared

crystalline and glassy thiophosphates and revealed that crystalline electrolytes, due to higher electronic conductivity and accelerated decomposition, suffer from interfacial degradation, contact loss, and pronounced volume changes, whereas glassy electrolytes suppress electronic conduction, stabilize interfaces, and deliver improved cycling [19]. Maus *et al* further demonstrated that postsynthetic processing affects crystallinity: moderate milling reduces particle size and enhances cathode composite performance, whereas excessive milling severely diminishes crystallinity, hinders ionic transport, and degrades cell behavior [20].

Taken together, these findings underscore the complexity of using 'crystallinity' as a materials descriptor. Although methods such as x-ray diffraction, total scattering with coherent length analysis, and scanning electron microscopy/transmission electron microscopy (SEM/TEM) observations, as well as relative intensity ratio methods, allow partial quantification of crystalline versus glassy fractions, the disentanglement of particle size, strain, and disorder effects remains unresolved. For practical implementation and sustained advancement, crystallinity must be addressed as a multifactorial parameter that resists simple computational predictions and still requires nuanced experimental investigation. As such, the systematic exploration of crystallinity, bridging atomic structure, processing, and electrochemical performance, remains an open frontier for the design of robust sulfide SEs.

Artificial intelligence (AI) has become a powerful tool for accelerating the discovery of SEs, particularly sulfide-based systems. By directly predicting key properties, such as ionic conductivity and migration barriers, AI enables high-throughput screening far beyond the reach of traditional methods. For example, Sendek *et al* combined ML with density functional theory to evaluate ∼12 000 candidates, raising the likelihood of finding fast-ion conductors by 2.7 times [21]. Zhao *et al* introduced the hierarchical encoded crystal structure descriptor to predict Li argyrodite migration barriers [22], while Kahle *et al* used high-throughput molecular dynamics to identify 130 promising lithium compounds [23]. Guo *et al* expanded this scale dramatically, screening 740 000 compounds with a universal ML interatomic potential [24]. Notably, Cho *et al* demonstrated experiment-driven active learning, which yielded a Li argyrodite with a conductivity of 13.02 mS $cm^{-1}$, showing how AI can guide synthesis as well as design [25].

More focused studies have illustrated AI's potential in the field of sulfide electrolytes. Kong *et al* employed a semisupervised framework with local structural order parameters to screen 3800 compounds, identifying 19 and synthesizing $Li_3LaP_2S_8$ derivatives [26]. Conductivity was initially modest but improved through Sr substitution, demonstrating the value of semisupervised approaches under conditions of data scarcity. Han *et al* applied a variational autoencoder with a multianion topological design, selecting $Li_7Si_2S_7I$ from 300 phase diagrams [27]. Despite being metastable, this compound achieved a conductivity of $\sim 10^{-2}$ S $cm^{-1}$ through multichannel transport, challenging conventional assumptions of single-pathway ion mobility.

Beyond property screening, large language models (LLMs) are emerging as a new tool. Wang *et al* integrated LLMs with metadynamics simulations to clarify ion migration in hydride electrolytes [28], while Li *et al* introduced a coevolutionary LLM–physics framework to combine literature mining with real-time physical modeling [29]. The Chemeleon model further showed that cross-modal contrastive learning can couple textual descriptions with structural data to generate stable phases in the Li–P–S–Cl space [30]. Such advances suggest that LLMs can overcome the limitations of traditional ML in mapping structure–property relations, opening new avenues for electrolyte design.

Despite these successes, critical challenges remain in bridging prediction and experiment. Current models often assume idealized stoichiometries, while real sulfide SEs display substantial compositional freedom. Substitutions and defect engineering, as in Sr-doped $Li_3LaP_2S_8$, can significantly enhance conductivity, but such effects are rarely built into AI models. Reliance on convex-hull thermodynamics also limits realism: many high-performance SEs, such as $Li_7Si_2S_7I$, are metastable and require careful kinetic control during synthesis. Furthermore, precursor chemistry plays a decisive role. In Li-argyrodite systems, different precursors alter phase purity and ionic transport; however, the choice of precursors remains underexplored in AI frameworks.

Looking forward, progress will depend on integrated, feedback-driven approaches that link modeling with experiment. Combining reaction energy network analysis, interfacial barrier modeling, and ML-accelerated molecular dynamics with high-throughput experimental feedback could enable predictive synthesis planning. The success of Cho's active-learning Li argyrodite highlights the promise of such frameworks. By incorporating compositional variability, metastability, kinetics, and precursor effects, AI can evolve from identifying initial targets to guiding the full design-to-synthesis pipeline. This will be crucial for realizing optimized sulfide SEs and advancing their deployment in next-generation SSBs.

High-entropy solid-state electrolytes (HE-SSEs) exploit configurational entropy to overcome the intrinsic limitations of conventional SEs [31]. Increasing configurational entropy in sulfide SEs can introduce beneficial structural disorder, which broadens ion migration pathways and lowers transport barriers. Such entropy-driven stabilization fosters highly conductive frameworks, demonstrating that HE design serves as a powerful strategy for enhancing ionic transport in SEs beyond the limits of conventional compositions [32]. Mechanistic studies, particularly by Ceder's group, reveal that multielement substitution introduces a broad distribution of site energies, enabling percolative ion transport via multiple low-barrier pathways rather than a single high-energy route [33]. Synergistic effects, including overlapping site energy distributions, interstitial site occupation, lattice softening, and the 'cocktail effect,' create an optimized energy landscape for charge transport [31]. Such insights form a foundation for the rational design of next-generation HE-SSEs with superior ionic transport and stability.

Experimental evidence supports these benefits. In HE argyrodites, such as $Li_{6.5}(Ge_{0.5}P_{0.5})(S_{2.5}Se_{2.5})(Cl_{0.33}Br_{0.33}I_{0.33})$, multianion and cation substitution reduce activation energies to ∼0.22 eV, though conductivity gains over optimized analogues are limited [34]. The cationic substitution effect in the argyrodite structure has also been explored in $Li_{6.5}[P_{0.25}Si_{0.25}Ge_{0.25}Sb_{0.25}]S_5I$, realizing an ionic conductivity of ∼13 mS $cm^{-1}$ with a very low activation energy (∼0.2 eV), attributed to local lattice distortions and sublattice softening [35]. High ionic conductivity has also been demonstrated in the LGPS-type electrolyte $Li_{9.54}[Si_{1-\delta}M_{\delta}]_{1.74}P_{1.44}S_{11.1}Br_{0.3}O_{0.6}$ (M = Ge, Sn), achieving 32 mS $cm^{-1}$ [16].

HE-SSEs show markedly improved ionic conductivities, often linked to reduced activation energies. However, key questions remain unresolved. The relationship between configurational entropy and the Arrhenius prefactor is unclear, limiting predictive control of transport. The proposed 'frustrated energy landscape' has not been clearly distinguished from disorder effects in glassy phases. Moreover, disentangling configurational and vibrational entropy contributions remains challenging, as lattice softening and phonon broadening may also lower barriers [31]. Finally, systematic design rules for selecting elemental combinations are lacking. Clarifying these aspects is essential for rational HE-SSE design.

From both materials development and device application perspectives, reproducibility is a critical factor for commercialization. However, this has not yet been sufficiently ensured, as standardized protocols for conductivity measurements and systematic discussions about the reproducibility of material functionality across synthesis batches are still lacking. For research aimed at advancing materials performance, a uniform comparison of transport properties is indispensable. Yet, a round-robin test conducted in 2020 revealed that even when identical sulfide powder samples were distributed, the measured conductivities showed a standard deviation exceeding 50% [36]. This indicates the possibility of significant discrepancies between reported literature values and laboratory-scale measurements. Factors such as crystallinity, fabrication pressure, and stack pressure during measurement [18], as well as sample history (e.g. storage environment) and the analysis methodology [37], have been suggested as contributing variables.

Even for nominally identical materials, transport reproducibility remains a critical challenge. Variations in conductivity often persist across different synthesis batches, even when synthesis methods and measurement environments are standardized. Using $Na_3SbS_4$, a representative Na–ion conducting sulfide electrolyte, as a model system, it has been suggested that such discrepancies stem from differences in defect concentrations caused by variations in the thermodynamic state of the material. In this context, while single-phase purity has been widely pursued, the potential benefits of deliberately utilizing coexisting phases have been highlighted [38]. Furthermore, the influence of trace oxygen impurities on the ionic transport properties of $Na_3PS_4$ has also been discussed [39], underscoring the need to balance industrial demands for high purity with the functional requirements of electrochemical performance.

Realizing battery devices requires the intimate integration of multiple functional materials, inevitably leading to the formation of complex and diverse interfaces. Thus, reproducibility at the interface level directly translates into the reproducibility of overall cell performance. Indeed, despite employing identical materials, a cell-level round-robin test conducted in 2024 revealed surprisingly significant variations in battery performance [40]. Considering the combined effects of thermodynamic states, crystallinity, and interfacial diversity, the importance of more standardized testing is reinforced. At the same time, these results raise concerns about the prevailing expectations for high battery performance even in fundamental materials research, suggesting that deepening fundamental understanding should not be conflated with demonstrating optimized device-level output.

Interfacial phenomena at the anodes and cathodes of sulfide-based SE interfaces critically govern the practical deployment of SSBs. In particular, contact with highly reducing Li(Na) metal or alloy-type electrodes [41, 42], as well as interactions at SE–active material interfaces within composite cathodes [43–45], often triggers SE decomposition, uncontrolled interphase formation, and loss of interface contact, which collectively limit cell cyclability [46]. Interfacial engineering, therefore, emerges as a unifying theme across materials, processing, and cell-design strategies. Stabilized interphases formed through chemical additives such as $Li_3N$, LiX (Cl, Br, I), $LiBH_4$, or irreducible SE [47] derivatives can mitigate reduction reactions at Li and C/Ag anodes while retaining fast Li-ion transport. Surface coatings, gradient layers, and optimized composite architectures can significantly improve compatibility at both anode and cathode interfaces [48]. For quantitative analysis of interfacial reactions occurring at Li/SE contacts, coulometric titration time analysis provides a particularly powerful method to assess interfacial competitiveness and stability [49]. In section 3, (electro)chemical compatibility at various interfaces is also discussed.

SSBs are often touted as intrinsically safe, largely because they do not rely on flammable organic liquid electrolytes. This assumption may hold true when oxide electrolytes are employed, but the situation is more complex for sulfide-based systems. Can a battery that generates toxic hydrogen sulfide gas upon exposure to air truly be considered safe? How should safety be assessed? While this may appear to go beyond laboratory-scale concerns, a critical evaluation of safety is indispensable for SSBs, especially as they are promoted as both high performance and inherently safe.

It is well established that conventional lithium-ion batteries (LIBs) undergo thermal runaway initiated by parasitic reactions at the anode; however, reports also demonstrate that sulfide-based SSBs are not immune to combustion [50]. When argyrodite electrolytes are combined with charged Ni-rich cathodes (e.g. $LiNi_{0.8}Co_{0.1}Mn_{0.1}O_2$, NCM811) and subjected to heating, explosive combustion occurs at around 150 °C, triggered by oxygen release from the cathode [51]. Subsequent studies have revealed that crystalline sulfide electrolytes are

relatively more stable, whereas glassy sulfides react strongly with released oxygen, generating substantial heat and $SO_2$ gas [52]. This has introduced crystallinity as a new dimension in the safety debate. In sulfide-based systems, oxygen and sulfur vapors reacting with lithium metal are considered the primary hazard [53], and although interfacial gas consumption can mitigate risk, it remains a major concern. Additional risks stem from $H_2S$ release upon moisture exposure [54]. Strategies such as oxygen substitution, the incorporation of softer acid species, and surface treatments of SEs have been proposed, yet gas evolution in confined environments can still lead to catastrophic failure.

Looking ahead, mitigating these risks will require integrated strategies across materials, cell design, and system levels. On the materials side, designing hybrid electrolytes that combine the high conductivity of sulfides with the chemical robustness of oxides and halides, as well as applying protective coatings, may suppress oxygen and moisture-driven decomposition. At the cell level, architectures that allow early gas adsorption and efficient heat dissipation, combined with packaging tailored for thermal management, hold promise. At the system level, incorporating gas and thermal sensors, active cooling, and AI-based early-warning diagnostics can provide additional safeguards. Crucially, *operando* characterization and multiscale modeling must be leveraged to quantify degradation pathways and define standardized metrics for safety evaluation under realistic stresses. Ultimately, bridging fundamental materials chemistry with engineering-scale safety design will be essential to ensure the reliability of sulfide-based SSBs and accelerate their deployment in practical applications.

## Conclusions and future perspectives

In this section, we have discussed the progress and future outlook of sulfide-based SEs from both materials design and device application viewpoints. Several directions can be highlighted for the coming years. HE effects have so far been mainly interpreted as averaged anion disorder, but a more constructive approach lies in multianion and complex-anion compounds, where different anions form the structural framework. The exploration that began with oxyhalides is now expanding toward sulfur–halogen systems. From both glass and crystal viewpoints, further refinement of design principles is needed. While many recent discoveries have emerged from glass systems, taking advantage of unique local structures to enhance crystallinity represents another promising strategy. The enormous chemical space still to be explored presents a significant challenge in identifying metastable but functional structures, yet AI-driven prediction may offer a practical route. Such compositional design could also help suppress interfacial decomposition by employing graded compositional modulation to improve stability near interfaces.

From the safety viewpoint, as demonstrated in verification studies, low-voltage cathodes such as $LiFePO_4$ are highly promising [51]. Sulfur cathodes, with their very high capacity, low operating potential, and absence of oxygen release, may ultimately provide a foundation for truly safe batteries [55]. On the industrial side, progress is accelerating: Mitsui Kinzoku has begun moving toward the mass production of argyrodites (September 2024), while Idemitsu has started developing cost-efficient synthesis routes for $Li_2S$ (February 2025). As for Na–ion conductors, although $Na_3SbS_4$ is available in small quantities from chemical vendors, sulfide-based electrolytes are not yet ready for mass production, and worldwide efforts to identify viable candidate materials are still ongoing. From a broader perspective, the commercial viability of Na-based systems remains uncertain, and continued materials innovation must be coupled with clear evidence that solid-state sodium batteries can offer competitive advantages in terms of cost, safety, and performance. Insights gained from scaling up will be crucial not only for established compounds but also for newly emerging materials [56]. With these advances, it is reasonable to expect that sulfide-based SEs will soon find their way into commercial vehicles and portable devices.

## Acknowledgments

This work was supported by the Toyota Physical and Chemical Research Institute through the Rising Fellow Program, by JSPS KAKENHI (Grant Number JP23K26762), and by the Japan Science and Technology Agency (JST) under the Adopting Sustainable Partnerships for Innovative Research Ecosystem (ASPIRE) program (Grant Number JPMJAP2419).

## Conflict of interest

The authors declare no conflict of interest.

## 3. Perspectives on halide-based SEs

*Xabier Martinez de Irujo-Labalde*[1] *and Wolfgang G Zeier*[1,2,*]

[1]Institute of Inorganic and Analytical Chemistry, University of Münster, Corrensstr. 28/30, 48149 Münster, Germany
[2]Institute of Energy Materials and Devices (IMD), IMD-4: Helmholtz Institute Münster, Forschungszentrum Jülich GmbH, 48149 Münster, Germany

[*]E-mail: wzeier@uni-muenster.de

### Status

One of the major bottlenecks in the development of SSBs is the design of an optimal SE [1, 57, 58]. Various classes of materials are currently under extensive investigation. Beyond sulfide- and oxide-based solid ionic conductors, halide-based materials have stood out due to their facile synthesis and processability in combination with their enhanced (electro)chemical stability in contact with cathode materials at high voltages (figure 3) [59–62]. However, our understanding of these materials is currently limited, and aspects such as ionic conductivity and chemical stability against their anode counterparts are still open questions.

This section of the roadmap discusses current challenges in improving the ionic transport and chemical stability of halide-based materials, and offers tools for designing future electrolytes based on this chemistry.

### Current and future challenges

Improving ionic conductivity and chemical stability remains a key challenge for the practical implementation of halide-based materials as electrolytes in SSBs (figure 4). On the one hand, the ionic conductivity of these materials has recently experienced a significant leap. For $Li^+$-based chlorides, it has been found that many of the most promising materials have nominal compositions of $Li_3MCl_6$ ($M$ = $Sc^{3+}$, $Y^{3+}$, $In^{3+}$, $Ho^{3+}$…) and crystallize in a rock-salt-related crystal structure, although the final structure is really dependent on the synthetic conditions. This framework offers low-energy ionic diffusion pathways, facilitating ion migration [63–67]. Ionic conductivity can be further enhanced through aliovalent cation substitution in these systems (e.g. $Li_{3-x}M_{1-x}Zr_xCl_6$), achieved by introducing $Li^+$ vacancies [68–72]. These vacancies facilitate ion transport, as the dominant diffusion mechanism in this system is vacancy-driven. In turn, an ionic conductivity boost can be achieved through isovalent anion substitution from $Cl^-$ to $Br^-$ or $I^-$, although the mechanism involved is still unclear. Some of the hypotheses being considered range from lattice polarizability [73] and lattice expansion [71] to the depression of superionic transition [74]. One of the most accepted hypotheses, however, is the introduction of disorder within the metal center arrangement [75]. Similarly, mechanochemical approaches can induce lattice disorder, boosting ionic conductivity [76].

In the case of $Na^+$-containing chlorides, the trend of ionic transport is hardly related to their $Li^+$ analogues. $Na_xMCl_6$ ($M$ = $Sc^{3+}$, $Y^{3+}$, $In^{3+}$, $Zr^{4+}$…) compositions offer very restricted $Na^+$ mobility, with ionic conductivities of approximately $10^{-5}$ mS cm$^{-1}$ [77–79]. The larger size of $Na^+$ compared to $Li^+$ prevents the formation of layered structures, favoring other crystal structures, such as ilmenite, cryolite, or caswellsilverite-related structures, depending on the metal center size. These frameworks show less energetically favorable ionic migration pathways, explaining their low ionic transport. To enhance ionic conductivity, a common approach of ion substitution has also been attempted in these systems. While isovalent anion substitution does not significantly impact ionic transport [80], aliovalent cation substitution enhances it, albeit in a limited manner, by up to $10^{-3}$ mS cm$^{-1}$ at optimal $Na^+$ vacancy concentrations [81, 82]. Recently, it has been shown that $Na^+$ transport can be greatly increased when the materials are mechanochemically treated after annealing or directly obtained by mechanochemical synthesis, as in the case of $Li^+$-containing materials. However, in these cases, the increase in conductivity has not been associated with the introduction of disorder within the crystal lattice. In ball-milling-prepared systems such as $Na_{3-x}In_{1-x}Zr_xCl_6$, $Na_{3-2x}In_{1-x}Ta_xCl_6$, and $Na_{2-x}Zr_{1-x}Ta_xCl_6$, reduced crystallite size has been linked to improved ionic conductivity [83–86]. Additionally, prolonged ball milling of $NaTaCl_6$ has been shown to enhance ionic conductivity, likely due to the increased amorphous content [87, 88].

In harmony with these findings, a new class of glassy superionic materials, either containing $Li^+$ [89–92] or $Na^+$ [93–95] cations and based on mixed-anion chemistries, has recently been discovered [96]. These materials generally exhibit $AMOCl_4$ compositions (A = $Li^+$ or $Na^+$, $M$ = $Nb^{5+}$ or $Ta^{5+}$) due to the partial replacement of $Cl^-$ by $O^{2-}$, where $O^{2-}$ anions are likely acting as glass formers that help to boost ionic conductivity to values greater than 10 mS cm$^{-1}$ and 1 mS cm$^{-1}$ in the case of $Li^+$- [89–91] and $Na^+$- [93–95] containing materials, respectively. Thus, the lower crystallinity associated with a smaller crystallite size and larger amounts of amorphous fractions seems to be the origin of the enhanced ionic transport in these materials, although the precise origin is yet to be determined. Therefore, although various tools have been developed to tune ionic conductivity in halide-based materials, a deeper mechanistic understanding—from both structural and microstructural perspectives—is still needed.

However, huge efforts have recently been devoted to investigating the chemical compatibility of these materials against their anode counterparts. In particular, halide SEs often face challenges when interfaced with highly reducing anode materials such as LiIn or NaSn alloys [97, 98]. The primary concern lies in undesirable interfacial reactions, where the halide electrolytes may undergo ion intercalation and eventually reductive decomposition, forming resistive interphases that hinder ion transport. For instance, when $Li_3InCl_6$ and $Li_3YCl_6$ contact anode materials, they form passivation layers composed of LiCl, indium metal, or other insulating species, which severely

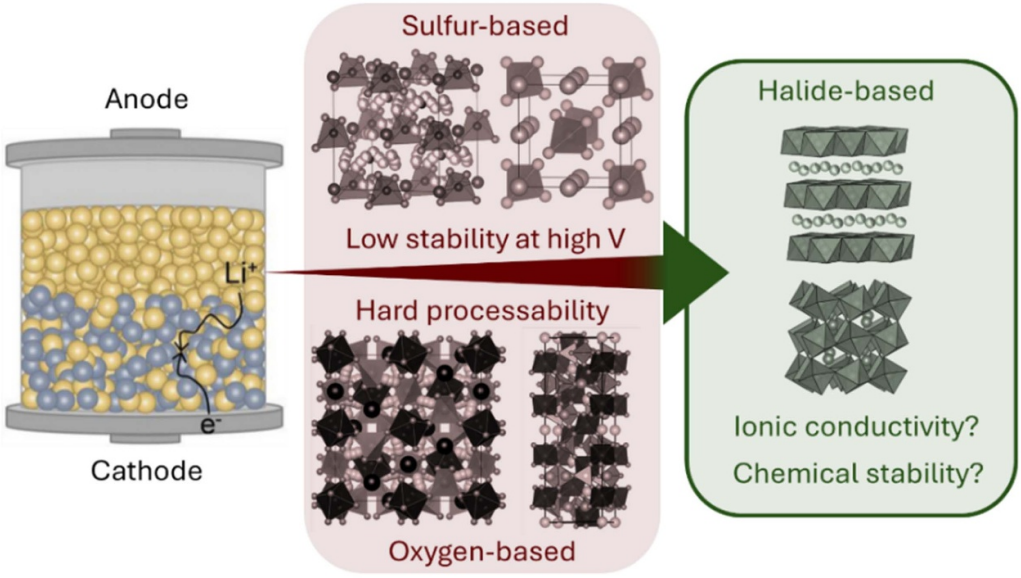


**Figure 3.** Halide-based materials as an alternative to sulfide- or oxygen-based electrolytes.

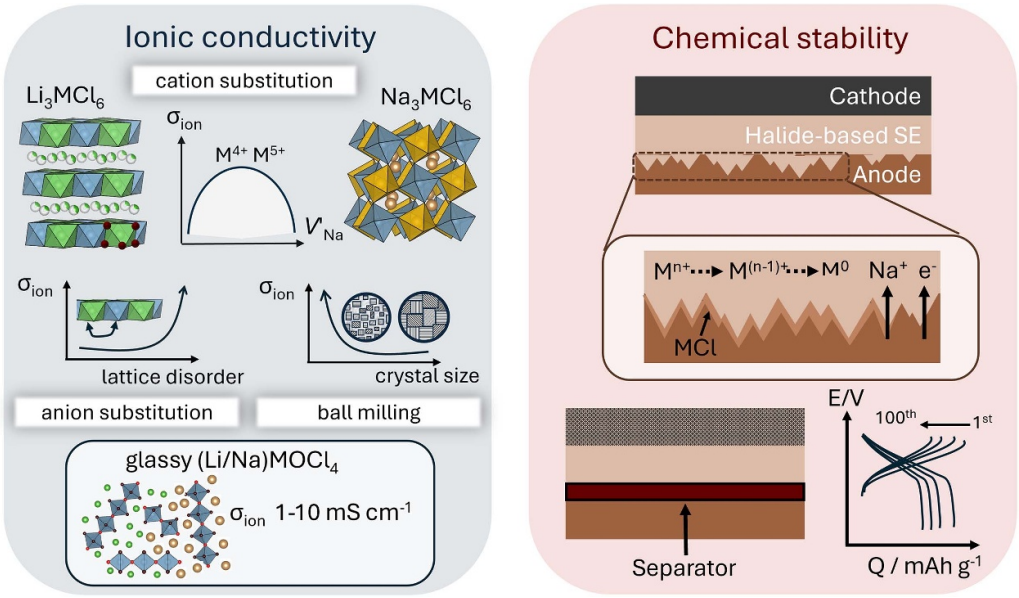


**Figure 4.** Ionic conductivity and chemical stability of halide-based materials represent major challenges for their implementation in SSB technologies today and in the near future.

impede ion transport [71]. Additionally, when $NaTaOCl_4$ contacts Na metal, it is reduced by $Na^+$ intercalation and decomposes into Na salts and/or Nb/Ta salts, or eventually into metals [94]. These detrimental reactions restrict the use of halide-based materials to catholyte configurations that prevent contact with their anode counterparts [46, 98, 99]. Consequently, interfacial regulation strategies based on cell configuration, such as avoiding direct contact between halide electrolytes and metal anodes by employing more chemically stable separator layers (e.g. sulfide-based SEs; see chapter 2), have emerged as an effective and pragmatic approach [46]. In turn, some of these $Na^+$- or $Li^+$-containing halides have been shown to take advantage of their redox activity, increasing the energy density and the areal discharge capacity of the battery when in contact with a cathode material [100–102]. However, if the full potential of halide-based SEs as 'free-standing' electrolytes in SSB systems is to be unlocked, it is critical to understand and control the undesired interfacial chemical interactions.

## Conclusions and future perspectives

Halide- and oxyhalide-based compounds represent a promising class of materials in terms of their ease of synthesis, processability, and (electro)chemical stability at elevated potentials. In recent years, the ionic conductivity of $Li^+$ and $Na^+$

halide materials has significantly improved, reaching values comparable to those of superionic sulfide and oxide conductors, particularly the newly discovered glassy oxyhalides. Nevertheless, if halide-based materials are to be used as 'free-standing' SEs, their chemical stability against the current anode materials should be improved. A promising approach to address this issue involves the careful selection of metal elements that are stable at low potentials, which could pave the way for designing the next generation of halide-based SEs. Furthermore, tailoring the approach by embedding these *M* centers within an amorphous mixed-anion matrix could offer a dual advantage: the previously mentioned suppression of their direct interaction with the anode, thus enhancing chemical stability while retaining the high ionic conductivities observed in disordered systems. Therefore, the development of halide-based materials with stabilized *M* centers in amorphous or glass-ceramic matrices represents a highly promising strategy. Such materials would not only overcome current stability limitations but also maintain or even enhance ionic conductivity, making them strong candidates for next-generation SEs in SSBs.

## Acknowledgment

This work was partially funded by the Bundesministerium für Forschung, Technologie und Raumfahrt (BMFTR, 03XP0525B).

## Conflict of interest

The authors declare no conflict of interest.

## 4. Post-Li/Na inorganic solid-state electrolytes

*Jelena Popovic-Neuber**

Department of Energy and Petroleum Engineering, University of Stavanger, Stavanger, Norway

*E-mail: jelena.popovic-neuber@uis.no

### Status

Post-Li and Na SSBs, similarly to their liquid electrolyte counterparts, address issues such as materials resourcing and diversification, sustainability, and energy density [103]. The electrochemical performance and properties of solid-state electrolytes depend on the quality of ion transport at multiple scales within the bulk, which is related to structural factors. It is also influenced by the suppression of electron conductivity. In addition, interfacial behavior, particularly reactivity and ion transport at the interphases, plays a critical role. These interfacial properties are often affected by dynamic degradation that occurs as a result of contact between electrolytes and high-energy anodes or cathodes (figure 5) [104]. Research typically focuses on materials exhibiting high room-temperature ionic conductivities, $\sigma_{\mathrm{ion,RT}}$, suitably small migration barriers or activation energies, $E_{\mathrm{A}}$, measured by electrochemical impedance spectroscopy (EIS), and a high effective transference number for the moving ions, $t_{\mathrm{i,eff}}$, as measured by polarization techniques. The reason for this is that these bulk performance factors are also directly affecting the battery application ones (figure 5). Additional important bulk transport factors include the ability to achieve a high concentration of charge carriers, most commonly vacancies, and high values of prefactor, $\sigma_0$, also available from EIS measurements, linked with the attempt frequency and migration entropy [105]. The materials in question are chemically reactive and are ultimately to be used in battery cells; they thus form buried and evolving interphases upon galvanostatic cycling. Such materials call for the use and development of advanced *in situ* and *operando* characterization techniques, in conjunction with modeling that considers the complex electro-chemo-mechanics involved, i.e. the interconnected influence of the electrical, chemical, and mechanical behaviors of the materials.

In the case of *K*, several inorganic materials have proven to be suitable for high performance at room temperature, including rhombohedral $\beta''$-alumina (e.g. $K$–$\beta''$–$Al_2O_3$), orthorhombic thioantimonates (e.g. $K_3SbS_4$), borohydrates (e.g. $KB_3H_8{\cdot}NH_3B_3H_7$, $KCB_9H_{10}\cdot 2C_3H_4N_2$), and tetragonal phosphidosilicates (e.g. $KSi_2P_3$) [106, 107]. The fact that the first three material classes are successful analogues of known $Li^+$ and $Na^+$ ionic conductors indicates similar satisfactory conduction mechanisms for alkali metal ions. Fine-tuning of $\sigma_{\mathrm{ion,RT}}$ and $E_{\mathrm{A}}$ in thioantimonates can be achieved by increasing the concentration of charge carriers through W- and Cl-doping and heat treatment of the electrochemical cell [108, 109]. The first instances of K metal use as an anode in full cells or electrodes to study interphase evolution showed that borohydrates and thioantimonates may offer kinetic stability, either in the form of low overpotentials or via the isolation of electronically conducting phases in highly blocking interphases, while long-term cycling in full cells leaves room for additional improvement through materials engineering [107–109].

Generally speaking, the higher charge density associated with divalency leads to stronger electrostatic interactions. In addition, $Ca^{2+}$ has a larger ionic radius than $Mg^{2+}$ because it possesses an additional electron shell. Together, these factors reduce the number of appropriate material classes for post-Li/Na SEs particularly in the case of Ca. This behavior can be compared to that of $O^{2-}$ inorganic conducting materials applied in high-temperature oxide fuel cells (e.g. $CeO_2$, $Zr_{1-x}Y_xO_{2-y}$, $La_{1-x}Sr_xGa_{1-y}Mg_yO_{3-\delta}$). However, a key difference is the larger size and lower charge density of the $O^{2-}$ ions. Despite this difference, the most important structural factors for ionic conduction remain the same: polarizability, flexibility, bottleneck size, disorder, and coordination environment [105]. In the case of Mg, Na superionic conductor (NASICON)-type oxides (e.g. $Mg_{0.5}Zr_2(PO_4)_3$), sulfide glasses (e.g. $MgS$-$P_2S_5$-$MgI_2$), halides (e.g. $MgAl_2Cl_{8-x}Br_x$), chalcogenide spinels ($MgX_2Se_4$, X = Sc, B, Yb), and borohydride derivatives (e.g. $\beta$-$Mg(BH_4){\cdot}CH_3NH_2$, $Mg(BH_4)_2(NH_3BH_3)_2$) have been investigated [110–113]. The chalcogenide spinels and borohydrates are currently the most promising, offering a suitably large distance between the mobile $Mg^{2+}$ and neighboring ions, while the somewhat stabilizing covalent character of the bonds and distortion of the lattice allow for an increased number of ionic pathways [112, 113]. However, none of the abovementioned electrolytes is stable with a Mg electrode. An additional complexity in studying these materials arises from the considerable electronic conductivity of the chalcogenide spinel phase, leading to the necessity of using ionogel interlayers for EIS measurements [113]. Borohydride derivatives (e.g. $Ca(CB_{11}H_{12})_2$, $Ca(BH_4)_2{\cdot}2NH_2CH_3$, and $Ca(BH_4)_2$-$3.30CO(NH_2)_2$) are also the most promising $Ca^{2+}$ conductors, offering open space and exclusive ionic conduction pathways [114–116]. Unfortunately, only monocarboranes have been tested in contact with $CaSn_3$ alloy electrodes with promising results; other electrolytes have not been employed in the relevant battery cells [114].

The main crystal structures that are currently under investigation for F-conductivity include cubic fluorite (e.g. $BaSnF_4$), which exhibits highly disordered mobile ion species and flattening of the mobile ion potential energy surface, and metastable alkaline-earth metal fluorides (e.g. $(CaF_2)_x(BaF_2)_{1-x}$), where the mixing of Ca and Ba atoms permits F-anion fluctuations, generating Frenkel pairs and low $E_{\mathrm{A}}$ [117, 118]. Although the current focus is on understanding the bulk

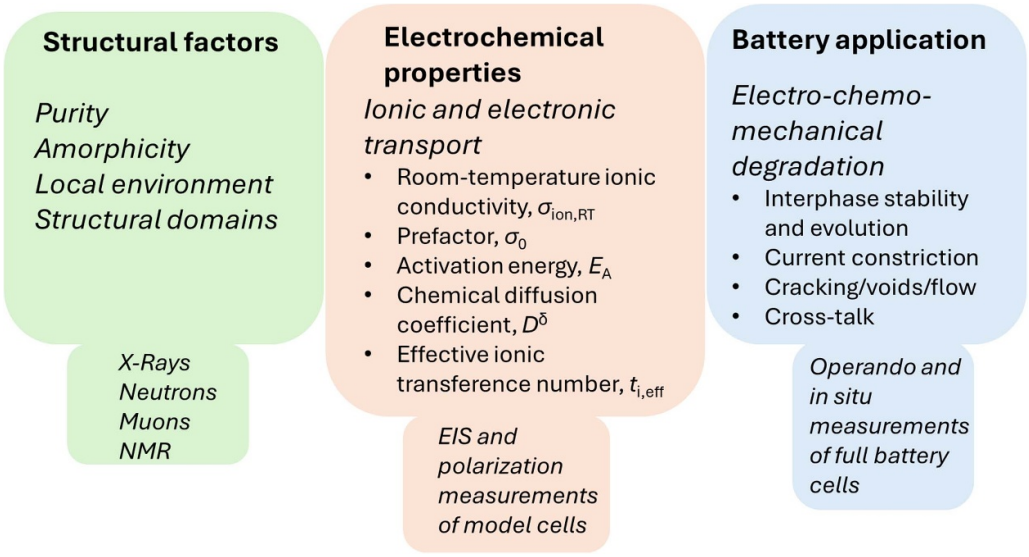


**Figure 5.** Triad of factors influencing the suitability of post-Li and Na SSB electrolytes, including different structural factors, electrochemical properties, and the factors influencing battery application. The boxes below each heading list suitable characterization techniques for the investigation of the specific factors.

behavior, some of the older publications reported full battery cell performance, which was particularly promising with Zn anodes ($Zn/BiSnF_4/BiF_3$ at 60 °C) and thus initiated wider interest in F-based SSBs [119].

In recent years, with the rise of metal–organic framework synthesis and applications in batteries, several such materials have been suggested as suitable electrolytes for post-Li technologies. These are not covered here, as they are, in essence, quasi-solid-state conductors exhibiting solvent-assisted hopping conduction mechanisms, allowing for higher $\sigma_{ion,RT}$ and lower $E_A$ [120]. As such, their performance and conduction mechanism must be compared to that of other composites, such as solid–liquid, gel, and hybrid polymer electrolytes. Unfortunately, given the interdisciplinary nature of the battery community, such treatment is not universal.

## Current and future challenges

Similarly to the Li and Na cases, the variety of chemical structures investigated does not allow comprehensive approaches for $\sigma_{ion,RT}$ and $E_A$ improvement. However, a deeper understanding of the relevance of the Meyer–Neldel rule and other considerations linking the two most relevant parameters is necessary for specific chemistries. In terms of EIS as a technique to track long-range ion movement (e.g. chemical diffusion), detailed information about the processing of the powder material into pellets, including its density and fabrication or measurement pressures, is necessary to understand whether the observed differences are materials-related or process-related. Thus, detailed reporting of experimental and processing procedures remains a challenge. If the materials are mixed conductors, exhibit contact problems, or contain/form interphases, it is necessary to develop more extensive and complex equivalent circuits or transmission-line models for treating EIS data.

The closer this field approaches the possible application domain, the more environmental sustainability aspects related to resourcing, recyclability, and materials' processability, which are currently not the focus, will become relevant. In fact, the typical advice for materials optimization in battery cells is to perform it synergistically and simultaneously, and not one material at a time, as is typically the case in the initial stages of these subtechnologies.

Finally, we should expect to see more use of approaches such as the integration of automation and digitalization through high-throughput experiments/simulations and big data/AI/ML approaches in a closed loop, with the hope that this will reduce cost and time-to-market in this field of materials research.

## Concluding remarks

Our general understanding and development of post-Li and Na solid-state electrolytes for K, Mg, Ca, and F-based SSBs are currently in the cradle phase and are largely driven by the demands of specific chemistries in the field of battery

technology or the necessity to understand the complex interplay of structure and ion movement in the fields of materials chemistry, physics, inorganic chemistry, and solid-state ionics. Ongoing research holds significant promise both in terms of fundamental scientific discoveries related to the movement of ions in solids and battery applications, and in particular for their necessary diversification and technological advancement. The high level of interdisciplinarity in this field calls for varied educational backgrounds on the part of involved scientists and a truly collaborative approach.

## Acknowledgment

Funding from FME BATTERY, a Norwegian Center for Environment-friendly Energy Research (FME), sponsored by the Research Council of Norway (Project Number 350373), is greatly appreciated.

## Conflict of interest

The author declares no conflict of interest.

## 5. Hydroborate SEs

*Hugo Braun*[1,2], *Arndt Remhof*[1,2] *and Corsin Battaglia*[1,3,4,*]

[1]Empa—Swiss Federal Laboratories for Materials Science and Technology, Duebendorf, Switzerland
[2]Institute for Inorganic and Analytical Chemistry, University of Freiburg, Freiburg, Germany
[3]Department of Information Technology and Electrical Engineering, ETH Zurich, Zurich, Switzerland
[4]Institute of Materials, School of Engineering, EPFL, Lausanne, Switzerland

[*]E-mail: corsin.battaglia@empa.ch

### Status

Hydroborates are salts with complex anions consisting of boron and hydrogen atoms (figure 6). The most stable anion is the divalent $B_{12}H_{12}^{2-}$ closo-hydroborate anion, consisting of twelve equivalent boron atoms forming a closed icosahedral cage, where each vertex boron is terminated by a hydrogen atom. The room-temperature cation conductivity of $Li_2B_{12}H_{12}$ and $Na_2B_{12}H_{12}$ is $<10^{-6}$ S cm$^{-1}$. However, $Li_2B_{12}H_{12}$ and $Na_2B_{12}H_{12}$ undergo a first-order phase transition at 350 °C [121] and 250 °C [122], respectively, from an ordered monoclinic low-temperature phase to a dynamically disordered cubic high-temperature phase, in which the $B_{12}H_{12}^{2-}$ anions form a body-centered cubic lattice, exhibiting cation conductivities on the order of $10^{-1}$ S cm$^{-1}$. The high-temperature cubic structure can be stabilized at room temperature by anion mixing, combining, e.g. $Na_2B_{12}H_{12}$ with $Na_2B_{10}H_{10}$ to form $Na_4B_{12}H_{12}B_{10}H_{10}$ [123], in which anions form a dynamically disordered face-centered cubic lattice, resulting in a room-temperature sodium-ion conductivity of several $10^{-3}$ S cm$^{-1}$. The role of librational anion motion and geometric frustration in reaching high cation conductivity has been studied in detail [124, 125]. Even higher cation conductivity of up to several $10^{-2}$ S cm$^{-1}$ can be achieved by replacing one boron atom in each anion with a carbon atom to form, for example, $Na_2CB_{11}H_{12}CB_9H_{10}$ [126]. These closo-hydrocarbaborates possess monovalent anions, reducing cation occupancy and the electrostatic interaction between ions in the lattice.

The integration of these mixed-anion hydroborates into SSBs was first demonstrated using relatively low-voltage cathodes, including $TiS_2$ [127–130], $LiFePO_4$ [130], and $NaCrO_3$ [131]. More recently, stable galvanostatic cycling over several hundred cycles was achieved for high-voltage cathodes, including $LiNi_{0.8}Mn_{0.1}Co_{0.1}O_2$ (NMC811) [132] and $Na_3(VOPO_4)_2F$ (figure 7) [133], where sufficient oxidative stability was achieved by increasing the ratio of $CB_{11}H_{12}^-$:$CB_9H_{10}^-$ and $CB_{11}H_{12}^-$:$B_{12}H_{12}^{2-}$ from 1:1 to 2:1. While the closo-hydroborates also exhibit excellent reductive stability and compatibility with lithium and sodium metal anodes [123], closo-hydrocarbaborates and the open-cage nido-hydroborates show lower reductive stability [127]. Despite excellent anodic and cathodic stability, dendrite formation remains a critical bottleneck, limiting current density and areal capacity in SSBs with hydroborate electrolytes.

Hydroborates offer a number of additional advantages over alternative SE materials. Since boron and hydrogen are both very light elements, the density of these materials is typically very low (1.0−1.2 g cm$^{-3}$). It is thus comparable to or even slightly lower than that of carbonate-based liquid electrolytes (1.2−1.3 g cm$^{-3}$) and significantly lower than those of argyrodite $Li_6PS_5Cl$ (LPSCl) (1.6 g cm$^{-3}$) and garnet $Li_7La_3Zr_2O_{12}$ (5.0 g cm$^{-3}$). Mixed-anion crystal structures are most often synthesized from precursor single-anion salts using chemo-mechanical synthesis. While mixed-anion crystal structures may dissolve in a number of solvents, hydroborate anions remain stable in air, water, and a number of solvents. The crystallization of highly conducting mixed-anion hydroborate crystal structures from solution has been demonstrated for several hydroborates and solvents, enabling solution-based infiltration of prefabricated porous electrode sheets with hydroborate electrolytes [134]. However, most cells described in the literature are fabricated using cold pressing, benefitting from the ductile mechanical properties of hydroborates. Stack pressure during galvanostatic cycling is not a strict requirement for electrode materials that have low volume expansion and contraction during cycling, such as $Na_3(VOPO_4)_2F$ [133], but is required for electrode materials with considerable volume expansion, such as NMC811 [132]. Hydroborate electrolytes typically also exhibit a high thermal stability of ∼400 °C and low toxicity (e.g. the toxicity of $Na_2B_{12}H_{12}$ is similar to that of NaCl) [135].

### Current and future challenges

While the community researching and developing hydroborate electrolytes has been limited to a handful of groups globally, hydroborates have surprisingly been able to keep up with the pace set by more intensively studied electrolyte materials, such as argyrodite LPSCl and garnet $Li_7La_3Zr_2O_{12}$. So far, almost all cells demonstrated in the literature have made use of lithium and sodium metal anodes but struggle with lithium and sodium metal dendrite formation, which consequently limits the achievable current density and areal capacity of the cells. A recent study compared the cycling stability of NMC811 cathodes vs. Li, InLi, and graphite electrodes, concluding that challenges with dendrites on the negative electrode mask the excellent performance and stability of the positive electrode [132]. Consequently, the hydroborate cells with higher positive electrode areal capacities >1 mAh cm$^{-2}$ reported so far have made use of either InLi [132] or NaSn anodes [134] with a redox potential above the onset of dendrite formation, thereby compromising the energy density of these cells. Cathode electrolyte interphase formation at the interface between hydroborates and high-voltage cathodes, such as $Na_3(VOPO_4)_2F$ [133] and NMC811 [132], has been observed indirectly using EIS but remains very difficult to study in more detail with x-ray or electron-beam-based techniques because both boron and hydrogen are light elements. A recent study concluded

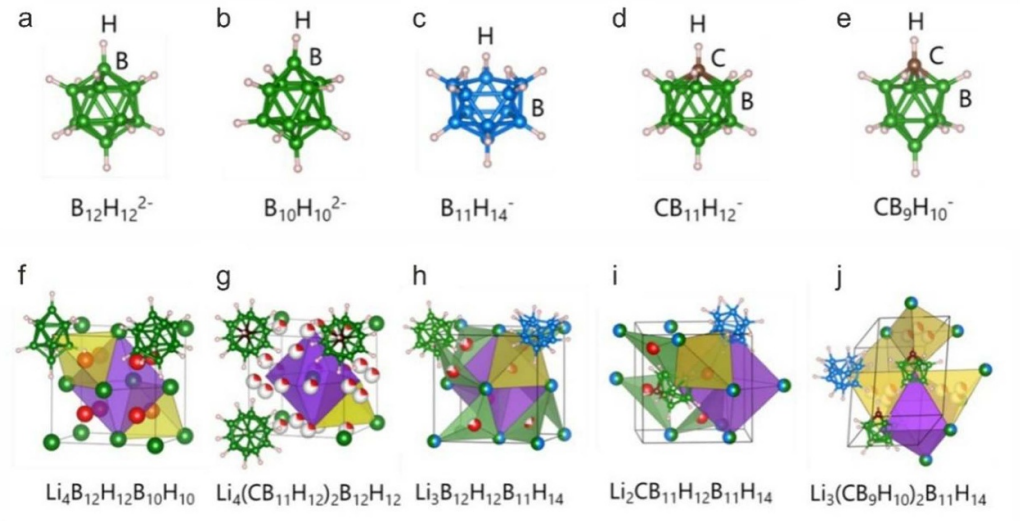


**Figure 6.** Examples of closo-hydroborates (a), (b); nido-hydroborate (c); closo-hydrocarbaborate anions (d), (e); and examples of mixed-anion crystal structures (f)−(j).

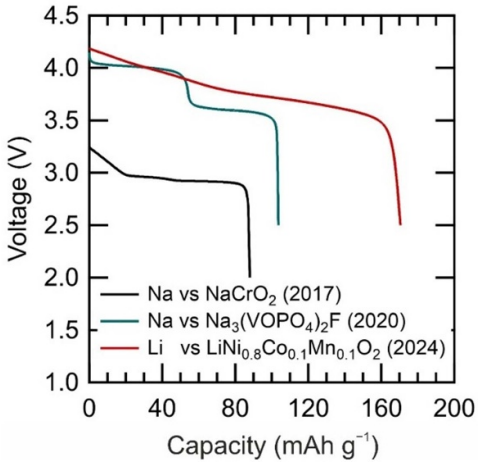


**Figure 7.** Evolution of cell voltage vs discharge capacity of hydroborate SSB cells fabricated in our laboratory.

that the electrochemical oxidation of $LiB_{12}H_{12}$ proceeds successively through the formation of hydrogen-interconnected larger closo-clusters, e.g. the dimerization of two $B_{12}H_{12}^{2-}$ anions into $B_{24}H_{23}^{3-}$ [136]. These clusters are expected to have even higher oxidative stability, thereby passivating the electrolyte/electrode interface. Analogous studies should also be conducted on the reductive stability of hydroborate electrolytes to better understand the interface stability of lithium and sodium metal anodes and ultimately mitigate dendrite formation. Some attempts have also been made to integrate hydroborates with other SEs to benefit from the best of both worlds [79, 137], while mitigating shortcomings, a strategy that may be worth pursuing in more detail in the future.

A major handicap of hydroborate electrolytes is the high cost of hydroborate salts due to their applications in medicine. Currently, the cost per kilogram is on the order of USD 10 000 for $Li_2B_{12}H_{12}$ and $Na_2B_{12}H_{12}$, USD 100 000 for $Li_2B_{10}H_{10}$ and $Na_2B_{10}H_{10}$, and as much as USD 500 000 for $LiCB_{11}H_{12}$. However, there have been multiple efforts to develop cost-effective synthesis methods for closo-hydroborate and closo-hydrocarbaborate salts [138–140]. While closo-hydroborate anions can be synthesized via low-temperature solvothermal synthesis [138], the synthesis of closo-hydrocarbaborate anions proceeds via nido-hydroborate intermediates and is more complex [127, 139, 140]. Most hydroborate salts can be synthesized from the precursor $NaBH_4$, which is cheap and widely available. Lithium salts can be easily obtained via ion exchange from the corresponding sodium salts [130]. However, so far, we are not aware of any successful scale-up of hydroborate salt synthesis to the kilogram or multikilogram scale, although there are no apparent conceptual barriers. Achieving this level of scale-up is a prerequisite to demonstrate cell fabrication at the MWh/y pilot line level. While boron chemistry has a reputation for being relatively difficult, NASA studied the synthesis of boranes ($BH_3$, $B_2H_6$, $B_5H_9$, $B_{10}H_{14}$) as rocket fuel in detail in the 1960s, so competences from this period may be beneficial.

## Conclusions and future perspectives

Hydroborate SEs have emerged as promising candidates for next-generation SSBs due to their unique combination of high ionic conductivity, wide electrochemical stability windows, low density, excellent thermal stability, and low toxicity. The development of mixed-anion hydroborates and hydrocarbaborates has demonstrated that cation conductivities comparable to or exceeding those of state-of-the-art SEs can be achieved while demonstrating compatibility with lithium and sodium metal anodes and high-voltage cathodes. Their ductile mechanical properties and solution processability are further advantages in the context of SSB manufacturing. Despite these advantages, several challenges, including SE interphase formation and dendrite formation, must be addressed before SSBs based on hydroborates can be commercialized.

Looking ahead, the most immediate bottleneck for commercialization lies in the scalable and cost-effective synthesis of hydroborate salts. While current production remains restricted to laboratory-scale quantities at high cost, routes based on inexpensive precursors, such as $NaBH_4$, and knowledge from historical boron chemistry research may offer promising opportunities for scale-up. The successful reduction of synthesis costs could unlock hydroborates as competitive SEs for both lithium and sodium SSBs.

In perspective, hydroborates represent a relatively underexplored but highly versatile class of electrolyte materials with untapped potential. Their continuous progress, despite limited global research activity, underscores the strong potential of hydroborate electrolytes. With coordinated efforts in synthesis, interfacial characterization, and cell engineering, hydroborates may evolve from a niche research topic into a cornerstone electrolyte class for competitive, high-performance, safe, and sustainable SSBs.

## Acknowledgment

This work was supported by the Swiss National Science Foundation (SNSF) under contracts CRSII2_160749/1 and 200021l_192191 and by Innosuisse—Swiss Innovation Agency under contract number 49729.1 IP-EE.

## Conflict of interest

The authors declare no conflict of interest.

## 6. Fully reduced (irreducible) SEs

*Theodosios Famprikis*[1,*] *and Marnix Wagemaker*[*]

Radiation Science and Technology, Faculty of Applied Sciences, Delft University of Technology, Delft, The Netherlands
[1]Current address: Inorganic Chemistry Laboratory, Department of Chemistry, University of Oxford, Oxford, United Kingdom.

[*]E-mail: t.famprikis@tudelft.nl and m.wagemaker@tudelft.nl

### Status

In contrast to most known high-performance electrolytes, irreducible electrolytes are defined as inert to reduction by the corresponding metal, i.e. thermodynamically stable against lithium metal or down to 0 V vs $Li/Li^+$ in the context of lithium-ion conductors. The key idea is that such electrolytes do not undergo decomposition when in contact with low-voltage electrodes, which could enable the practical application of high-performance anodes, such as lithium metal and silicon. This approach is an alternative to relying on the kinetically stabilized decomposition of the SE into a favorable—ionically conducting and electronically insulating—solid-electrolyte interphase (SEI) [104], as exemplified by lithium phosphorus oxynitride (LiPON) [141, 142].

Irreducibility is a stringent constraint that, in practice, limits the chemical composition of the electrolytes in most cases to a combination of mobile cations (e.g. $Li^+$) and anions in their lowest oxidation state (i.e. fully reduced, e.g. $O^{2-}$, $Cl^-$) while precluding reducible framework cations. Many such irreducible compounds are known (table 1) and are often identified as components of the SEI formed by reductive decomposition of high-performance electrolytes. For example, when the argyrodite LPSCl contacts lithium metal, it is reduced to the irreducible binaries $Li_2S$, $Li_3P$, and LiCl [143], while the aforementioned LiPON is reduced to $Li_3N$, $Li_2O$, and $Li_3P$ [141, 142]. The issue is that these binary irreducible compounds are usually ionic insulators.

An exception to this rule is the binary pnictides $Li_3P$ ($\sim 10^{-4}$ S cm$^{-1}$ [146]) and particularly $Li_3N$, which has long been studied as an SE precisely because of its high ionic conductivity [144] and stability against reduction. A mechanochemically prepared $\beta$-$Li_3N$ electrolyte has recently reached $2 \times 10^{-3}$ S cm$^{-1}$ and shows promising results as an anolyte in lithium-metal SSBs [145].

Recent work has focused on the (re)exploration of the mixed-anion phase space bounded by irreducible binaries with the goal of identifying new materials with enhanced ion conduction while maintaining irreducibility. In this vein, many lithium and sodium mixed-anion antiperovskites have been identified, with the general formula $A_3XY$ (A = Li/Na; X = $O^{2-}$/$H^-$; Y = $Cl^-$/$Br^-$/$I^-$/$S^{2-}$/$Se^{2-}$/$Te^{2-}$) [155]. These typically suffer from low-to-modest ionic conductivities and/or reproducibility issues and will not be discussed further here. The previously identified $Li_7N_2I$ has recently been demonstrated as an anolyte in an SSB [154]. $Li_7N_2I$ crystallizes in its own structural type (related to argyrodite via their similar $MgCu_2$-type anion arrangement) and exhibits a modest ionic conductivity of $3 \times 10^{-4}$ S cm$^{-1}$.

Significant promise has been demonstrated in the identification of anion-disordered antifluorite-like materials in the pseudo-tie lines LiCl–$Li_3N$ [157–159], $Li_2S$-$Li_3P$ [161], $Li_2S$-$Li_3N$ [149, 160], and $Li_2Se$–$Li_3As$ [147]. The anion disorder is achieved by mechanochemical synthesis, and most of these materials contain more than two Li ions per anion; they can thus be described as intermediates between the antifluorite and $Li_3Bi$ structural types. Their structure is based on a face-centered cubic (FCC) arrangement of anions forming a network of tetrahedral and octahedral sites for Li, where the tetrahedral sites are preferentially occupied (i.e. antifluorite-like), while the octahedral sites act as reservoirs for extra Li and interstitial sites for ion migration. Furthermore, it has recently been demonstrated that ternary and quaternary mixed-anion compositions are accessible (e.g. $Li_{2.65}S_{0.35}N_{0.15}P_{0.5}$ [162]; $Li_{2.31}S_{0.41}Br_{0.14}N_{0.45}$ [159]), showing high ionic conductivities along with tunable anodic stability. These open up a vast space for exploration and property optimization. As such, we focus the following discussion on antifluorite-like materials.

### Current and future challenges

Irreducible electrolytes show potential for application as anolytes in multielectrolyte battery designs. Irreducible SEs are intrinsically stable at low potentials, but their typically low anodic stability (<2 V vs $Li^+/Li$) precludes their application as the sole electrolyte in a battery, as they would decompose at the operating voltage of any typical battery cathode (>3 V vs $Li^+/Li$). Multielectrolyte battery architectures leverage multiple electrolytes to ensure interfacial stability. In its simplest form, a dual-electrolyte architecture is demonstrated in figure 8. An irreducible SE can be used as an anolyte, inert for reduction by the anode active material and protected from oxidation by the catholyte. In turn, the catholyte selected would be resistant to oxidation by the cathode active material and protected from reduction by the anolyte. This concept can easily be extended to triple- (or generally multi-) electrolyte designs, and such prototypes leveraging irreducible anolytes and low-potential anodes have already shown promising results in terms of cycling stability and power capability [145, 149, 154, 157, 160, 162].

In the context of multielectrolyte architectures, the key properties of irreducible electrolytes become their ionic conductivity and stability to oxidation, as listed in table 1. Although $Li_3N$, with its high room-temperature ionic conductivity ($\sim 10^{-3}$ S cm$^{-1}$), might seem like the obvious anolyte choice, its extremely limited stability window ($\sim$0−0.5 V vs $Li^+/Li$) makes it questionable whether it can form stable interfaces with other SEs. Electrochemical compatibility between different electrolytes has not been systematically investigated and represents a clear direction for future work; still, preliminary calculations indicate that antifluorite-like irreducible electrolytes would be less prone to reactions with

**Table 1.** Key properties of irreducible electrolytes. Experimental data are preferentially reported where available (n/a: not available).

| Phase/class | Ionic conductivity (S cm$^{-1}$, RT) | Anodic stability limit (vs Li$^+$/Li) | References |
|---|---|---|---|
| $Li_3N$ | $\sim10^{-3}$ | ∼0.5 V | [144, 145] |
| $Li_3P$ | $\sim10^{-4}$ | ∼1 V[a] | [146] |
| $Li_3As$ | $<10^{-7}$ | n/a | [147] |
| $Li_2O$ | $\sim10^{-12}$ | ∼ 3 V[a] | [148] |
| $Li_2S$ | $<10^{-8}$ | ∼2.2 V | [149, 150] |
| $Li_2Se$ | $<10^{-7}$ | n/a | [147] |
| LiH | n/a | ∼1 V[a] | — |
| LiF | $<10^{-14}$ | ∼6.3 V[a] | [151] |
| LiCl | $<10^{-10}$ | ∼4.2 V[a] | [152] |
| LiBr | n/a | ∼3.6 V[a] | — |
| LiI | $\sim10^{-7}$ | ∼2.8 V[a] | [153] |
| $Li_7N_2I$ | $\sim3 \times 10^{-4}$ | ∼1.1 V | [154] |
| Antiperovskites | | | |
| $Li_3OX$ (X: Cl, Br) | $\sim10^{-4}$[b] | ∼3 V[a] | [155] |
| $Li_3HCh$ (Ch: S, Se, Te) | $\sim10^{-9}-10^{-7}$ | n/a | [156] |
| Antifluorite-like | | | |
| $Li_{1+2x}Cl_{1-x}N_x$ | $\sim10^{-5}$ | ∼0.7−1.4 V | [157–159] |
| $Li_{2+x}S_{1-x}N_x$ | Up to $2 \times 10^{-4}$ | ∼1.2−2.2 V | [149, 159, 160] |
| $Li_{2+x}S_{1-x}P_x$ | Up to $2 \times 10^{-4}$ | n/a | [161] |
| $Li_{2+x}Se_{1-x}As_x$ | $\sim10^{-5}-10^{-4}$ | n/a | [147] |
| $Li_{2.65}S_{0.35}N_xP_{0.65-x}$ | $\sim10^{-3}$ | ∼1.1 V | [162] |

[a] Experimental data not available, calculated stability limit from Richards *et al* [163].
[b] It is debated whether these compositions are synthesizable in bulk form; the initial reports could not be reproduced. See discussion in [155].

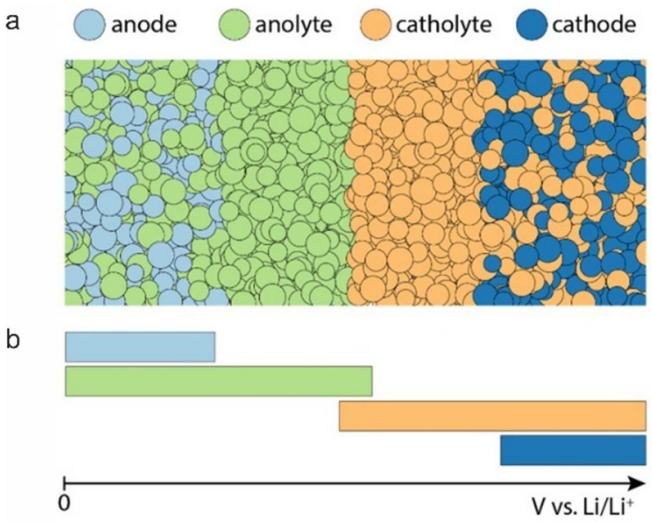


**Figure 8.** (a) Schematic of a dual-electrolyte SSB. (b) Schematic of the working potentials (for anode, cathode) and electrochemical stability windows (anolyte, catholyte). The anolyte is inert to reduction by the anode and is protected from oxidation by the catholyte. The catholyte is inert to oxidation by the cathode and is protected from reduction by the anolyte.

various potential catholytes compared to $Li_3N$ [158]. It has recently been shown that antifluorite-like materials can effectively show higher anodic stability than $Li_3N$ (table 1) while maintaining a high ionic conductivity ($\sim10^{-3}$ S cm$^{-1}$ for $Li_{2.65}S_{0.35}N_{0.15}P_{0.5}$ [162]).

Another area in which the extended anodic stability of antifluorites could prove critically advantageous is the application of next-generation silicon anodes. Reversible (de)lithiation of silicon proceeds through various phases and over a wide potential window (∼0–1 V vs Li$^+$/Li), meaning that $Li_3N$ would be

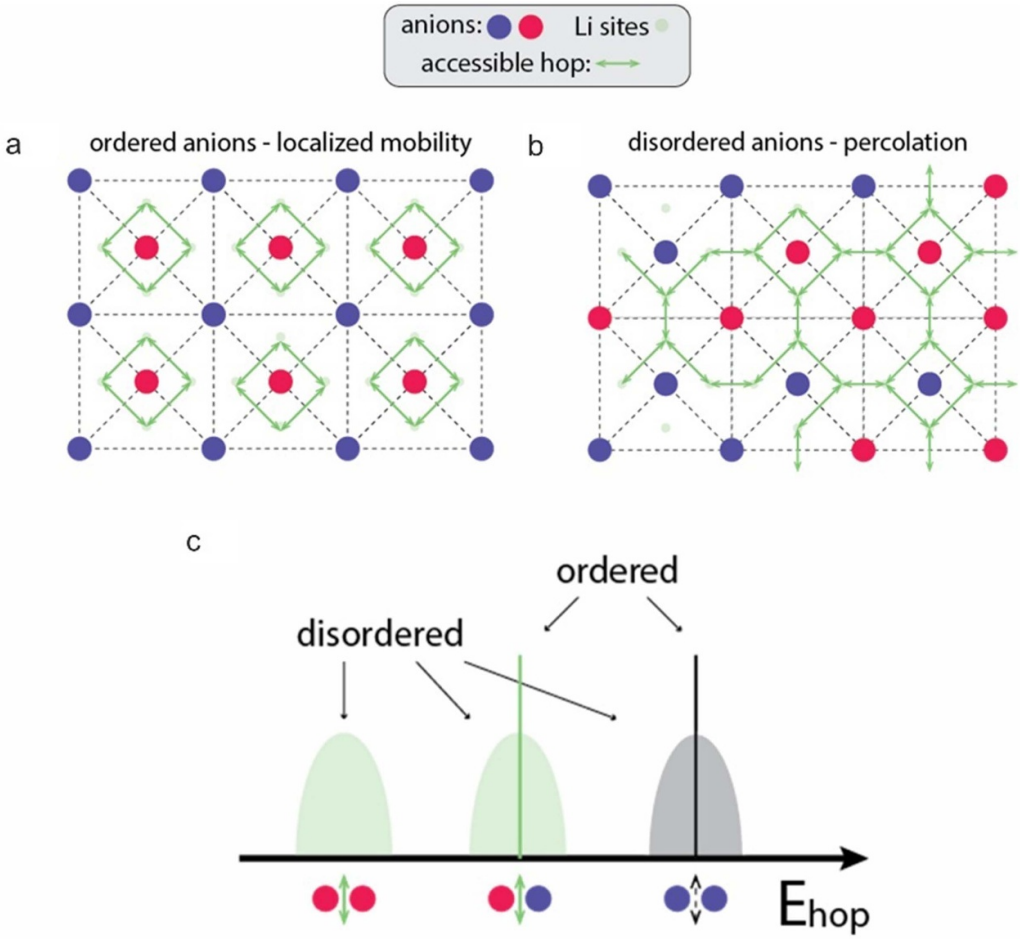


**Figure 9.** Effects of anion disorder on lithium diffusivity. It is assumed in this schematic example that lithium hops are only allowed in the vicinity of a red anion. (a) Lithium mobility is localized in anion-ordered frameworks. (b) Anion disorder creates interconnected percolation pathways by (c) breaking the degeneracy of ion-hopping energies ($E_{hop}$) and creating new local environments conducive to ion hopping.

prone to oxidation against the anode at more than ∼0.5 V vs $Li^+$/Li. In contrast, antifluorites are able to encompass the silicon operational potential window within their electrochemical stability window and could, as such, be key in enabling silicon-anode SSBs.

Structural disorder can be leveraged as a rational design knob for irreducible SEs. Mechanochemical treatment of mixtures of irreducible binaries has been shown to favor the formation of single-phase antifluorite-like materials with anion disorder as a key structural feature. These anion-disordered materials are likely metastable: it has been shown (for some [147, 149] and assumed for others) that they can decompose into the corresponding binaries upon high-temperature treatment. Their kinetic stabilization is predicated on the configurational (and/or vibrational) entropy associated with anion disorder and the high activation barrier for anion rearrangement (ordering) near room temperature. In practice, they are accessible through the high local instantaneous effective temperature (and pressure) afforded by mechanochemistry [147], which effectively emulates quenching and successfully stabilizes the metastable disordered configurations of anions at room temperature. Further advancements will be facilitated by a better understanding of the formation thermodynamics (the balance between entropy and enthalpy) as well as the optimization of out-of-equilibrium mechanochemical (and/or high-pressure [147, 156]) synthesis protocols. It would also be necessary to quantify the thermal stability of irreducible antifluorite-like SEs against decomposition (exsolution [147]) in the context of practical battery device fabrication and operating temperatures.

Beyond its critical effect on synthesis, anion disorder intimately influences the ionic conductivity of antifluorite-like irreducible electrolytes. We have recently developed a computational protocol based on molecular dynamics simulations and percolation analysis to quantify this effect of local anion environments on ionic diffusivity in disordered antifluorite [149] (and argyrodite [164]) SEs. For irreducible antifluorites, we have shown that lithium ions preferentially hop through pnictide-rich regions [149, 162], explaining the trend of higher ionic conductivity with higher pnictide content, $x$, in $Li_{2+x}S_{1-x}N_x$ [149], $Li_{2+x}S_{1-x}P_x$ [161], and $Li_{2+x}Se_{1-x}As_x$ [147]. We have preliminarily interpreted this correlation based on steric arguments, though our latest results on ternary mixed-pnictide compositions $Li_{2.65}S_{0.35}N_xP_{0.65-x}$ indicate that the chemical rationale (i.e. bonding nature, electronegativity, etc.) needs to be included for a full mechanistic

picture. Our analysis clearly shows that the disordered anion arrangements produce interconnected percolation pathways, critically facilitating long-range ion diffusion compared to ordered variants of the same compositions (figure 9) [149, 164]. Further refinements should aim to derive transferable descriptors linking composition to ionic conductivity via local-hopping-environment analysis and percolation arguments. It also remains unclear whether the anion disorder in these phases is in fact random or correlated [165]. In the latter case, it remains to be seen whether there is scope for chemical tuning of the anion distribution and thus properties through, for example, composition or synthetic optimization.

## Conclusions and future perspectives

Irreducible electrolytes offer a direct route to the elimination of anode-side electrolyte decomposition and associated performance losses in SSBs. Recent discoveries have established design rules that now enable purposeful materials discovery:

(1) Enforce irreducibility for thermodynamic stability to Li metal.
(2) Use out-of-equilibrium synthesis to stabilize otherwise inaccessible disordered structural frameworks.
(3) Exploit mixed-anion disorder to achieve high ionic conductivity, greater than $10^{-3}$ S $cm^{-1}$ at room temperature.
(4) Deploy multielectrolyte architectures that combine irreducible anolytes with oxidation-stable catholytes to enable high-energy-density and high-power-density SSBs.

Further work will focus on (i) consolidating phase maps and processing windows for irreducible electrolytes, (ii) benchmarking anodic limits and interfacial stability against leading sulfide/halide catholytes, and (iii) investigating lithium-plating-related properties, such as lithiophilicity, electronic conductivity, and the mechanical properties of irreducible SEs. In parallel, multielectrolyte prototypes leveraging irreducible anolytes with silicon and lithium-metal anodes at practical areal capacities will be validated. With these directions in mind, irreducible SEs can provide the missing anolyte link in practical multielectrolyte SSBs, unlocking the full promise of silicon and lithium-metal anodes without sacrificing cycle life, rate capability, or safety.

Finally, it is likely that the mixed-anion fully reduced electrolytes presently being identified and studied in bulk will be found to actually form *in situ* upon reductive decomposition of other (reducible) electrolytes, such as the LPSCl and LiPON examples discussed in the introduction, i.e. forming components of their respective SEIs. Thus, the exploration of the irreducible electrolyte phase space outlined above could also effectively contribute to a better fundamental understanding of SEI composition and behavior, leading to transferable insight into the development of SSBs in general, regardless of the choice of electrolyte.

## Acknowledgments

TF acknowledges funding provided by the European Union's HORIZON EUROPE program in the form of a Marie Skłodowska-Curie individual postdoctoral fellowship (Project Number 101066486) and by the Dutch Research Council (NWO) in the form of an open-competition XS grant (OCENW.XS22.4.210). MW acknowledges financial support from the 'BatteryNL—Next Generation Batteries based on Understanding Materials Interfaces' project NWA.1389.20.089 of the NWA research program 'Research on Routes by Consortia (ORC)' funded by the Dutch Research Council (NWO).

## Conflict of interest

The authors declare no conflict of interest.

## 7. Amorphous SEs: ionic conductivity and conduction mechanisms

*Ke Huang, Yan Zeng and Bin Ouyang*[*]

Department of Chemistry & Biochemistry, Florida State University, Tallahassee, FL 32306, United States of America

[*]E-mail: bouyang@fsu.edu

### Status

The growing demand for large-scale energy storage drives the search for safer, high-energy-density batteries. Solid-state electrolytes SEs have the potential to replace flammable liquid solvents and can pair with lithium metal anodes, improving both safety and energy density in all-solid-state batteries (ASSBs) [2, 104, 166, 167]. Unlike crystalline SEs, amorphous SEs allow ionic conductivity to be tuned through structural disorder while also suppressing dendrite growth [168, 169] and eliminating grain-boundary resistance [141, 170, 171]. Certain metal-halide-based amorphous electrolytes have been shown to exhibit remarkable mechanical flexibility [172, 173], facilitating battery processing during manufacturing. A widely used amorphous SE is LiPON [174], which has been extensively employed to demonstrate stable SSBs [141, 175–178]. Beyond LiPON, amorphous electrolytes have been explored in oxide [179–182], sulfide [183–186], halide [87, 172, 173, 187], and several mixed-anion systems [91, 169, 188–190]. The best reported ionic conductivities can reach up to $\sim 10^{-2}$ S cm$^{-1}$ [187, 191–193], comparable to those of commercial liquid electrolytes. Despite this rapid progress, rational design principles for optimizing the accessible chemical space and maximizing ionic conductivity remain underdeveloped. In the following sections, we provide a comprehensive overview of the reported chemical spaces for amorphous battery electrolytes and discuss the proposed mechanisms of ion conduction.

The reported amorphous electrolytes can be classified, depending on anion chemistry, as sulfides, oxides, halides, or mixed anions. The reported conductivities for Li, Na, K, and Mg electrolytes obtained from experimental measurements and various simulation approaches are summarized in figure 10. Among all amorphous electrolytes, sulfide-based amorphous electrolytes have attracted the most attention in recent decades [12, 183, 194], which is particularly attributed to the possibility of approaching the ionic conductivity of liquid electrolytes [36, 192]. The extracted ionic conductivity of this group can be represented by S-G1, S-G2, and S-G3, respectively. In general, the chemical formula follows $x$M$_2$S-$(1-x)$P$_2$S$_5$ (M = Li or Na), which allows tuning by changing the M$_2$S-to-P$_2$S ratio [195, 196]. Glass-ceramic thiophosphates (S-G1) are often argued to conduct better than their glassy counterparts (S-G2) due to the fast crystalline pathways precipitating inside the amorphous matrix [184, 197, 198]. A notable example is the glass-ceramic $Li_7P_3S_{11}$, which achieves 17 mS cm$^{-1}$ at room temperature after melt quench and heat treatment [192], exceeding the $\sim$10 mS cm$^{-1}$ of conventional liquid electrolytes [199]. In other cases, the amorphization of LGPS generally reduces conductivity relative to that of the crystal form [6, 200]. Simulations sometimes report very high conductivities for sulfide glasses, such as gc-$Li_{42}P_{16}S_{61}$ (33.1 mS cm$^{-1}$) [195] and $Li_3PS_4$ (19 mS cm$^{-1}$) [201], but these values are extrapolated from high temperature and may be overestimated [202].

Oxide amorphous SEs, including garnet-based (O-G1), borate (O-G2), phosphate (O-G3), and other families (O-G4), are much less developed in contrast to sulfide-based amorphous conductors. Moreover, they are always developed through doping and tuning of synthesis conditions to adopt a well-known crystalline phase, e.g. LISICON, NASICON, garnet, etc. In contrast to sulfide-based systems, there has been significantly less work on oxide amorphous SEs. The intention to pursue a more systematic exploration of oxide-based systems is likely discouraged by the fact that the amorphous phase shows lower or similar ionic conductivity compared to the crystalline reference in many situations [203–209]. Moreover, most oxide amorphous SEs tend to show much lower ionic conductivity than the best of the oxides. Nevertheless, there are some notable exceptions to this statement. For instance, a NASICON-based amorphous SE formed during the electrochemical process was reported to achieve an ionic conductivity of 4.1 mS cm$^{-1}$ [210]. Moreover, the chemical space of oxides extends far beyond the region that has been explored and warrants more thorough investigation.

Halide amorphous SEs are another high-conductivity family. Ball milling mixtures of halide glass formers (such as $TaCl_5$, $NbCl_5$, $AlF_3$, $GaF_3$) with alkali or alkaline-earth salts can produce amorphous halides [172, 173, 187, 193, 211]. Some pairings, such as 3LiCl-$GaF_3$ or $MgCl_2$-$GaF_3$, form soft clay-like mixtures (H-G1) through partial anion exchange [172, 173, 212]. These show good conductivities, $10^{-4}$–$10^{-2}$ S cm$^{-1}$, and make intimate electrode contact during cycling [172]. Nonclay binary or ternary halide glasses (H-G2) can be even more conductive. $TaCl_5$ and $NbCl_5$-based Li conductors are notable, benefiting from larger free volume and polyanion rotation rather than lower migration barriers [193, 211, 213]. The 2LiCl-0.5$AlF_3$-0.5$GaF_3$ composition achieves 16 mS cm$^{-1}$ at room temperature, attributed to a deep eutectic phase that enhances Li transport [187]. Li electrolytes generally outperform Na, Mg, and K analogs because larger ionic radii raise barriers [214], and $Mg^{2+}$ can be strongly bound to the anion framework [215].

We further group mixed-anion systems into chalcohalides (M-G1), LiPON and analogs (M-G2), oxyhalides (M-G3), oxysulfides (M-G4), thiophosphate-boron hydrides (M-G5), and other variants (M-G6). As can well be expected, any mixed-anion system with sulfur and a halogen as anions tends to show higher ionic conductivity, which is inherited from the single-anion systems. In contrast, oxide-based systems generally show lower ionic conductivity, as exemplified by the LiPON family. A typical motivation for creating mixed anions is the hope of a trade-off between phase and electrochemical stability, as well as the hope of a potentially synergistic effect leading to enhanced ionic conductivity. For example, chalcohalides (M-G1), oxysulfides (M-G4), and oxyhalides (M-G3)

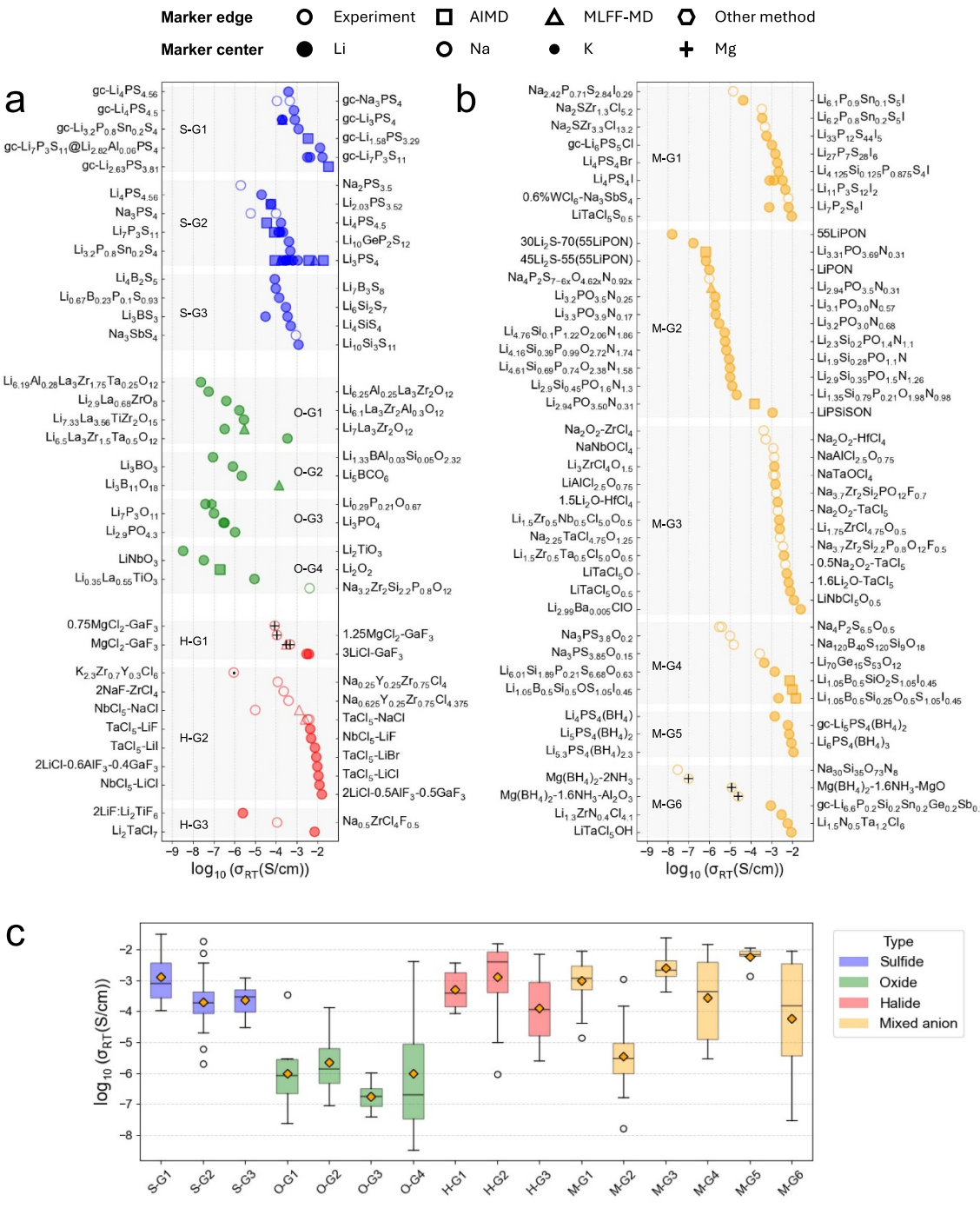


**Figure 10.** Room-temperature ionic conductivities of amorphous SEs. (a) Single-anion systems: sulfides (blue), oxides (green), and halides (red). Sulfides: S-G1, glass-ceramic thiophosphates; S-G2, glassy thiophosphates; S-G3, other sulfides. Oxides: O-G1, amorphous garnets; O-G2, borates; O-G3, phosphates; O-G4, other oxides. Halides: H-G1, clay-like binary halide mixtures; H-G2, non-clay-like binary or ternary halides; H-G3, other halides. (b) Mixed-anion systems (orange), grouped into: M-G1, chalcohalides; M-G2, LIPON and analogs; M-G3, oxyhalides; M-G4, oxysulfides; M-G5, thiophosphate-boron hydrides; M-G6, other mixed-anion compositions. (c) Corresponding box plots of ionic conductivities. The black line and orange diamond inside the box represent the median and mean value, respectively. Total numbers of reported amorphous SEs by type: sulfide $n = 52$, oxide $n = 23$, halide $n = 26$, and mixed anion $n = 85$. For detailed data on the ionic conductivity of all reported amorphous SEs, see table S1 in the supporting information.

have attracted increasing attention recently, as these designs can lead to a reasonable balance between good moisture stability, broad electrochemical window, easier processability, and high ionic conductivity [91, 92, 169, 189, 216–219].

Understanding ion conduction in amorphous SEs is challenging due to structural disorder and the lack of unified descriptors, even within a single class. Strategies to enhance conductivity mainly focus on lowering the activation bar-

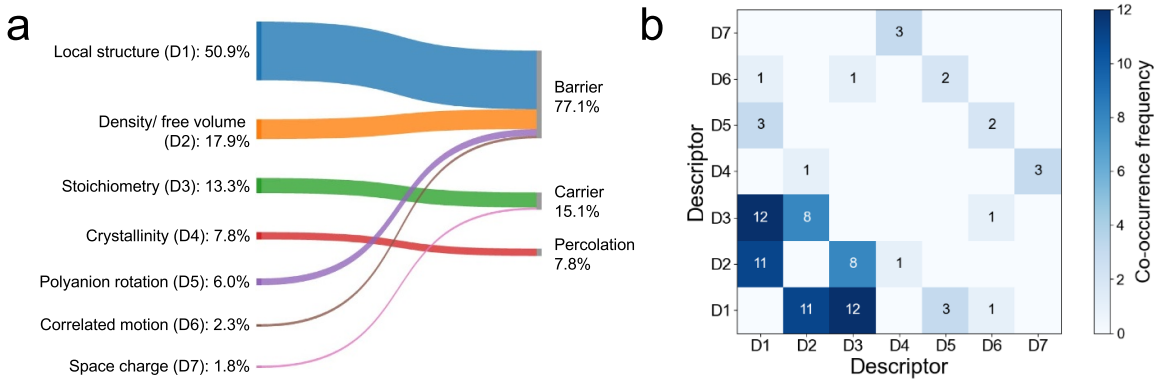


**Figure 11.** Descriptor landscape for ionic conductivity mechanisms in amorphous SEs. (a) Use frequency of each descriptor across the reported amorphous SEs, defined as each descriptor's occurrence count divided by the total occurrences of all descriptors. The descriptors are grouped according to their contribution to $\sigma$ from the migration barrier $E_a$ (77.1%), charge-carrier concentration $n$ (15.1%), or both (7.8%). (b) Descriptor co-occurrence matrix. Each cell ($D_i$, $D_j$) counts pairs that appear together in the same SE; the diagonal ($D_i$, $D_j$) is excluded. For detailed data on the descriptors of all reported amorphous SEs, see table S1 in the Supporting Information.

rier for ion hopping, increasing carrier concentration, or both, to form continuous percolation pathways. We classify the mechanisms discussed in 132 studies into seven categories (figure 11): local structure [219–222], density/free volume [185, 223–225], stoichiometry [191, 216, 226, 227], crystallinity [192, 194, 197], polyanion rotation [201, 228–230], correlated motion [173, 181, 201], and space charges [197, 231, 232]. Among these, crystallinity is dominant in glass-ceramic SEs, where percolating crystalline motifs within the amorphous matrix are believed to boost conductivity. Stoichiometry and space charges primarily affect carrier concentration, while the other four factors mainly reduce activation barriers. Notably, polyanion rotation represents a dynamic coupling between polyanion motion and ion diffusion, constituting a distinct type of local structural effect. We highlight it separately to emphasize its emerging importance, which has also led to occasional conflicting reports [201, 230, 233–236] that warrant further case-by-case theoretical and experimental investigations.

Figure 11(a) exhibits the use frequency of the above descriptors across all amorphous SEs. For crystalline ionic conductors, recent studies suggest that high conductivity arises from three factors: (i) crystalline frameworks that minimize the fluctuation of coordination environments, thereby lowering diffusion barriers [237], (ii) compositional disorder that promotes ion percolation [33, 238, 239], and (iii) framework–stoichiometry [240] interplay that influences both carrier concentration and activation barriers. In contrast, amorphous SEs urgently require tools to probe local structures, as over half of the reports attribute high conductivity to this factor. Ion percolation is further complicated by the absence of symmetry, demanding careful statistical treatment from both experiments and simulations. More accessible descriptors include density and composition, shown to strongly affect conductivity in 17.9% and 13.3% of cases, respectively. Building systematic datasets correlating these variables with conductivity would provide an efficient entry point for understanding amorphous SEs. Finally, these descriptors are often interdependent. As illustrated in figure 11(b), multiple descriptors, particularly local structure, density, and stoichiometry, frequently coexist. This overlap suggests that, in practice, one may substitute difficult-to-measure descriptors with more accessible ones to advance design rules for amorphous SEs.

## Current and future challenges

In contrast to crystalline electrolytes, it is somewhat surprising that there has been much less systematic work on expanding the chemical space of amorphous electrolytes, while many crystalline electrolyte systems have been well explored with the aid of high-throughput computational screening [241–245]. Moreover, the compositional design of amorphous electrolytes is largely driven by heuristic hypotheses from experienced experimentalists, while in many cases, researchers tend to start from some crystalline analog when designing amorphous electrolytes. There could be broader spaces for further extending the viable chemical spaces of amorphous materials if state-of-the-art high-throughput virtual screening, ML, and automated synthesis approaches were adapted for the discovery of amorphous electrolytes [246, 247].

Meanwhile, extending the length and time scales for molecular statistical simulation of SEs through molecular dynamics, Monte Carlo, or other methods is always a challenge. For amorphous SEs, such a challenge is more severe, particularly considering two factors: (i) the melt and quench

process typically requires a much longer time to equilibrate and (ii) there is a possibility for amorphous materials to evolve at different temperatures [248–250], which further contributes to the evolution of ionic conductivity.

## Conclusions and future perspectives

To summarize, we have compiled a curated dataset of amorphous SEs from 132 published studies. This dataset captures the reported distributions of ionic conductivity and the proposed ion-conduction mechanisms. Our analysis highlights that amorphous SEs hold significant promise not only for achieving high ionic conductivity but also for enabling flexible synthesis and processing strategies in SSBs. At the same time, the relatively limited exploration and understanding of ion transport in amorphous systems underscore a major opportunity to expand the viable chemical space.

## Acknowledgment

All authors acknowledge startup funding from Florida State University in support of this work.

## Conflict of interest

The authors declare no conflict of interest.

## 8. Glass-ceramic SEs: halides

*Juhyoun Park*[1] *and Yoon Seok Jung*[1,2,*]

[1]Department of Chemical and Biomolecular Engineering, Yonsei University, Seoul 03722, Republic of Korea
[2]Department of Battery Engineering, Yonsei University, Seoul 03722, Republic of Korea

[*]E-mail: yoonsjung@yonsei.ac.kr

### Status

Glass ceramics are metastable phases positioned between amorphous and crystalline materials; they comprise an amorphous matrix with embedded crystalline domains formed through partial nucleation (figure 12(a)). The field emerged in 1953, when $Li_2O$-$2SiO_2$ synthesized at high temperatures was unexpectedly found to exhibit superior mechanical strength compared to conventional glass [251]. This discovery established the concept of 'controlled crystallization,' which became the foundation for glass-ceramic manufacturing and was later extended to SE applications [252].

Glass/glass-ceramic SEs offer distinct advantages. For example, the structural disorder in glass provides compositional flexibility, which can enhance ionic conductivity, chemical and interfacial stability, and mechanical ductility [254]. Additionally, the absence of grain boundaries allows for the densification of cold-pressed pellets [254, 255]. A representative example is the $Li_2S$-$P_2S_5$ system, in which crystallinity plays a decisive role in ionic conductivity (figures 12(b) and (c)). For instance, $70Li_2S$-$30P_2S_5$ ($Li_7P_3S_{11}$) exhibits an ionic conductivity of ∼0.05 mS cm$^{-1}$ in the ball-milled glass state, ∼$10^{-8}$ S cm$^{-1}$ in the fully crystalline state, and ∼3 mS cm$^{-1}$ in the glass-ceramic state [253].

Halide SEs have attracted increasing attention due to their superior oxidative stability (>4 V) compared to their sulfide counterparts [71, 256]. Notably, after the rediscovery of $Li_3YCl_6$, it was confirmed that mechanochemically synthesized materials exhibit higher ionic conductivity than those obtained by simple annealing, as ball milling often yields distinct structural motifs that enhance transport [71, 257]. Although sulfide SEs can deliver $Li^+$ conductivities exceeding 10 mS cm$^{-1}$ [6], no crystalline halide SEs have yet achieved comparable levels. Recently, however, the emergence of glass/glass-ceramic halide SEs has renewed interest in the subject, as glassy phases offer opportunities to improve both ionic conductivity and mechanical properties.

Most crystalline halide SEs exhibit hexagonal close packing (trigonal $P\bar{3}m1$ and orthorhombic $Pnma$ $Li_3YCl_6$ structure) or cubic close packing (monoclinic $C2/m$ $Li_3InCl_6$ structure) [256]. Compared to sulfides, these frameworks provide narrower $Li^+$ migration channels, thereby imposing intrinsic upper limits on ionic conductivity [256]. Consequently, despite extensive compositional screening, no crystalline halide SE has surpassed 5 mS cm$^{-1}$. In contrast, glassy halide SEs lack long-range periodicity and are free from such structural constraints, spurring growing interest in their development as highly conductive electrolytes.

Glass/glass-ceramic halide SEs are typically synthesized from a combination of glass formers and network modifiers [258]. Glass formers include low-melting-point or sublimable metal chlorides, such as $AlCl_3$, $ZrCl_4$, and $TaCl_5$, whereas network modifiers include Li-based salts, such as $Li_2O$, $Li_2O_2$, $Li_3PO_4$, and LiCl (or analogous Na salts). Upon ball milling or annealing, these precursors undergo anion rearrangement, generating diverse structural motifs with varying coordination environments. In this short review, we highlight the compositional design, structural characteristics, synthesis methods, and potential applications of glassy halide SEs and outline the key problems that must be addressed for their future commercialization.

Jung *et al* reported that mechanochemically prepared $n$LiCl-$GaF_3$ ($n$ = 2, 3) exhibits a clay-like behavior with a modulus of less than 1 MPa [172]. NMR and x-ray absorption spectroscopy analyses revealed an amorphous phase containing $GaCl_mF_{n-m}$-complex anions [259], which Gupta *et al* linked to the observed ductility [212]. Specific Al-based compositions were subsequently identified with similar mechanical softness and ionic conductivities of up to 1–16 mS cm$^{-1}$ [260]; even $Mg^{2+}$-conducting analogs have been demonstrated [173]. Although this ductility enables intimate interfacial contact with active materials, some compositions suffer from compatibility problems with other SEs, necessitating careful consideration in ASSB designs [172].

$ZrCl_4$ and $TaCl_5$ are inorganic, molecular solids that can act as glass formers [258], enabling the synthesis of both crystalline and amorphous SEs. The heat treatment of $Li_aMCl_6$ (M = Zr, Ta) yields low-conductivity crystalline phases, whereas oxygen incorporation or prolonged ball milling produces highly conductive glassy halide SEs [261]. For example, crystalline $LiTaCl_6$ exhibits a low ionic conductivity of ∼$10^{-8}$ S cm$^{-1}$ [262], whereas glass-ceramic $LiMOCl_4$ (M = Nb, Ta) forms glass-ceramic phases with conductivities of more than 10 mS cm$^{-1}$ [89]. Similarly, annealed $Li_2ZrCl_6$ crystallizes in a monoclinic phase with an ionic conductivity of 0.006 mS cm$^{-1}$ [257], whereas mechanochemically prepared $Li_2ZrCl_6$ and $ZrO_2$-$2Li_2ZrCl_6$ achieve ionic conductivities of 0.4 and 1.3 mS cm$^{-1}$, respectively (figures 13(a) and (b)) [257, 263]. These findings highlight the growing trend of resynthesizing crystalline halide compositions into glass/glass-ceramic phases containing amorphous domains to markedly improve their ionic conductivity.

Structurally, the crystalline Zr/Ta-based halide SEs contain isolated $MCl_6$ octahedra without corners or edge-sharing linkages [257, 262]. In contrast, glassy halides feature disordered arrangements of multiple coordination units, such as trigonal bipyramids and tetrahedra [91]. Zhang *et al* demonstrated that oxygen atoms could bridge $TaCl_{5-a}O_a$ units in $1.6Li_2O$-$TaCl_5$ [91], reminiscent of conductivity enhancements in oxysulfide glass-ceramic SEs [194]. However, due to the inherent disorder of glass structures, current characterizations have largely been limited to identifying the building-unit types. Quantitative insights into the degree and connectivity of

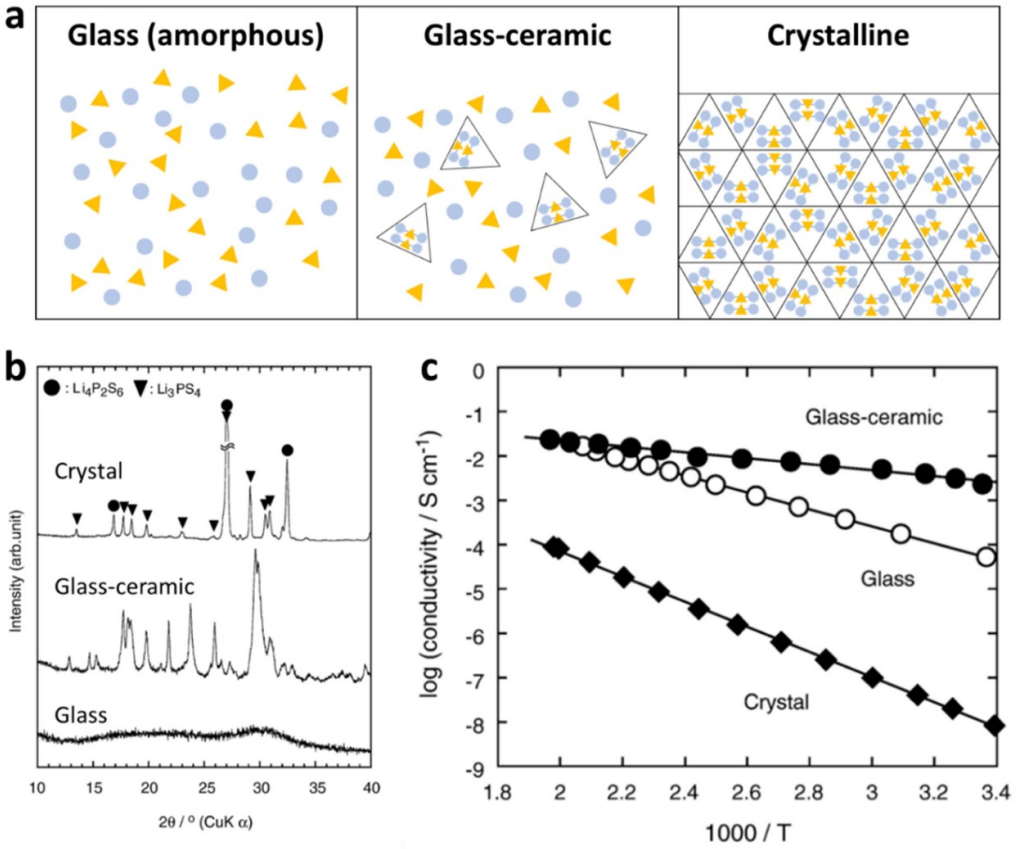


**Figure 12.** Structural and ionic transport characteristics of glass, glass-ceramic, and crystalline SEs. (a) Schematic illustrating glass, glass-ceramic, and crystalline materials; blue circles and yellow triangles represent anionic and cationic constituents, respectively, and black hollow triangles indicate the crystalline domains. (b) X-ray diffraction (XRD) patterns and (c) Arrhenius plots of $70Li_2S$-$30P_2S_5$ SEs. (b), (c) Reprinted from [253], Copyright (2006), with permission from Elsevier.

these units are scarce, highlighting the need for more advanced structural investigations.

Li–Al–O–Cl (LAOC) systems have recently garnered attention owing to their cost-effectiveness, soft mechanical properties, and high ionic conductivities (>1 mS cm$^{-1}$), which are likely related to the low melting point (<200 °C) of $AlCl_3$. Dai *et al* synthesized oxychloride SEs with polymer-like mechanical properties by oxidizing $LiAlCl_4$ using $Sb_2O_3$ (equation (1)) [260]. Alternative oxygen sources such as $AlCl_3 \cdot 6H_2O$ or $Li_2O_2$ can also be employed (equations (2) and (3)) [264–266], although these reactions are invariably accompanied by gas evolution:

$$4LiAlCl_4 + Sb_2O_3 \rightarrow LiAlCl_{2.5}O_{0.75} + 2SbCl_3(g) \quad (1)$$

$$aLiCl + bAlCl_3 + cAlCl_3{\cdot}6H_2O \rightarrow 6Li_{a/6}Al_{(b+1)/6} \times OCl_{(a+3b-9)/6} + 12HCl(g) \quad (2)$$

$$aLi_2O_2 + bAlCl_3 \rightarrow Li - Al - O - Cl + \text{unidentified gas.} \quad (3)$$

Cyclic voltammetry has indicated that the oxidation stability of LAOC is limited to less than 4 V, and long-term cycling with layered oxide cathodes (cutoff at 4.8 or 4.3 V) has been enabled by passivation through $LiAlO_2$ formation at the cathode interface [260, 261, 266]. On the anode side, a comparable passivation mechanism derived from oxygen-rich Al environments allowed stable cycling with Li–In anodes [261]. Additionally, the low melting point allowed interfacial wetting and infiltration into cathode interparticle voids, thereby forming integrated $Li^+$ transport channels within the electrode (figures 13(c) and (d)) [267].

## Current and future challenges

The particle size of the SEs strongly influences the effective ionic conductivity of the composite electrodes [268]. Even with comparable intrinsic conductivities, smaller particles generally exhibit higher effective conductivities. However, controlling the particle sizes of glassy halide SEs can be challenging. The particle sizes of sulfide SEs can be readily tuned by wet milling or synthesis [269, 270]. In contrast, halide SEs are highly solvent sensitive and remain unstable even in nonpolar solvents, with $Li_3InCl_6$ being a rare exception [256]. According to the hard and soft acid-base (HSAB) theory, this instability arises from structural units such as $AlCl_3$, $ZrCl_4$, and $TaCl_5$, which not only serve as precursors but can also persist in the products. As harder acids

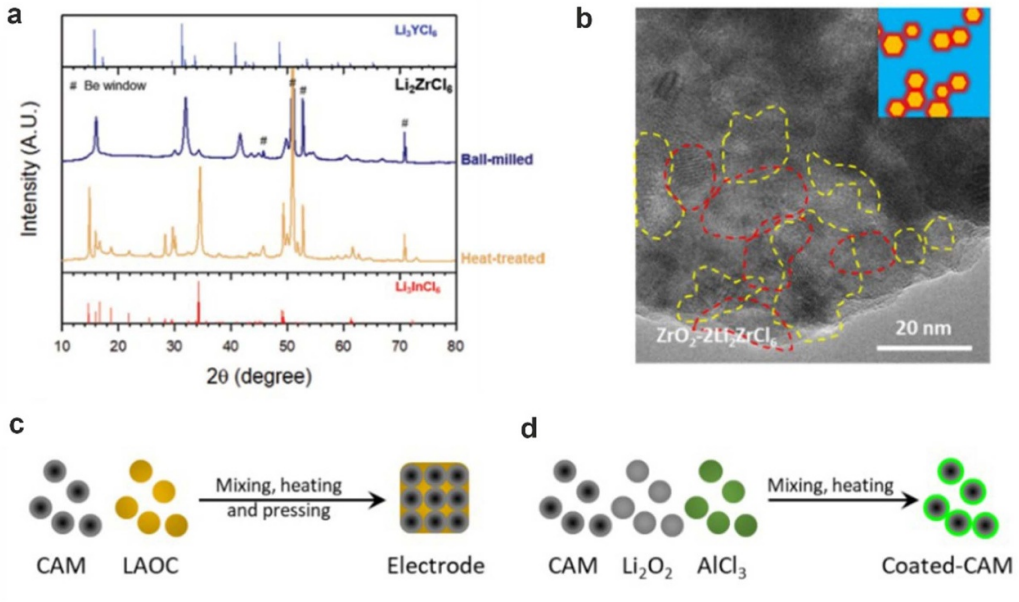


**Figure 13.** Glassy halide SEs with their structural characteristics and electrode-level applications. (a) XRD patterns of heat-treated $Li_2ZrCl_6$ and mechanochemically prepared samples of $Li_2ZrCl_6$ [257]. John Wiley & Sons.© 2021 Wiley-VCH GmbH. (b) TEM image of $ZrO_2$-$2Li_2ZrCl_6$. Reproduced from [263]. CC BY 4.0. Schematic of the electrode-level application of Li–Al–O–Cl (LAOC) via thermal infiltration using (c) preformed LAOC and (d) precursors.

than $InCl_3$, they react more readily with solvents, thereby imparting pronounced solvent sensitivity to glassy halide SEs. Consequently, solution-based methods of controlling the particle size are impractical. Instead, dry processes such as jet milling, which have proven to be effective for sulfide SEs [271], may also be applicable to halide SEs.

The air stability of amorphous halide SEs can be expected to be lower than that of conventional crystalline halides. According to the HSAB theory, $Al^{3+}$, $Zr^{4+}$, $Ta^{5+}$, and $Ga^{3+}$ are harder metal cations than $Y^{3+}$ and $In^{3+}$ [272] and thus exhibit higher reactivity toward moisture. For example, $Zn^{2+}$ substitution in $Li_2ZrCl_6$ improves air stability [273], suggesting that incorporating softer metal elements can be effective, albeit with inherent compositional limitations. Alternatively, surface modifications that impede moisture exposure, such as vapor-phase coatings with hydrophobic polymers—for example, fluorinated poly(dimethylsiloxane)—provide a promising approach [274].

Due to their poor intrinsic reductive stability and limited passivation ability, the direct application of halide SEs to anodes is inherently restricted [256], which can necessitate hybrid configurations with anolytes such as sulfides, oxides, or nitrides. This makes interfacial compatibility a critical consideration in cell design. Kwak *et al* first reported side reactions at the $Li_2ZrCl_6$|LPSCl interface and proposed mitigation through the incorporation of F or O [263]. Rosenbach *et al* revealed the formation of a resistive $InS^-$-containing layer at the $Li_3InCl_6$|LPSCl interface [46], whereas Samanta *et al* correlated the resistance evolution with the electronegativity of the metal element in halide SEs [275]. Because $Al^{3+}$, $Zr^{4+}$, $Ta^{5+}$, and $Ga^{3+}$ are more electronegative than $In^{3+}$, amorphous halide SEs are likely to exhibit more pronounced incompatibility with sulfides than with $Li_3InCl_6$.

Beyond sulfides, attention has recently been extended to 'irreducible' SEs with ionic conductivities of approximately 1 mS $cm^{-1}$, which can be paired with halides to enable stable cycling with Li metal anodes [276, 277]. As the name suggests, these materials are composed of anions such as $F^-$, $O^{2-}$, $OH^-$, and $N^{3-}$, which cannot be further reduced. Shen *et al* reported that a $LiInO_2$-containing passivation layer forms at the $Li_3OCl$|$Li_3InCl_6$ interface [278], enabling the stable operation of full cells with Li metal anodes. More recently, the concept of 'dynamic' reductive stability has been proposed for $Li_3YCl_6$ and $Li_3YCl_3Br_3$, with stability extending down to 0.2 V (vs $Li^+$/Li) [100]. Although still insufficient for the direct use of Li metal, this finding demonstrates the feasibility of pairing halide SEs with alternative high-capacity phosphorus anodes, thereby highlighting potential paths toward high-energy all-halide ASSBs.

## Conclusions and future perspectives

In summary, glass/glass-ceramic SEs represent a unique class of materials exhibiting higher ionic conductivities than their crystalline counterparts. Among these, halide-based systems are promising candidates because of their superior conductivity and ductility, which are enabled by their compositional, structural, and processing flexibility. Nevertheless, several problems must be addressed for their practical implementation:

(1) Severe solvent incompatibility necessitates solvent-free particle size control, via jet milling, for example, to enhance effective ionic transport in composite electrodes.

(2) Poor air stability requires compositional tuning or surface modifications to ensure compatibility with dry-room processing.
(3) Cell-level strategies—including hybrid stacking with different SEs and the adoption of alternative anodes—must be further developed.

In the long term, establishing fundamental correlations between the building-unit distribution/connectivity and ionic, mechanical, and chemical properties could transform the structure–property relationships into predictive design tools, accelerating rational compositional screening. With these advances, glassy halide SEs could emerge as key enablers of high-energy and high-power ASSBs.

## Acknowledgments

This work was supported by the National Research Foundation of Korea (NRF) Grant funded by the Korean government (MSIT) (No. RS-2024-00343349) and through the Human Resources Development Program (No. 20214000000320) of the Korea Institute of Energy Technology Evaluation and Planning (KETEP), funded by the Ministry of Trade, Industry, and Energy of the Korean government.

## Conflict of interest

The authors declare no conflict of interest.

## 9. Redox-active SEs

*Jingui Yang, Siyuan Guo, Torsten Brezesinski and Florian Strauss**

Institute of Nanotechnology, Karlsruhe Institute of Technology (KIT), Kaiserstr. 12, 76131 Karlsruhe, Germany

*E-mail: florian.strauss@kit.edu

### Status

SEs are indispensable components of SSBs because they determine ion transport and play an important role in interfacial stability. Ideally, SEs should combine superionic conductivity with high (electro)chemical stability toward both the cathode and anode across the entire operating voltage range. However, modern SEs, including sulfide-, halide-, and polymer-based materials, are not electrochemically inert. Instead, they often exhibit intrinsic redox activity that triggers parasitic reactions at the interface between the electrolyte and the other electrode components. These interfacial processes are usually only partially reversible and often lead to the formation of resistive interphases that block charge transfer and ultimately limit long-term cycling stability [279].

Previous research efforts have largely focused on mitigating such adverse side reactions. Common strategies include applying protective surface coatings to electrode materials, substituting elements into the SEs to expand their (electro)chemical stability window, or developing dual-electrolyte architectures to decouple cathode and anode chemistries [280–282]. These approaches are based on the long-standing paradigm of the necessity of having an inert SE, viewing it as a passive cell component whose only function is to enable fast ion transport between the active materials. However, this paradigm has recently been called into question. There is growing evidence that redox activity in SEs may not necessarily be detrimental. Under certain circumstances, the intrinsic redox processes can be exploited in a reversible manner, thereby providing additional capacity for the battery. This paradigm shift defines SEs no longer as passive components but as functional materials that directly contribute to cell performance.

As illustrated in figure 14, SEs can be classified according to their redox behavior. Redox-inert SEs have a wide electrochemical stability window, with the anodic and cathodic limits lying beyond the working potential of the active materials and thus contributing no additional capacity. Redox-passive SEs undergo redox processes within the operating voltage range. However, these reactions are either irreversible or, if reversible in nature, occur at potentials that do not overlap with those of the active materials. In contrast, redox-reversible SEs exhibit redox activity in the working potential ranges of the active materials, enabling them to participate in reversible charge storage. Such materials not only provide ion conduction but also contribute to additional capacity, thereby increasing the specific energy at the cell level. This classification invites a more comprehensive rethinking of the functionality of SEs.

In the following sections, we highlight recent advances in sulfide- and halide-based redox-active SEs for lithium-sulfur and LIBs. However, the general design strategies are also promising for extension to post-Li systems.

### Current and future challenges

Sulfide SEs have attracted great attention due to their exceptionally high ionic conductivities at room temperature. However, their electrochemical stability windows are relatively narrow [6]. On the cathode side, oxidative stability is limited by sulfur chemistry: $S^{2-}$ anions are prone to oxidation at relatively low potentials. On the anode side, reductive stability is defined by the reduction of framework cations, such as $P^{5+}$, $Ge^{4+}$, or $Si^{4+}$, depending on the specific composition. In combination with high-voltage (intercalation) cathodes, sulfide SEs often behave as redox passive. They undergo irreversible decomposition into polysulfides and/or elemental sulfur and other poorly conductive species that impede lithium transport and accelerate impedance growth [283]. Despite this apparent instability, recent studies have shown that sulfur redox can be reversible in sulfide SEs [284]. In solid-state lithium–sulfur batteries (SSLSBs), sulfide SEs are actively involved in redox processes and contribute significantly to reversible capacity. Interestingly, several systems have been found to deliver capacities that exceed the theoretical limit of sulfur alone [285, 286]. The reason for this is that, in these cases, the sulfide SEs act not only as passive ion conductors but also as an additional electrochemically active phase. Building on this insight, the introduction of new redox-reversible chemistries offers a promising strategy for overcoming the sluggish sulfur conversion that limits SSLSBs. An effective approach is the incorporation of iodine species [287]. Iodine has a redox potential slightly higher than sulfur's, with strongly overlapping voltage windows and intrinsically faster kinetics. This allows it to act as a redox mediator, accelerating sulfur conversion, especially during charging, enabling SSLSBs to compete with or even outperform liquid-electrolyte-based counterparts. Such a targeted design thus opens up new avenues for improving battery performance. However, the advantageous redox activity comes with trade-offs. It inevitably involves structural and morphological changes, which can negatively affect ionic conductivity and add to the overall volume changes in the composite electrode. These problems are particularly serious in lithium-sulfur battery systems, where sulfur undergoes a volume expansion of about 80% upon lithiation ($Li_2S$ formation), and the different species suffer from inherently low electronic conductivities. Overall, these effects accelerate mechanical degradation, interfacial instability, and capacity loss, highlighting the delicate balance between exploiting redox activity and maintaining long-term cycling stability.

Halide SEs typically have much higher anodic stability because their oxidation chemistry is determined by halide anions rather than $S^{2-}$. In general, the high oxidative stability makes halides particularly attractive as catholytes for high-voltage oxide cathodes. However, due to the presence of transition-metal cations that tend to undergo reduction,

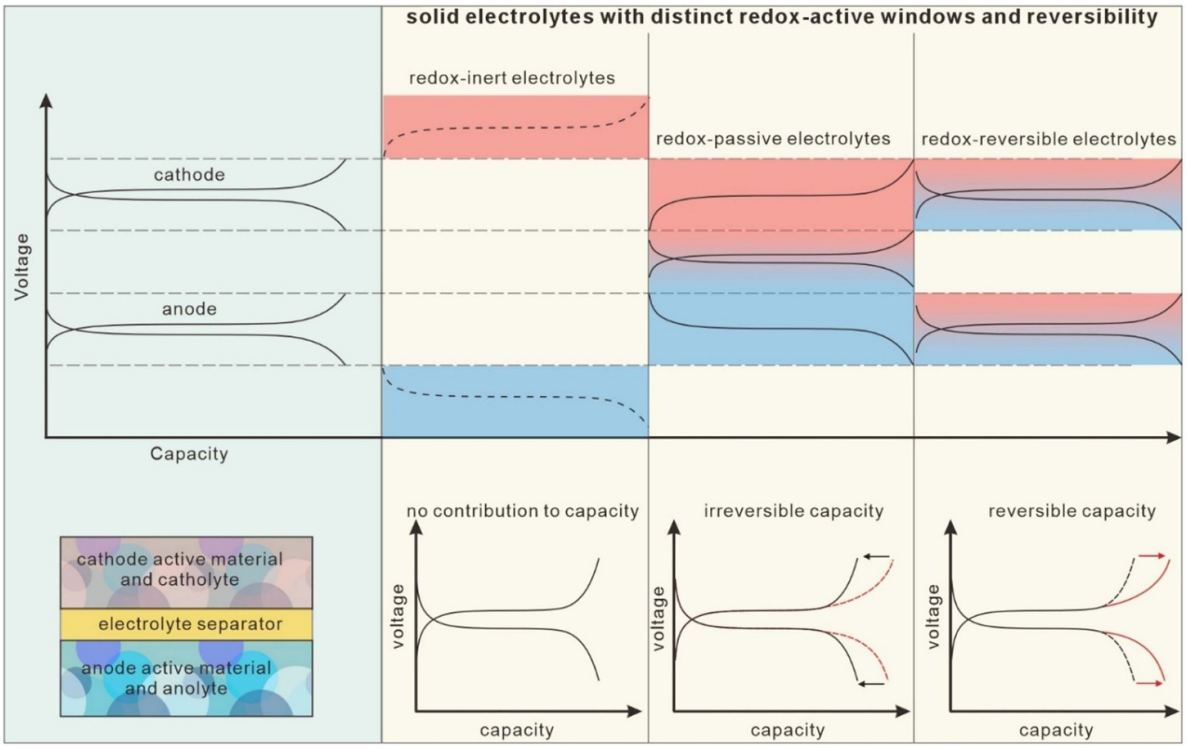


**Figure 14.** Classification of SEs for SSBs: redox-inert materials only provide ion conduction; redox-passive materials decompose irreversibly and only contribute to capacity over the first few cycles; and redox-reversible materials align reversible redox reactions with electrode potentials, adding reversible capacity and increasing the specific energy.

they generally exhibit poor cathodic (reductive) stability [288]. Interestingly, unlike sulfide SEs, which undergo conversion reactions, halide SEs exhibit (de)lithiation behavior. The latter is expected to offer better reversibility and have fewer negative effects on ionic conductivity, as their structural framework remains intact [100, 289]. Fe-based halides, such as $Li_{2.9}Fe_{0.9}Zr_{0.1}Cl_6$ and $Li_{1.3}Fe_{1.2}Cl_4$, utilize the $Fe^{2+}/Fe^{3+}$ redox couple with an average potential of ∼3.6 V vs $Li^+/Li$ and can be combined with various cathode active materials, including $LiCoO_2$ and layered Ni-rich oxides [290, 291]. Notably, $Li_{1.3}Fe_{1.2}Cl_4$ has also been found to show promising properties as an all-in-one material (catholyte and cathode active material) for SSBs [290]. Other transition-metal halides further enrich the available redox chemistry. $Li_3VCl_6$ operates with the $V^{2+}/V^{3+}$ redox couple at ∼3.06 V, delivers an intrinsic specific capacity of ∼80 mAh $g^{-1}$, and shows good compatibility with $LiFePO_4$ cathodes [289]. $Li_3TiCl_6$ stands out for its dual redox activity, combining $Ti^{3+}/Ti^{4+}$ at 3.62 V and $Ti^{2+}/Ti^{3+}$ at 1.86 V [292]. Halide SEs have also proven to be promising redox-reversible anolyte materials. For example, $Li_3YCl_3Br_3$ (with $Y^{3+}/Y^{2+}/Y^+$ redox) exhibits a dynamic stability window with a lower limit of about 0.2 V vs $Li^+/Li$ and is compatible with red phosphorus anodes [100]. Similar design strategies have also been extended to various sodium systems, with promising results [102, 293]. Despite this progress, and although it is assumed that the (de)lithiation behavior of halide SEs has less of an impact on their transport properties than conversion reactions, significant fluctuations in ionic conductivity were observed at different states of charge [100, 291]. Since halides already have lower conductivities than common liquid electrolytes, this dependence could become a major obstacle to practical SSB operation. In addition, they also undergo volume changes during cycling, which compromises electrode integrity over time.

## Conclusions and future perspectives

Redox activity in SEs, long considered a disadvantage, is increasingly recognized as an opportunity. With suitable anode/cathode combinations, redox-active SEs can directly contribute to electrode capacity and thus improve energy density. Due to their shared chemistry with lithium–sulfur battery systems, sulfides are natural candidates for redox-reversible catholytes. The incorporation of iodine or other redox mediators offers a promising way to overcome sluggish sulfur kinetics and boost performance. In halides, the stable anion framework enables reversible redox activity in transition-metal species, making them attractive for high-voltage cathode applications. However, to exploit the potential of redox-reversible SEs, several key challenges must be overcome:

(1) The redox behavior of SEs is still poorly understood. In the case of sulfides, there is a considerable discrepancy between experimentally and theoretically determined stability windows [57]. While this has often been attributed to kinetic effects, a recent study suggests that sulfides degrade via indirect pathways involving initial

(de)lithiation followed by thermodynamic decomposition [294]. *In situ* spectroscopic and electrochemical probes will be essential for elucidating these mechanisms and will enable the rational design of redox-reversible SEs.

(2) The ionic conductivity in redox-reversible SEs is not stable but evolves with the state of charge, i.e. the redox behavior, often decreasing upon decomposition. This increases the internal resistance, reduces the utilization of active material, and limits the rate capability. Future work should focus on the coupled transport of ions and electrons across complex electrode/electrolyte interfaces while optimizing the electrode's microstructure to maximize both the capacity contribution from the electrolyte and the ionic conduction.

(3) Redox-active SEs are subjected to volume changes during battery operation. Together with the expansion/contraction of the active material, this increases mechanical stress and accelerates degradation. Mitigation strategies could include combining them with active materials exhibiting opposite volume change behaviors to compensate for dimensional fluctuations. Furthermore, current findings suggest that state-of-charge-dependent SE softening could enable self-healing mechanisms [290]. Exploiting this behavior may open up a new dimension in electrolyte design.

In summary, embracing rather than avoiding redox activity in SEs could reshape the future of SSBs. By combining mechanistic insights with strategic materials design, redox-reversible SEs promise higher energy density, improved cycling stability, and major advances in next-generation batteries.

## Acknowledgments

J Y and F S are grateful to the German Federal Ministry of Research, Technology and Space (BMFTR) for funding within project MELLi (03XP0447). S G and F S acknowledge financial support from the Innovation Pool Automat, a project within the Helmholtz Research Program 'Materials and Technologies for the Energy Transition (MTET), Topic 2: Electrochemical Energy Storage.'

## Conflict of interest

The authors declare no conflict of interest.

## 10. Processing/large-scale manufacturing

*Shuo Wang* and Shu-Bo Wang*

School of Materials Science and Engineering, Wuhan University of Technology, Wuhan 430070, People's Republic of China

*E-mail: shuowang@whut.edu.cn

### Status

Preparation processes play a pivotal role in tailoring the crystal structure and ionic conductivity of SEs. In this chapter, the manufacturing methods for polymer, oxide, sulfide, and halide SEs, along with composite electrolyte membranes, are discussed (figure 15). Their merits and drawbacks are then analyzed, and a roadmap for future advancements in manufacturing processes is provided.

### Current and future challenges

For polymer electrolytes, a typical processing technique is the solution-casting method. First, a lithium salt is dissolved in a polar solvent, followed by the dissolution of the polymer. The homogeneous solution is then cast onto a substrate and evaporated to yield a freestanding polymer SE film [295]. This method is straightforward and amenable to large-scale continuous production. However, the utilization of toxic organic solvents raises environmental and safety concerns. Alternatively, for thermoplastic polymers such as polyethylene oxide (PEO), a solvent-free approach has been employed. This method typically involves the dry mixing of PEO and lithium salt powders—via ball milling or manual grinding—followed by hot pressing into a dense composite electrolyte film. This dry processing method eliminates the utilization of toxic solvents, making it more environmentally benign and time-efficient [296]. Nevertheless, it faces challenges in achieving continuous manufacturing compared to solution-casting processes.

For oxide SEs, the conventional solid-state reaction method is widely employed. Typical synthesis involves the stoichiometric weighing of precursor powders, such as $Li_2O$, $La_2O_3$, $ZrO_2$, and $Ta_2O_5$, with excess lithium salt to compensate for volatilization during high-temperature treatment. The mixture is then thoroughly homogenized via manual grinding or wet ball milling, followed by calcination in an alumina crucible at approximately 950 °C for 8 h. The resulting product is then reground, pressed into pellets, and sintered at 1150 °C–1200 °C to obtain dense $Li_{6.8}La_3Zr_{1.8}Ta_{0.2}O_{12}$ (LLZTO) ceramics, which typically exhibit a high ionic conductivity of 0.9 mS $cm^{-1}$ [297]. Similar procedures could also be used for the preparation of $Na_3Zr_2Si_2PO_{12}$ SEs.

Sulfide and halide SEs are highly sensitive to moisture, resulting in the degradation of ionic conductivity [298]. Therefore, they are typically synthesized and manufactured under an inert atmosphere. Based on their crystal structure, they can be broadly categorized into three primary types: glassy, glass-ceramic, and crystalline [19]. Glassy sulfides are primarily synthesized via melt quenching or high-energy ball milling. The melt-quenching process involves the following steps: initially, the precursors, such as $Li_2S$, $P_2S_5$, and $B_2S_3$, are dry mixed and then pressed into pellets. Subsequently, the pellets are placed in a carbon-coated quartz tube and heated to the molten state, followed by rapid cooling in ice water or liquid nitrogen to obtain glassy sulfide electrolytes with room-temperature ionic conductivities of approximately 0.1–1 mS $cm^{-1}$ [299]. However, this method is complex, time-consuming, and energy-intensive. Notably, the successful preparation of purely glassy halide electrolytes via melt quenching has not been reported to date.

High-energy ball milling is a popular technique for amorphizing sulfide and halide electrolytes through mechanical collisions at high rotational speeds, producing substantial heat and facilitating the formation of glassy SEs. The rotational speed and duration of ball milling significantly influence the phase composition and crystallinity of the final product. Only higher speeds promote the formation of glassy phases [300]. For example, ball milling of a mixture of $Li_2S$ and $P_2S_5$ in a 70:30 molar ratio at 500 rpm for 24 h yields the glassy sulfide electrolyte $70Li_2S{\cdot}30P_2S_5$ [19, 301]. Similarly, the glassy halide electrolyte $LiTaCl_6$ can also be obtained via high-energy ball milling [193]. Subsequent heat treatment of the glassy $70Li_2S{\cdot}30P_2S_5$ intermediates can produce glass-ceramic electrolytes containing $P_2S_7^{4-}$ or $PS_4^{3-}$ groups [301]. However, the ball-milling method suffers from poor batch-to-batch consistency, material adherence to container walls, time consumption, and limited scalability due to equipment size constraints.

The solid-state reaction method is commonly used to prepare crystalline sulfide SEs. The precursors are typically dry-mixed, pressed into pellets, sealed in a vacuum tube, and then annealed at high temperatures to obtain crystalline materials, such as LPSCl (3.4 mS $cm^{-1}$) [286], $Li_{5.5}PS_{4.5}Cl_{1.5}$ (8.4 mS $cm^{-1}$) [302], $Li_{5.5}PS_{4.5}Cl_{0.8}Br_{0.7}$ (9.6 mS $cm^{-1}$) [32], and $Li_2In_{1/3}Sc_{1/3}Cl_4$ (2 mS $cm^{-1}$) [303]. However, the high cost and size of quartz tubes impede large-scale production. Recently, Wang *et al* reported a scalable synthesis strategy for sulfide SEs, specifically LPSCB with a high ionic conductivity of 13 mS $cm^{-1}$, based on rapid mixing followed by heat treatment. This process enables the reproducible production of kg-scale batches and offers notable advantages in simplicity, making it suitable for mass production [56].

The liquid-phase method is also widely used for synthesizing sulfide/halide electrolytes. Preparation details are as follows: to begin with, the precursors are dissolved in a solvent. The solvent is then heated and stirred to facilitate reaction, followed by evaporation to yield an intermediate product. Finally, this intermediate is annealed to obtain the final SE [304]. Notably, this method enables the synthesis of several SEs that are challenging to prepare via traditional solid-state reaction routes, such as $Li_7P_2S_8I$ and $0.6LiI{\cdot}0.4Li_4SnS_4$ [305]. Similarly, halide electrolytes such as $Li_3InCl_6$ can be prepared by reacting LiCl and $InCl_3$ in water, followed by heat treatment at 200 °C for 4 h under vacuum [66]. Additionally,

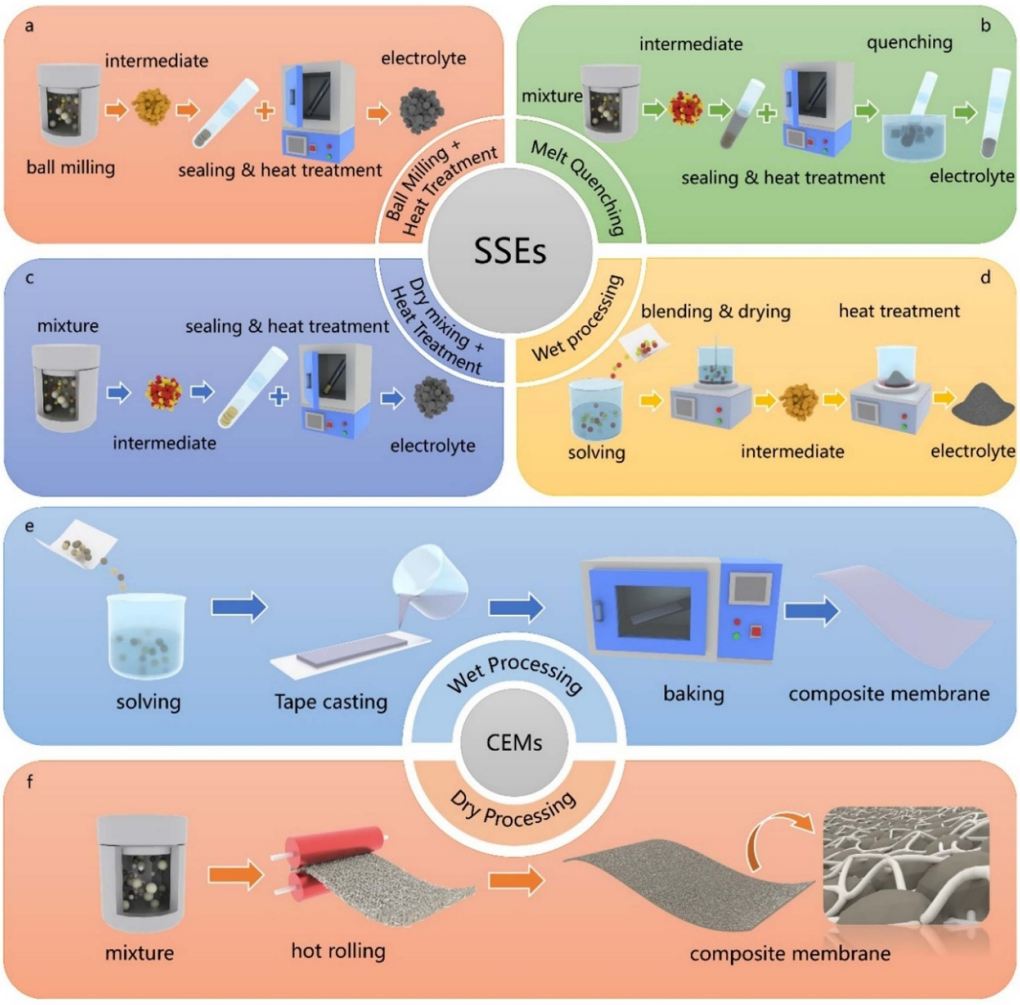


**Figure 15.** Methods used to prepare SEs, including (a) ball milling followed by heat treatment, (b) melt quenching, (c) dry mixing followed by heat treatment, and (d) wet processing. Methods used to process composite electrolyte membranes, including (e) wet and (f) dry processing.

using $NH_4Cl$ solutions, intermediates such as $(NH_4)_3[MCl_6]$ (M = Y, Sc, Er) can be obtained, which are subsequently converted to $Li_3MCl_6$ halide electrolytes [306].

Composite SEs are generally classified into two main categories: polymer-based composites incorporating inorganic fillers and inorganic-based composites with polymer additives. To produce polymer-based composite electrolytes, lithium salts and polymers are typically dissolved in a solvent. Then, a small amount of inorganic ceramic powder, such as inert $Al_2O_3$ or an ion-conductive oxide, sulfide, or halide electrolyte, is added to the solvent and stirred to achieve uniform dispersion. Finally, the slurry is tape cast and dried to produce a polymer-based composite electrolyte membrane. Currently, the ionic conductivity is relatively low, typically ranging from 0.1 to 1 mS $cm^{-1}$ [307]. To produce inorganic-based composite electrolyte membranes, the binder is first dissolved in a solvent, followed by the addition of a high fraction ($\geqslant$80 wt%) of inorganic SE. The mixture is then tape cast and dried to obtain an inorganic-based composite electrolyte film [308]. However, sulfide electrolytes are particularly sensitive to polar solvents and often undergo deleterious decomposition, significantly degrading ionic conductivity. Even in weakly polar and nonpolar solvents, the ionic conductivity of $Li_{5.5}PS_{4.5}Cl_{1.5}$ decreases from 10 to 6 mS $cm^{-1}$. When $Li_{5.5}PS_{4.5}Cl_{1.5}$ is used as the electrolyte, the ionic conductivity of the composite electrolyte film is typically around 1–3 mS $cm^{-1}$ [308].

To mitigate the conductivity loss of sulfide electrolytes during wet-film processing, dry-film processing techniques have attracted increasing attention. This method typically involves dry-mixing inorganic SEs with a polytetrafluoroethylene (PTFE) binder, followed by thermal rolling to fibrillate the PTFE, thereby forming a composite electrolyte membrane [309]. As an example, $Li_{5.4}PS_{4.4}Cl_{1.6}$ was dry-mixed with PTFE to obtain a composite film with a high ionic conductivity of 8.4 mS $cm^{-1}$ [309]. Due to the instability of halide electrolytes in solvents, they can even decompose in nonpolar solvents such as p-xylene, resulting in very low conductivity. Hence, halide-based composite membranes are also

commonly fabricated using PTFE as a binder via a dry process, resulting in, for example, a $Li_3InCl_6$-PTFE composite electrolyte membrane (1 mS $cm^{-1}$) [310]. However, PTFE-based composite membranes exhibit poor stability against lithium metal and are prone to decomposition, causing a sharp increase in electronic conductivity and leading to battery failure [309].

## Conclusions and future perspectives

For the manufacture of inorganic ceramic SEs, the solid-state high-temperature reaction method is more suitable for large-scale industrial production. In the future, more efforts should focus on optimizing the particle size distribution of SEs. The synthesis of ultrafine powders with particle size distributions ranging from tens to hundreds of nanometers is of great significance for increasing the active material loading and effective ionic conductivity of composite cathodes. Due to limitations in ball-milling capacity and the size of quartz tubes, it is also essential to develop new scalable production technologies for glass-type sulfide electrolytes. For sulfide-based composite electrolyte membranes, future work should prioritize optimizing the type and content of binders to enhance mechanical strength, reduce thickness, and maintain high room-temperature ionic conductivity. Regarding halide-based composite membranes, improving the solvent resistance of halides and selecting appropriate solvents are critical for enabling the large-scale, liquid-phase processing of halide-based composite films.

## Acknowledgments

S W acknowledges the Natural Science Foundation of China (Grant Number 52302305) and the Natural Science Foundation Exploration Program of Wuhan (Morning Light Plan) (Grant Number 202401jc0089).

## Conflict of interest

The authors declare no competing interests.

## 11. Outlook for high-throughput and ML-guided synthesis of SEs

*Eric McCalla**

Department of Chemistry, McGill University, Montreal, Canada

*E-mail: eric.mccalla@mcgill.ca

### Status

High-throughput experiments have long been utilized to optimize various components in modern rechargeable batteries. Early efforts by Dahn's group, for example, focused on thin-film anodes, where combinatorial sputtering was used to synthesize a variety of materials at once, and an electrochemical cell that could test 64 materials simultaneously was used for battery testing [311, 312]. The first attempts to use high-throughput experiments for SEs also involved thin-film synthesis. Here, perovskites were tested as interlayers between the SE and the cathode materials [313, 314]. These studies involved the mapping of ionic conductivity across varied compositions, but they were limited to compositions easily explored via thin-film deposition techniques and did not consider other necessary properties for SEs.

The all-solid electrolytes discussed so far in this roadmap have undergone a significant amount of research and development primarily aimed at optimizing ionic conductivity. This has resulted in quite complex compositions (e.g. garnet oxide SEs typically consist of four or more metals plus oxygen) and thus reside in highly underexplored composition spaces. Furthermore, a very limited amount of research has attempted to systematically screen such materials while determining the multitude of properties required to make a viable SE. Thus, it has become imperative to develop accelerated synthesis systems that can create samples using traditional synthesis routes (e.g. solid-state, co-precipitation, and sol-gel), so as to avoid being limited solely to compositions accessible by thin-film deposition techniques. Beyond synthesis, the new workflows must be effective in determining not only ionic conductivity but also electronic conductivity, the electrochemical stability window, chemical stability with metallic anodes, mechanical compatibility with electrodes, etc. Thus, it is essential that all relevant characterization tools keep up with synthesis without introducing bottlenecks.

The current push toward accelerating SE design revolves around a combination of automation and ML to guide experiments. Some fully automated systems exist, such as the A-lab at Berkeley, but these systems are currently limited to x-ray diffraction [315]. To date, these workflows have not screened electrolyte properties, and developing this aspect remains an important objective for fully automated battery material development. In contrast, some semiautomated systems that can screen electrolyte properties have been developed. Figure 16 illustrates the workflow in the McCalla lab, where a researcher can synthesize about 1500 materials per year while determining structures and key electrolyte properties [316, 317]. The group has used this system to develop SEs for both Li and Na batteries, including oxide ceramics, glasses, glass-ceramic composites, and ceramic-ionic liquid composites [317–319]. So far, the throughputs of both approaches (fully and semi-automated) are comparable for moderate group sizes (>10 000 samples/year) [320], though progress is certainly still being made in this regard. In both the fully automated and semiautomated cases, the use of ML is proving highly effective in closing the design loop and reducing the number of samples that need to be made in any given composition space [321].

In this chapter, I focus on further progress required to address challenges encountered in accelerating SE development by harnessing both high-throughput experiments and ML to explore complex compositions more efficiently.

### Current and future challenges

Both the fully and semiautomated systems discussed in the previous section are currently being used to effectively explore oxide materials. For example, the A-lab has been used to synthesize 41 materials that were previously only studied computationally out of a list of 58 attempted targets [315]. The McCalla lab, by contrast, optimizes previously known materials and has studied the impact of a huge list of dopants (>60) in promising oxide electrolytes [322]. This approach has yielded improvements in the key intrinsic properties needed for SEs (e.g. [322]). There is also no obvious limit to the level of complexity of the material that can be screened. For example, hybrid ceramic oxide/liquid electrolyte composites are currently of high interest in the literature and in industry due to their potential to yield viable oxide-based electrolytes [323]. Such materials could easily be studied using the methods developed previously for a ceramic–ionic liquid composite [319].

ML algorithms certainly continue to develop, but current tools seem sufficient to dramatically reduce the number of samples that need to be produced. For cathodes, we have recently been successful in screening triple doping (15 million combinations) using only about 1000 samples when guided by ML pretrained on the materials project as described in [324]. This success is due in part to the fact that it is acceptable to have numerous failures when each batch of samples contains 64 materials; there is no need for ML algorithms to be error-free. There is therefore no obstacle to ML being of immediate use to any accelerated experimental platform. In contrast, when computations/ML are used on their own with only low-throughput experimentation, there is a tendency to narrow down the candidate list extremely aggressively to match the low experimental throughput, and the result can be over-screening (e.g. the study described in [278] down-selected the candidate list from >20 000 to 1 candidate without experimental data). There is also a current lack of computational tools that can calculate all the intrinsic properties needed to make viable electrolytes.

In regard to using accelerated materials platforms for SE development, there remain two important capabilities that need to be developed. The first is the ability to perform

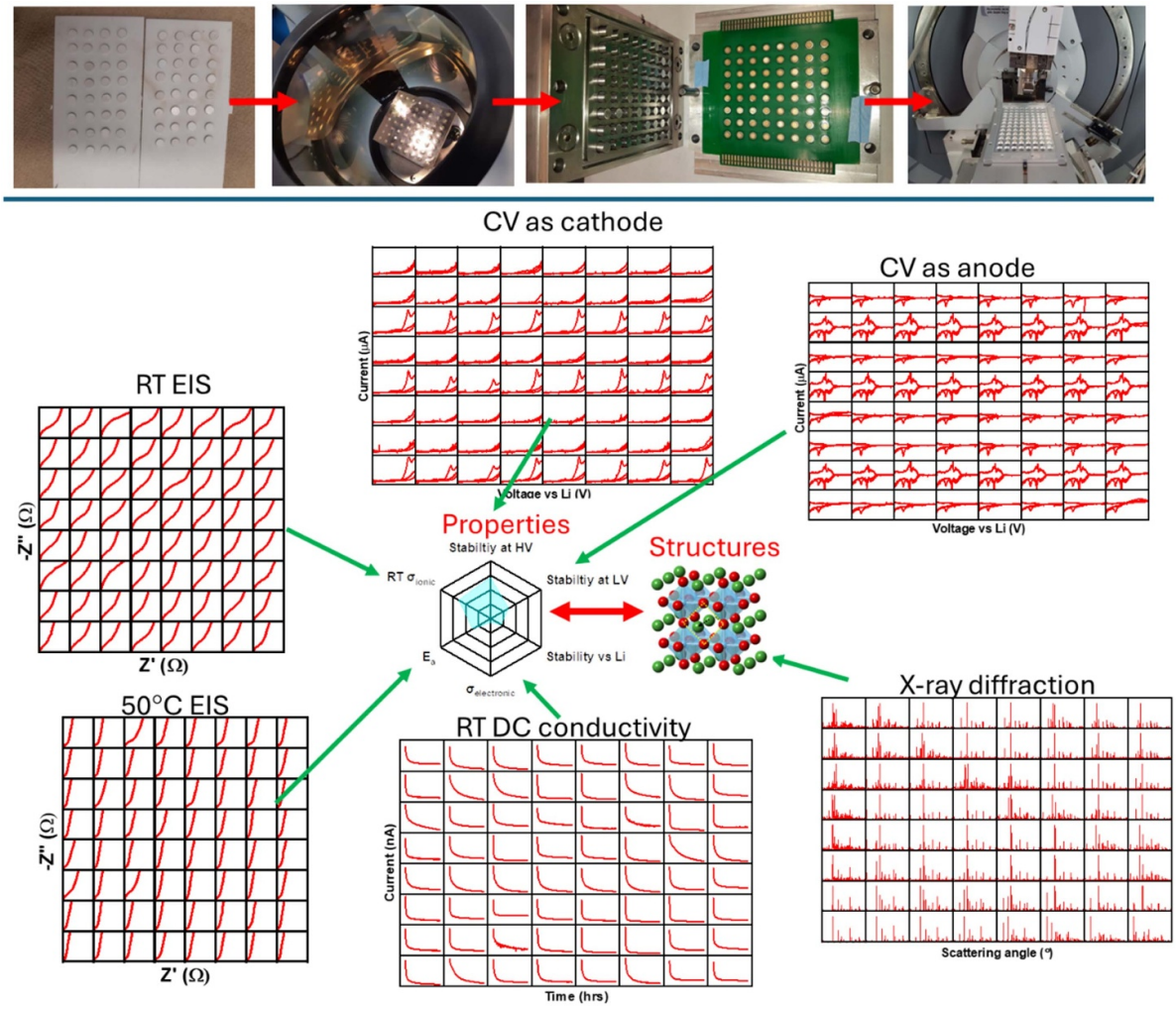


**Figure 16.** Top: pictures of key steps in the combinatorial screening of SEs, showing pellets, gold coating, an EIS cell with spring-mounted contacts, and automated x-ray diffraction. Bottom: resulting data used to generate high-throughput radar plots of key electrolyte properties. Reproduced from [316]. © 2022 The Electrochemical Society (ECS). Published on behalf of ECS by IOP. All rights reserved.

syntheses under entirely inert atmospheres. A number of chapters in this roadmap focus on materials that are inherently unstable in air, as even low moisture levels are sufficient to degrade them rapidly. In such cases, the experimental workflows utilized must exclusively employ inert atmospheres. While this is nontrivial to implement in high-throughput environments, a few groups are in the process of doing this. The McCalla group, for example, has connected a tube furnace to a glove box that has a gold coater in it, and this now permits us to make competitive halide materials on the combinatorial scale, though the throughput is not as high as for air-stable workflows [325, 326]. There are also efforts underway to establish an A-lab 2.0, which would have an inert atmosphere workflow for fully automated synthesis/XRD without compromising on throughput [327].

The second required innovation is the ability to test fully solid batteries in high-throughput workflows. It is certainly useful to determine a variety of intrinsic properties, but at some point, the electrolyte needs to be designed with particular cathodes and anodes in mind. Thus, the preparation of electrolyte/cathode composites needs to be developed for high-throughput workflows. Importantly, metallic anodes need to be deposited from a melt or vapor in such a way that they overcome interfacial resistance. This would enable effective high-throughput critical current density (CCD) testing, which to date has not occurred except on a down-selection of materials [318]. There is also a very important concern regarding reproducibility here. QuantumScape has recently published a combinatorial CCD study, where they measured the CCD of the same sample many times by depositing numerous Li contacts via vapor deposition. The results show a very large variation in the CCD values obtained, such that at certain currents, only a small fraction of cells failed; this means that to ensure there are no failures at a certain current, many measurements must be performed [328]. This raises serious concerns about the maximum throughput achievable in CCD measurements, given that a single measurement of each sample might be insufficient. Presumably, similar variations would occur in full solid

batteries, such that efforts must be made to develop approaches that either reduce the variability or obtain meaningful values despite the variability.

## Conclusions and future perspectives

Accelerated testing is enabling broader exploration of potential SEs, but the progression toward the screening of all necessary properties must continue. This will enable rapid development of each of the oxides, sulfides, halides, and hybrids/composites, as well as other emerging candidates. Efficiently tuning the properties of promising materials can be enhanced by coupling experiments with ML. Such workflows are not overly costly, especially if automation is only used when required [320]. This will be especially true moving forward, as the cost of automation will continue to decrease. This will lead to a situation where there are no longer just a few select labs that can do this, but the tools will become more widely accessible and enable a greater democratization of high-throughput research. ML-driven accelerated experimental approaches are poised to become game-changers in applications such as SSBs, where there is a high degree of device complexity.

## Acknowledgment

The author acknowledges support from the Natural Sciences and Engineering Research Council of Canada under the auspices of a Discovery Grant.

## Conflict of interest

The author declares no conflict of interest.

## 12. Advanced *operando* investigation of SSBs

*Benjamin Mercier-Guyon, Ove Korjus, Patrice Perrenot and Claire Villevieille**

Université Grenoble Alpes, Université Savoie Mont Blanc, CNRS, Grenoble INP, LEPMI, 38000 Grenoble, France

*E-mail: claire.villevieille@grenoble-inp.fr

### Status

SSBs are widely regarded as one of the most promising candidates for the next generation of electrochemical energy storage systems. However, realizing this vision requires overcoming several critical challenges, particularly those associated with ionic and electronic transport properties within solid matrices. To accelerate progress in this field, *operando* techniques have emerged as a powerful approach, providing excellent insight into the fundamental processes that govern battery performance. Unlike *ex situ* approaches, which only offer snapshots before or after cycling, *operando*-based investigations allow real-time monitoring of structural, chemical, and mechanical changes occurring within the cell. This capability is essential to identify degradation pathways, interfacial instabilities, and failure mechanisms that ultimately determine device lifetime and efficiency [329, 330]. A wide range of experimental techniques is now available to probe reaction mechanisms in SSBs. These techniques can be broadly classified into two categories. The first encompasses bulk-sensitive methods, such as x-ray and neutron scattering, which provide information on structural evolution, phase transitions, and lattice dynamics within electrolyte and electrode materials. The second category focuses on microstructural investigations, often achieved through advanced imaging approaches (e.g. tomography and electron microscopy), which reveal morphological changes, grain connectivity, and interfacial degradation at different length scales. Together, these complementary methods enable a multiscale understanding of transport phenomena and degradation processes, paving the way toward rational design strategies for improved solid-state systems.

*Operando* imaging has emerged as a transformative approach for probing electrochemical systems, enabling real-time observation of morphological evolution under realistic operating conditions. By minimizing artifacts typically introduced by sample preparation (mechanical fracture, air exposure) and *postmortem* cell relaxation, this methodology provides a more accurate and faithful representation of the system's behavior.

*Operando* imaging is primarily confined to synchrotron x-ray facilities, whose high-brilliance sources allow rapid and noninvasive investigations of the majority of battery systems. Despite inherent challenges in detecting lithium with x-rays due to its low electron density, significant studies have successfully captured the formation and growth of lithium dendrites under *operando* conditions, unveiling the origin of short-circuiting in SSBs (figures 17(a) and (b)) [331, 332]. In contrast, neutron imaging exhibits remarkable sensitivity to $^{6}$Li, and recent advances in brighter neutron sources have enabled *operando* $^{6}$Li tracking and the visualization of lithium concentration evolution. Studies have revealed ionic networks as critical bottlenecks both in separators and in thick solid-state composite electrodes, although $^{6}$Li spontaneous isotopic diffusion affecting quantification is often overlooked [333, 334]. However, the limited neutron flux currently available precludes 3D *operando* imaging without stopping the cycling and relaxing the system. In addition, due to the miniaturization of materials within the new-generation battery systems, both large-scale facilities lack investigations at the nanoscale (x-ray synchrotrons are limited to a resolution of 50 nm, and neutron sources are limited to a few micrometers).

Unlike organic liquid electrolytes, whose formulation has to be modified to meet the requirements of the imaging techniques, SSBs permit realistic and meaningful investigations via electron microscopy. *Operando* SEM [336, 337] and TEM [338] have already provided critical insights into interfacial evolution and failure mechanisms. Although *operando* SEM has enabled substantial progress, a major limitation remains: the buried nature of critical electrochemically active interfaces, which are often inaccessible in conventional setups. In this context, *operando* FIB (focused ion beam)-SEM is emerging as a promising technique. By uniting advanced electron-based imaging with site-specific milling, FIB-SEM offers the capability to reconstruct 3D morphologies at nanometer resolution while simultaneously probing electrochemically relevant interfaces (figures 17(c) and (d)) [335].

Scattering measurements can help identify crystalline phase evolution occurring during cycling at the electrolyte and composite electrode levels. Ideally, the measurement should be performed *operando* to ensure that the dynamics of the processes is maintained, giving a real vision of the degradation processes [339–341]. Neutron powder diffraction (NPD) is particularly valuable for studying Li–ion batteries, both *operando* and *ex situ*, because it enables the determination of the positions and site occupancies of light elements, such as lithium. It also allows for a clear differentiation between transition metals (e.g. Fe, Ni, Co, and Mn), which is often challenging with x-ray diffraction. Numerous *operando* cell designs have been developed for liquid electrolyte systems [342–344], but for SSBs, the cell design is more complex, as it must maintain sufficient pressure to allow cycling of thick electrodes—necessary due to the high mass loading required for neutron measurements. Despite these challenges, this remains a rapidly expanding field, with new SSB cell designs under active development (figure 18(a)) [340].

In contrast to neutrons, which have weak interactions (neutrons/matter), synchrotron x-ray diffraction (s-XRD) offers several advantages for *operando* studies. First, due to its significantly higher flux (compared to neutrons), s-XRD enables measurements on samples with very low mass loading. Second, s-XRD allows for depth profiling, enabling the investigation of inhomogeneities across electrodes during cycling. Several research groups have used this technique to reveal nonuniform lithiation within electrodes and the formation of lithiation gradients during cycling (figure 18(b)) [345, 347]. Li *et al* [347] demonstrated that in thick $LiNi_{0.8}Mn_{0.1}Co_{0.1}O_2$

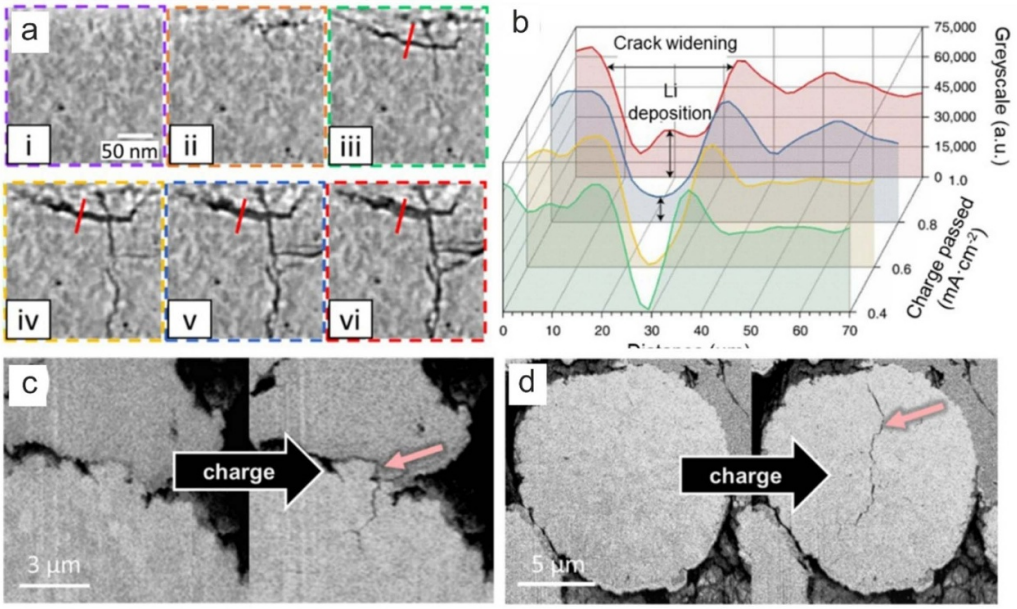


**Figure 17.** (a) *In situ* phase-contrast X-ray computed tomography (XCT) of virtual cross-sections during a single plating event in a Li|LPSCl|Li cell; (b) analysis of lithium deposition showing that cracks propagate ahead of Li. (a), (b) Reproduced from [332] with permission from Springer Nature. *Operando* focused ion beam (FIB)-SEM cross-section of a composite containing $LiNi_{0.6}Mn_{0.2}Co_{0.2}O_2$ (NMC622) and amorphous $Li_3PS_4$ (LPS), highlighting (c) decohesion of the active material from the ionic network and (d) intergranular fracturing of the polycrystalline active material. (c), (d) Reprinted (adapted) with permission from [335]. Copyright (2024) American Chemical Society.

(NMC811) electrodes, localized charging can occur even during the electrode discharging process.

Combining techniques such as three-dimensionally resolved x-ray diffraction computed tomography (XRD-CT) [346, 348, 349] and x-ray microdiffraction imaging [350, 351] can shed light on novel processes. XRD-CT has already been widely applied, primarily for phase identification and quantification. Multiple *ex situ* XRD-CT studies have been used to investigate decomposition products formed during cycling. For example, Villevieille *et al* [352] demonstrated that LPSCl undergoes partial decomposition throughout the entire electrolyte during cycling, producing LiCl and $Li_2S$. Similarly, Hu *et al* [348] revealed the formation of local stress hotspots in LPSCl electrolytes during both cycling and cell fabrication. Despite these advances, XRD-CT is less frequently employed for full Rietveld refinement in SSB studies due to technique-related artifacts. Furthermore, long measurement times limit its widespread application in *operando* investigations. Sottmann *et al* [346] conducted *operando* XRD-CT (figure 18(c)) on liquid sodium-ion batteries, illustrating its potential for broader application, including future studies on SSBs.

## Current and future challenges

Several critical issues must still be addressed before the full potential of advanced characterization techniques can be exploited for SSB research. The first challenge relates to the design of the electrochemical cells used in the literature. In the absence of standardized protocols, it is nearly impossible to make meaningful comparisons between studies [353]. One of the main sources of discrepancy lies in the applied pressure. Since the pressure applied to the different cell components is rarely controlled or reported, the observed decomposition pathways and interfacial reactions can vary drastically from one study to another.

Ohno *et al* highlighted this issue by comparing ionic conductivities from different research groups working on the same standardized material [36]. This discrepancy is largely attributed to differences in measurement setups. Based on these considerations, several groups have proposed innovative configurations to better control the pressure applied to the stack during measurements and cycling tests. For example, the study by Chen *et al* [354] suggests using a liquid medium to apply pressure to the stack, rather than a solid medium, as is generally the case in compression devices. Lee *et al* [355] used a variable-height compression device employing springs. As a result, after the initial pressure was set, volume changes in the active material during lithiation and delithiation no longer affected the pressure applied to the stack.

A second limitation concerns the mass loading of the electrodes employed. Many reports suggest that the loading is far from realistic values typically required for practical applications. This not only affects the electrochemical performance of the cell but can also lead to misinterpretations, for instance, regarding the presence or absence of concentration gradients within the electrode. The third issue arises from beam-induced damage during *operando* or *in situ* experiments. High-intensity x-ray and neutron beams can trigger unwanted side reactions, alter interfacial chemistry, or modify

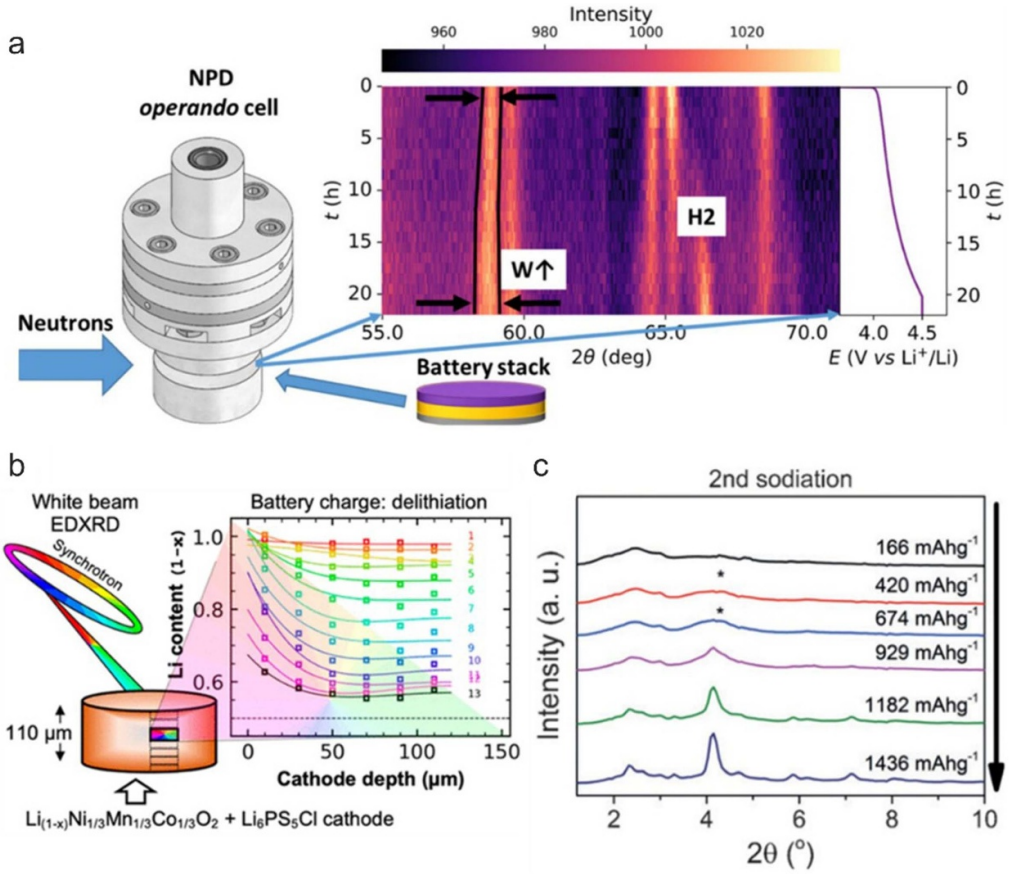


**Figure 18.** (a) *Operando* TiZr NPD during the charging of $LiNi_{0.5}Mn_{0.3}Co_{0.2}O_2$ (NMC532), showing the broadening of NMC532 reflections and the formation of the $H_2$ phase. Reprinted with permission from [340]. Copyright (2025) American Chemical Society. (b) Depth-resolved *operando* XRD of an $LiNi_{0.33}Mn_{0.33}Co_{0.33}O_2$ (NMC111) electrode at a synchrotron, revealing the development of a de-lithiation gradient. Reproduced from [345]. CC BY 4.0. (c) Reconstructed XRD-CT data from a single voxel ($1.2 \times 1.2\ \mu m^2$) in a $Na_3P$ electrode during *operando* sodiation. The asterisks denote P nanoparticles [346]. John Wiley & Sons. © 2017 Wiley-VCH Verlag GmbH & Co. KGaA, Weinheim.

microstructures, thereby biasing the conclusions drawn from the data. Addressing these limitations requires the development of new cell designs that combine several key features: the application of controlled and reproducible pressure, the use of electrodes with realistic (high) mass loadings, and the development of mitigation strategies to minimize beam-induced artifacts. Establishing such standardized protocols will be essential to generate reliable, comparable, and application-relevant insights into the mechanisms that govern SSBs.

## Acknowledgment

ANR Grant OpInsolid is acknowledged for its financial support for this work, as well as PEPR Batteries, France Relance 20230, and the Openstorm project.

## Conflict of interest

The author declares no conflict of interest.

## 13. NMR—a key that unlocks defect structure and dynamics in emerging SEs

*H Martin R Wilkening*

Institute of Chemistry and Technology of Materials, Stremayrgasse 9, Graz University of Technology, 8010 Graz, Austria

*E-mail: wilkening@tugraz.at

### Status

The SE, either as a ceramic or a hybrid material composed of ceramics and polymers, is a central component in all-solid-state and quasi-solid-state batteries, ensuring efficient transport of charge carriers between the two electrochemically active compartments. NMR spectroscopy [356, 357] is exceptionally well-suited to investigate local structural environments using high-resolution techniques, such as fast magic angle spinning (MAS). NMR has been employed not only to identify the structural motifs associated with spin-active charge carriers (e.g. $^{6}$Li, $^{7}$Li, $^{23}$Na, $^{19}$F, and $^{17}$O) but also to probe the local coordination geometry of framework elements in SEs (e.g. $^{31}$P, $^{19}$F, $^{119}$Sn, $^{11}$B, $^{29}$Si, and $^{27}$Al). Such site-specific information, derived from chemical shifts, anisotropies, and coupling constants, is essential for elucidating both the typical and defect structures of emerging (electrolyte) materials [356]. In addition, NMR can detect structural disorder, polymorphs, and local phase heterogeneity, providing insight into how these variations influence ionic mobility and overall electrolyte performance [358]. When combined with complementary methods, such as diffraction and scattering, NMR contributes to a comprehensive understanding of structure–dynamics relationships, which are critical for advancing electrolyte design [27, 359].

To investigate ion dynamics, NMR offers a uniquely versatile set of techniques capable of noninvasively probing ionic motion over an exceptionally broad timescale, spanning, in some cases, more than ten orders of magnitude. Figure 19 provides an overview of the various NMR methods [360–363] that can quantify microscopic jump rates and macroscopic diffusion coefficients.

These results can be directly compared with dynamic parameters obtained from complementary nuclear and nonnuclear techniques, enabling a comprehensive understanding of ion transport processes. Furthermore, NMR-derived jump rates and site occupancies can serve as benchmarks for computational models and molecular dynamics simulations, providing a quantitative link between experiments and theory [364, 365].

In recent years, time-domain and high-resolution $^{7}$Li and $^{23}$Na NMR measurements have been employed to investigate sequentially activated diffusion processes in some of the most prominent SEs, including LGPS-type compounds [365], argyrodite materials [359, 362, 366, 367], and $LiTi_2(PS_4)_3$ (LTPS) [368]. The results from the latter are exemplarily shown in figure 20. Future studies will aim to deepen our understanding of how local defect structures influence both short-range and long-range ionic dynamics, within the bulk and particularly in interfacial regions, i.e. in the contact zones between the SE and the electrochemically active materials.

### Current and future challenges

The properties of SEs are highly sensitive to structural, compositional, and processing factors, which can strongly influence both short- and long-range ion transport [369]. Even slight variations in preparation conditions, such as small changes in composition, annealing, or calcination protocols, can strongly affect the transport parameters of an SE. Even if long-range transport remains essentially unchanged, the elementary jump processes that govern ion dynamics on shorter length scales may be significantly altered. NMR, depending on the temperature and frequency window chosen for relaxation-rate measurements, can probe both regimes: short-range motion and long-range transport. This makes it a powerful tool for unraveling the impact of defect structures that emerge from different preparation conditions [370]. The next step would be to benchmark such findings against commercially available electrolytes to assess their quality in terms of ionic transport properties [371].

In general, the strength of NMR lies in its ability to provide not only average transport parameters but also site-specific information on dynamic processes [372]. Future studies may therefore apply high-resolution techniques, such as 2D exchange spectroscopy, to identify energetically favored diffusion steps and exchange mechanisms. For very fast ion conductors, such methods must be carried out at sufficiently low temperatures, as 2D NMR is most sensitive to slow exchange processes. At higher temperatures, coalescence effects may obscure the off-diagonal cross-peaks that encode this site-specific information. A limitation arises from the narrow chemical shift range of $^{6}$Li, the preferred isotope for these experiments, since second-order quadrupolar effects are largely suppressed. In diamagnetic materials, this range may be insufficient to resolve the relevant processes. In contrast, in materials containing moderate concentrations of paramagnetic centers [373], hyperfine (Fermi contact) interactions provide enhanced spectral separation, provided that longitudinal relaxation times remain long enough. Such studies require low magnetic fields and fast magic-angle spinning, a combination that has been available for many years. For diamagnetic electrolytes, extending both the frequency and temperature ranges [365] will be crucial to capture the various diffusion steps of charge carriers across different material classes, including oxides, sulfides, thiophosphates, halides, and hydrides [374].

As already noted, understanding degradation processes at macroscopic interfaces in all-solid-state batteries poses a further challenge for NMR spectroscopy. *Operando* and *in situ* studies are often limited by low spin densities in interfacial regions, leading to weak NMR signals. Polarization transfer methods are expected to help overcome this limitation [375]. An early approach is $\beta$-NMR, where the polarization of the $^{8}$Li isotope, generated, for example, after neutron capture, is independent of the Boltzmann factor [376]; other approaches

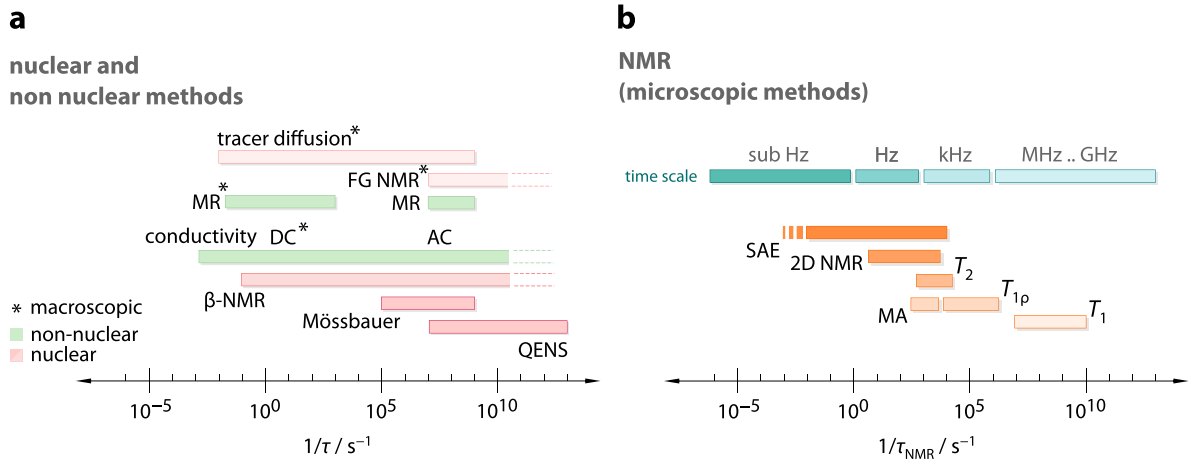


**Figure 19.** (a) Overview of nuclear and nonnuclear methods used to probe diffusion properties, along with the characteristic timescales over which they are sensitive (FG NMR: field-gradient NMR; QENS: quasi-elastic neutron scattering; MR: mechanical relaxation; DC, AC: direct-current and alternating-current measurements). (b) Selected NMR techniques (time-domain and high-resolution 2D NMR) and their respective timescales spanning a dynamic window from the subhertz regime to the gigahertz regime (SAE: spin-alignment echo NMR; MA: motional averaging of NMR lines; $T_{1(\rho),2}$ relaxation NMR methods). Reproduced from [362]. CC BY 4.0.

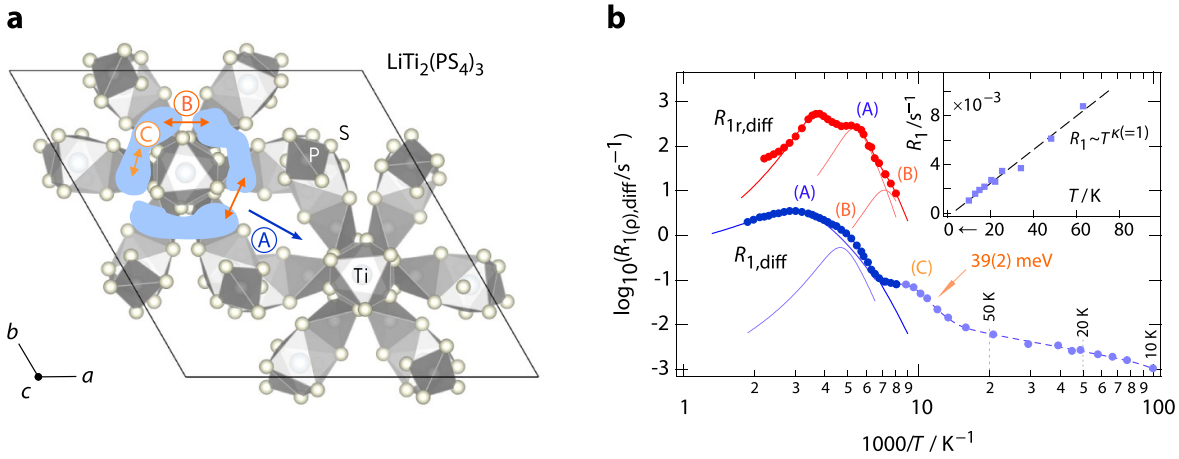


**Figure 20.** (a) Crystal structure of $LiTi_2(PS_4)_3$, a fast ionic conductor, showing several $Li^+$ diffusion pathways: strictly localized motions within pocket-like regions (C), interpocket jumps (B), and inter-ring hopping (A). The latter is the rate-determining step that governs long-range ion transport. (b) Using $^7$Li NMR relaxation rate $R_1 = 1/T_1(1/T)$ measurements, these processes can be studied separately, provided a sufficiently wide temperature range is accessible. For example, fast intrapocket motions are characterized by an activation energy of only 0.04 eV and give rise to peak C, observed at temperatures as low as $T \approx 100$ K. At even lower temperatures, the relaxation rate enters a regime $R_1 \sim T^{\kappa=1}$, where it is dominated by coupling to conduction electrons. Reproduced from [368]. CC BY 4.0.

benefit from ion-implantation methods [377, 378]. Similar sensitivity issues arise when studying microscopic interfacial dynamics in hybrid electrolytes [379, 380] that combine polymer and ceramic phases. In these cases, signal-enhanced NMR can provide key insights not only into ion dynamics but also into the local environments of Li ions at interfaces. Nanocrystalline materials, with their high fraction of interfacial regions (thicknesses on the order of ∼2 nm), already provide sufficiently high spin densities to be probed by NMR [381–384]. Alternatively, ion dynamics in interfacial regions may be studied by suitable *ex situ* measurements, provided that larger samples can be prepared to mimic *operando* conditions [385].

Finally, care must be taken when interpreting *in situ* or *operando* NMR experiments carried out under strong external magnetic fields [386], as these fields can influence the formation of metallic Li phases compared to cells cycled in zero-field conditions. In such cases, *ex situ* high-resolution measurements, taking into account and overcoming NMR skin effects, remain an indispensable complement.

## Conclusions and future perspectives

NMR, widely used in medicine, life sciences, and materials research, is also an indispensable tool in battery science due to the excellent NMR receptivity of key charge carriers, such as $Li^+$ and $Na^+$. Their nuclear spin interactions with local magnetic and electric fields enable detailed characterization of atomic-scale structures and dynamic processes.

In the study of ion dynamics, future research should move beyond measuring the average transport behavior toward probing individual ion hopping events [368]. In particular, the investigation of rotational–translational couplings remains an important research area for fundamentally understanding interrelation effects in electrolytes with polyanion host frameworks [387, 388].

In battery devices, *operando* and *in situ* NMR [375, 389, 390], even under MAS conditions [391], will be crucial for visualizing local structural changes, particularly those associated with degradation mechanisms, and for tracking the corresponding dynamics at interfaces. Importantly, NMR can directly detect the formation of Li metal, enabling monitoring of dendrite growth under operating conditions [392–394]. However, because interfacial regions often contain only a small number of NMR-active nuclei, achieving sufficient signal intensity remains a significant challenge. Advanced methods for enhancing spectral resolution and NMR sensitivity [375, 390] will therefore be essential for future studies aiming to understand the diverse interfacial phenomena in all-solid-state batteries. Emerging NMR approaches [356], such as ultrafast MAS, multinuclear correlation experiments, and particularly dynamic nuclear polarization [390, 394], are expected to enable the study of dilute nuclei not only at interfaces but also in low-abundance phases. Combined with time-domain relaxation rate measurements across broad frequency and temperature ranges [368], these techniques will allow detailed mapping of ion dynamics over multiple timescales. Together, these advances promise to extend the reach of NMR, providing deeper insight into both bulk and interfacial transport processes in SEs.

## Acknowledgment

Financial support from the Deutsche Forschungsgemeinschaft (DFG) is highly appreciated (former Research Unit 1277 (molife)).

## Conflict of interest

The author declares no conflict of interest.

## 14. Recycling of SEs in SSBs

*Kerstin Wissel* and Oliver Clemens**

University of Stuttgart, Institute for Materials Science, Heisenbergstr. 3, 70569 Stuttgart, Germany

*E-mail: oliver.clemens@imw.uni-stuttgart.de
and kerstin.wissel@imw.unistuttgart.de

### Status

The recycling of SSBs represents a more recent area of research compared to the recycling of conventional LIBs. Recent studies are beginning to address specific challenges associated with the diverse cell formats and material combinations used. SSBs employ SEs, such as oxides, sulfides, halides, or polymers, and often incorporate lithium metal anodes; in this respect, they differ from LIBs. These components improve performance; however, they also complicate end-of-life processing due to their reactivity and limited recyclability when applying procedures initially designed for conventional LIBs.

The recycling of conventional LIBs generally utilizes pyrometallurgical and hydrometallurgical methods to recover critical elements (e.g. lithium, cobalt, and nickel) [395, 396]. Recovering these metals using pyrometallurgy requires high temperatures and reducing atmospheres. Hydrometallurgical recycling uses aqueous solution chemistry to dissolve battery materials, enabling the selective extraction of individual elements via solvent extraction and precipitation. These processes are effective; however, they are energy-intensive, require complete material decomposition, and involve complex resynthesis. Direct recycling serves as an alternative approach for the recovery and regeneration of functional battery components; nevertheless, research in this area remains in its early stages [397]. This approach preserves the structure and chemistry of the original materials, potentially reducing energy consumption and processing costs compared to other strategies. Recycling processes typically involve additional mechanical pretreatment steps for battery disassembly and separation into recoverable fractions (e.g. black mass, current collectors, housings).

To adapt these methods for the recycling of SSBs, it is necessary to address material-specific challenges, specifically the handling of (partially) sensitive SEs and the safe recovery of lithium metal. Mechanical separation is challenging due to strong interfacial bonding (e.g. separating adhesive lithium metal and (intermixed) SEs from other cell components is not easy). Moreover, electrolyte-specific strategies are necessary due to the diverse chemical and physical properties of different SE classes.

So far, most research into SSB recycling has been theoretical or conceptual. Experimental studies are scarce and often concentrate on simplified material systems with varying levels of compositional complexity instead of full cells. Consequently, extensive research and development remain necessary to establish scalable and economically viable recycling methods for SSBs.


**Figure 21.** Future challenges for the recycling of solid-state batteries.

### Current and future challenges

Despite recent progress in developing recycling strategies for SSBs, numerous significant challenges persist that hinder the implementation of these strategies. The next section addresses these challenges and introduces strategies related to different types of SEs. In addition, future challenges are discussed (figure 21).

For oxidic SSBs based on, for example, garnet-type (e.g. $Li_7La_3Zr_2O_{12}$), NASICON-type (e.g. $Li_{1+x}Al_xTi_{2-x}(PO_4)_3$), or perovskite-type (e.g. $Li_{3x}La_{2/3-x}TiO_3$) SEs, pyrometallurgical processes are only partially suitable, as they may cause redistribution of chemical elements and formation of undesired, thermodynamically stable phases, particularly when dealing with complex material mixtures of different electrolytes and electrode materials [398]. Hydrometallurgical approaches possess greater potential and are also essential for further processing of slags produced during pyrometallurgy. Materials can be either completely or selectively dissolved [399, 400]. Lithium can be recovered, for example, by supercritical $CO_2$ extraction [401]. Direct recycling methods for relithiation may be based on solid-state reactions or hydrothermal processes [402].

The main challenge in recycling SSBs that utilize sulfides and thiophosphates as SEs is that they are unstable upon exposure to air or humidity. To mitigate safety hazards and prevent electrolyte degradation, handling in dry rooms or under inert atmospheres is required. Consequently, pyrometallurgical and hydrometallurgical processes are unsuitable. However, due to their high solubility in organic solvents, solvent-based separation methods, including dissolution followed by recrystallization, are a promising alternative. This strategy has been investigated for separating argyrodite-type $Li_6PS_5X$ (X = Cl, Br, I) [403, 404] and $\beta$-$Li_3PS_4$ [405] from different transition-metal

oxide electrode materials using solvents such as ethanol and N-methylformamide. The dissolved electrolytes may chemically interact with other components of the battery, particularly electrode active materials [404, 405]. This suggests that electrode materials may require further purification or treatment via hydrometallurgy. Further investigations are required to determine the compatibility of these solvent-based methods when using lithium metal. Solvent-based methods, as well as thermal and mechanochemical treatments, provide approaches for the (direct) resynthesis or reconditioning of deteriorated SEs through relithiation [406].

For halide-based SSBs, the same concerns regarding moisture sensitivity apply; thus, processing in a dry environment is just as crucial. Halide and sulfide SEs share many similarities regarding recycling, resynthesis, and reconditioning. For example, for $Li_3InCl_6$, the concept of a solvent-based separation technique using a solvent as simple as water can be applied. This is due to the SE's ability to reversibly convert between its hydrated and dehydrated forms after dissolution [66]. However, side reactions that degrade both the SE and active materials may occur [407].

To process polymer SSBs, solvent-based dissolution can also be employed to effectively separate polymers and active materials [408]. As both the polymers and conducting lithium salts decompose at relatively low temperatures, conventional high-temperature approaches are unsuitable due to the formation of hazardous byproducts and significant material loss [409]. Hydrometallurgical recycling of other battery components can be significantly hindered by any polymer impurities [410]. Furthermore, the low cost of polymeric SEs is a major problem from an economic point of view when considering recycling, requiring processes to be cost-effective and energy-efficient.

As SSBs approach commercial readiness, recycling strategies must be significantly improved to address the increasing complexity and diversity of next-generation battery systems. Implementing techniques that perform well in optimal laboratory conditions is often inadequate when applied to 'real-world' cell architectures, which typically contain various SEs and lithium metal anodes and feature tightly integrated designs. Thus, the scaling-up of recycling requires solutions that meet higher demands for process robustness and safety. In this context, translating promising lab-scale techniques into industrially feasible processes remains a major hurdle. Several issues, including mechanical wear caused by the shredding of hard materials, the necessity for an inert or moisture-free environment, and the requirement for high-purity separation, must be resolved. Systems must be scalable, flexible, and automated to effectively accommodate the wide array of cell chemistries and formats expected in future applications. Consequently, cell formats and treatment protocols must be standardized. However, recycling different types of electrolytes may require distinctly specialized methods. This differs from the recycling of conventional LIBs, which typically involves a certain degree of compatibility between materials, particularly for the recovery of metals from the active material. The integration of AI and robotics may also facilitate the automation of disassembly, optimize sorting and separation procedures, and increase process adaptability.

Designing for recycling will be pivotal in enabling more efficient end-of-life management. Future battery modules should feature, for example, easy-to-disassemble housings, reversible bonding agents, and accessible current collectors. These design principles simplify disassembly, minimize cross-contamination, and enhance the value of recovered fractions. To do this, battery designers, materials scientists, process engineers, and recycling specialists must collaborate closely from the earliest stages of development.

Conducting comprehensive life cycle assessments is essential for evaluating the environmental and economic effects of SSB recycling. Beyond recovering critical elements, future strategies should aim to directly recycle individual functional battery materials. Such an approach would reduce emissions and the necessity for energy-intensive resynthesis.

Finally, for large-scale industrial implementation, robust regulations must be established. Policies promoting circular designs could accelerate market adoption. Furthermore, recycling infrastructure must be developed, or existing infrastructure must be modified. Ultimately, only a concerted effort between academia, industry, and policymakers will enable the advancement of safe, economically viable, and scalable recycling solutions for SSBs. This will ensure their long-term sustainability and contribution to the energy transition.

## Conclusions and future perspectives

Significant progress has been made in the development of recycling strategies for SSBs; nonetheless, many challenges remain. Recent research has already demonstrated that effective separation processes can be defined, enabling the recovery of different battery components. These initial successes lay an important foundation for future developments while also underscoring the need for continued research efforts as cell chemistries and designs diversify. Importantly, the field still offers a rare opportunity to shape an emerging battery technology from the ground up with circularity in mind. While early findings suggest that some material combinations are more difficult to process than others, it is not yet clear which configurations will ultimately prove most compatible with recycling. SSBs might even provide benefits over conventional LIBs in terms of recyclability and resource requirements during end-of-life processing.

Future research should include post-Li technologies, such as lithium-sulfur batterie or SSBs based on other ions (e.g. $Na^+$, $K^+$, $Mg^{2+}$). These technologies may introduce new challenges, although they use analogous materials, indicating that insights gained from SSB recycling could be transferable. A coordinated effort to integrate recycling considerations into early-stage battery development, combined with technological advancements and policy support, will be essential to realize a sustainable and economically viable circular battery economy.

## Acknowledgment

K W is grateful to the Baden-Württemberg Stiftung for financial support through the postdoctoral fellowship for leading earlycareer researchers.

## Conflict of interest

The authors declare no conflict of interest.

## ORCID iDs

Florian Strauss 0000-0001-5817-6349
Torsten Brezesinski 0000-0002-4336-263X
Hugo Braun 0000-0001-9903-5614
Arndt Remhof 0000-0002-8394-9646
Corsin Battaglia 0000-0002-5003-1134
Theodosios Famprikis 0000-0002-7946-1445
Yoon Seok Jung 0000-0003-0357-9508
H Martin R Wilkening 0000-0001-9706-4892
Kerstin Wissel 0000-0003-4418-0595
Oliver Clemens 0000-0002-0860-0911

## References

[1] Janek J and Zeier W G 2023 Challenges in speeding up solid-state battery development *Nat. Energy* **8** 230–40
[2] Schmaltz T, Hartmann F, Wicke L, Weymann L, Neef C and Janek J 2023 A roadmap for solid-state batteries *Adv. Energy Mater.* **13** 2301886
[3] Sung J, Heo J, Kim D-H, Jo S, Ha Y-C, Kim D, Ahn S and Park J-W 2024 Recent advances in all-solid-state batteries for commercialization *Mater. Chem. Front.* **8** 1861–87
[4] Huang J, Wu K, Xu G, Wu M, Dou S and Wu C 2023 Recent progress and strategic perspectives of inorganic solid electrolytes: fundamentals, modifications, and applications in sodium metal batteries *Chem. Soc. Rev.* **52** 4933–95
[5] Yu T, Haoyu L, Sun Y, Guo S and Zhou H 2025 Ductile inorganic solid electrolytes for all-solid-state lithium batteries *Chem. Rev.* **125** 3595–662
[6] Kamaya N *et al* 2011 A lithium superionic conductor *Nat. Mater.* **10** 682–6
[7] Weng W, Lan Y, Tang D, Fu L, Tan W and Zhong S 2025 Research progress on lithium sulfide synthesis: a review *ACS Appl. Energy Mater.* **8** 13139–54
[8] Ohno S *et al* 2020 Materials design of ionic conductors for solid state batteries *Prog. Energy* **2** 022001
[9] Kraft M A, Culver S P, Calderon M, Böcher F, Krauskopf T, Senyshyn A, Dietrich C, Zevalkink A, Janek J and Zeier W G 2017 Influence of lattice polarizability on the ionic conductivity in the lithium superionic argyrodites $Li_6PS_5X$ (*X*=Cl, Br, I) *J. Am. Chem. Soc.* **139** 10909–18
[10] Robert G, Malugani J and Saida A 1981 Fast ionic silver and lithium conduction in glasses *Solid State Ion.* **3–4** 311–5
[11] Kondo S, Takada K and Yamamura Y 1992 New lithium ion conductors based on $Li_2S$–$SiS_2$ system *Solid State Ion.* **53–56** 1183–6
[12] Mercier R, Malugani J-P, Fahys B and Robert G 1981 Superionic conduction in $Li_2S$–$P_2S_5$-LiI-glasses *Solid State Ion.* **5** 663–6
[13] Deiseroth H-J, Kong S-T, Eckert H, Vannahme J, Reiner C, Zaiß T and Schlosser M 2008 $Li_6PS_5X$: a class of crystalline Li-rich solids with an unusually high $Li^+$ mobility *Angew. Chem., Int. Ed.* **47** 755–8
[14] Minami K, Hayashi A, Ujiie S and Tatsumisago M 2009 Structure and properties of $Li_2S$–$P_2S_5$–$P_2S_3$ glass and glass–ceramic electrolytes *J. Power Sources* **189** 651–4
[15] Kato Y, Hori S, Saito T, Suzuki K, Hirayama M, Mitsui A, Yonemura M, Iba H and Kanno R 2016 High-power all-solid-state batteries using sulfide superionic conductors *Nat. Energy* **1** 16030
[16] Li Y *et al* 2023 A lithium superionic conductor for millimeter-thick battery electrode *Science* **381** 50–53
[17] Saito M, Araki T, Onodera Y, Ohara K, Seto M, Yoda Y and Wakabayashi Y 2025 Discovery of collective nonjumping motions leading to Johari–Goldstein process of stress relaxation in model ionic glass *Acta Mater.* **284** 120536
[18] Cronau M, Szabo M, König C, Wassermann T B and Roling B 2021 How to measure a reliable ionic conductivity? the stack pressure dilemma of microcrystalline sulfide-based solid electrolytes *ACS Energy Lett.* **6** 3072–7
[19] Wang S *et al* 2021 Influence of crystallinity of lithium thiophosphate solid electrolytes on the performance of solid-state batteries *Adv. Energy Mater.* **11** 2100654
[20] Maus O *et al* 2025 Influence of post-synthesis processing on the structure, transport, and performance of the solid electrolyte $Li_{5.5}PS_{4.5}Cl_{1.5}$ in all-solid-state batteries *Adv. Energy Mater.* **15** 2403291
[21] Sendek A D, Cubuk E D, Antoniuk E R, Cheon G, Cui Y and Reed E J 2019 Machine learning-assisted discovery of solid li–ion conducting materials *Chem. Mater.* **31** 342–52
[22] Zhao Q, Avdeev M, Chen L and Shi S 2021 Machine learning prediction of activation energy in cubic Li-argyrodites with hierarchically encoding crystal structure-based (HECS) descriptors *Sci. Bull.* **66** 1401–8
[23] Kahle L, Marcolongo A and Marzari N 2020 High-throughput computational screening for solid-state Li-ion conductors *Energy Environ. Sci.* **13** 928–48
[24] Guo X, Wang Z, Yang J-H and Gong X-G 2024 Machine-learning assisted high-throughput discovery of solid-state electrolytes for Li–ion batteries *J. Mater. Chem. A* **12** 10124–36
[25] Cho M Y, Pyo K, Lee B D, Kim H, Shin J, Seo J Y, Park W B and Sohn K-S 2025 Discovering multi-compositional li-argyrodite solid-state electrolytes via experimental active learning *Small* **21** 2410008
[26] Kong S, Matsui N, Hori S, Hirayama M, Mori K, Saito T, Kanno R and Suzuki K 2025 Exploration of lithium-ion conductors based on local coordination environments using crystallographic site fingerprints *J. Am. Chem. Soc.* **147** 24336–46
[27] Han G *et al* 2024 Superionic lithium transport via multiple coordination environments defined by two-anion packing *Science* **383** 739–45
[28] Wang Q *et al* 2025 Unraveling the complexity of divalent hydride electrolytes in solid-state batteries via a data-driven framework with large language model *Angew. Chem., Int. Ed.* **64** e202506573
[29] Li J, Hu Y, Xia G, Mo W, Li B, Jia Y, Gao Y, Xuan F, Liu H and Lian C 2025 Coevolution of large language models with physical models boosts advanced battery research *Cell Rep. Phys. Sci.* **6** 102553
[30] Park H, Onwuli A and Walsh A 2025 Exploration of crystal chemical space using text-guided generative artificial intelligence *Nat. Commun.* **16** 4379
[31] Schweidler S *et al* 2024 High-entropy materials for energy and electronic applications *Nat. Rev. Mater.* **9** 266–81
[32] Li S, Lin J, Schaller M, Indris S, Zhang X, Brezesinski T, Nan C-W, Wang S and Strauss F 2023 High-entropy lithium argyrodite solid electrolytes enabling stable all-solid-state batteries *Angew. Chem., Int. Ed.* **62** e202314155

[33] Zeng Y, Ouyang B, Liu J, Byeon Y-W, Cai Z, Miara L J, Wang Y and Ceder G 2022 High-entropy mechanism to boost ionic conductivity *Science* **378** 1320–4

[34] Strauss F, Lin J, Duffiet M, Wang K, Zinkevich T, Hansen A-L, Indris S and Brezesinski T 2022 High-entropy polyanionic lithium superionic conductors *ACS Mater. Lett.* **4** 418–23

[35] Lin J, Cherkashinin G, Schäfer M, Melinte G, Indris S, Kondrakov A, Janek J, Brezesinski T and Strauss F 2022 A high-entropy multicationic substituted lithium argyrodite superionic solid electrolyte *ACS Mater. Lett.* **4** 2187–94

[36] Ohno S *et al* 2020 How certain are the reported ionic conductivities of thiophosphate-based solid electrolytes? An interlaboratory study *ACS Energy Lett.* **5** 910–5

[37] Kalyk F, Pescara L, Drüschler M and Vargas-Barbosa N M 2026 Toward robust ionic conductivity determination of sulfide-based solid electrolytes for solid-state batteries *Adv. Funct. Mater.* **36** e09479

[38] Shimoda M, Maegawa M, Yoshida S, Akamatsu H, Hayashi K, Gorai P and Ohno S 2022 Controlling defects to achieve reproducibly high ionic conductivity in $Na_3SbS_4$ solid electrolytes *Chem. Mater.* **34** 5634–43

[39] Schnaubelt F, Panda A, Wagner D, Ziegler M, Dang H A, Zeier W G, Bielefeld A and Janek J 2025 Impurities in $Na_2S$ precursor and their effect on the synthesis of W-substituted $Na_3PS_4$: enabling 20 mS $cm^{-1}$ thiophosphate electrolytes for sodium solid-state batteries *Adv. Energy Mater.* **15** e03047

[40] Puls S *et al* 2024 Benchmarking the reproducibility of all-solid-state battery cell performance *Nat. Energy* **9** 1310–20

[41] Li J, Su H, Liu Y, Zhong Y, Wang X and Tu J 2024 Li alloys in all solid-state lithium batteries: a review of fundamentals and applications *Electrochem. Energy Rev.* **7** 18

[42] Lee Y-G *et al* 2020 High-energy long-cycling all-solid-state lithium metal batteries enabled by silver–carbon composite anodes *Nat. Energy* **5** 299–308

[43] Lei Y-J, Liu H-W, Yang Z, Zhao L-F, Lai W-H, Chen M, Liu H, Dou S and Wang Y-X 2023 A review on the status and challenges of cathodes in room-temperature Na–S batteries *Adv. Funct. Mater.* **33** 2212600

[44] Koerver R, Zhang W, de Biasi L, Schweidler S, Kondrakov A O, Kolling S, Brezesinski T, Hartmann P, Zeier W G and Janek J 2018 Chemo-mechanical expansion of lithium electrode materials–on the route to mechanically optimized all-solid-state batteries *Energy Environ. Sci.* **11** 2142–58

[45] Walther F, Koerver R, Fuchs T, Ohno S, Sann J, Rohnke M, Zeier W G and Janek J 2019 Visualization of the interfacial decomposition of composite cathodes in argyrodite-based all-solid-state batteries using time-of-flight secondary-ion mass spectrometry *Chem. Mater.* **31** 3745–55

[46] Rosenbach C, Walther F, Ruhl J, Hartmann M, Hendriks T A, Ohno S, Janek J and Zeier W G 2023 Visualizing the chemical incompatibility of halide and sulfide-based electrolytes in solid-state batteries *Adv. Energy Mater.* **13** 2203673

[47] Zhao W, Lavrinenko A K, Tu M-F, Huet L, Vasileiadis A, Famprikis T, Wagemaker M and Ganapathy S 2025 Irreducible solid electrolytes: new perspectives on stabilizing high-capacity anodes in solid-state batteries *ACS Energy Lett.* **10** 5363–72

[48] Wan H, Wang Z, Zhang W, He X and Wang C 2023 Interface design for all-solid-state lithium batteries *Nature* **623** 739–44

[49] Aktekin B, Riegger L M, Otto S K, Fuchs T, Henss A and Janek J 2023 SEI growth on lithium metal anodes in solid-state batteries quantified with coulometric titration time analysis *Nat. Commun.* **14** 6946

[50] Luo Y, Rao Z, Yang X, Wang C, Sun X and Li X 2024 Safety concerns in solid-state lithium batteries: from materials to devices *Energy Environ. Sci.* **17** 7543–65

[51] Kim T, Kim K, Lee S, Song G, Jung M S and Lee K T 2022 Thermal runaway behavior of $Li_6PS_5Cl$ solid electrolytes for $LiNi_{0.8}Co_{0.1}Mn_{0.1}O_2$ and $LiFePO_4$ in all-solid-state batteries *Chem. Mater.* **34** 9159–71

[52] Rui X *et al* 2023 Distinct thermal runaway mechanisms of sulfide-based all-solid-state batteries *Energy Environ. Sci.* **16** 3552–63

[53] He Y, Wang J, Rong C, Li W, Gao Z, Wang D and Chen Y 2024 Status of cell-level thermal safety assessments toward optimization of all-solid-state batteries *Cell Rep. Phys. Sci.* **5** 102056

[54] Lu P, Wu D, Chen L, Li H and Wu F 2022 Air stability of solid-state sulfide batteries and electrolytes *Electrochem. Energy Rev.* **5** 3

[55] Ohno S and Zeier W G 2021 Toward practical solid-state lithium–sulfur batteries: challenges and perspectives *Acc. Mater. Res.* **2** 869–80

[56] Wang S *et al* 2025 Large-scale manufacturing sulfide superionic conductor for advancing all-solid-state batteries *Matter* **8** 102135

[57] Zhang Z *et al* 2018 New horizons for inorganic solid state ion conductors *Energy Environ. Sci.* **11** 1945–76

[58] Kerman K, Luntz A, Viswanathan V, Chiang Y-M and Chen Z 2017 Review—practical challenges hindering the development of solid state li ion batteries *J. Electrochem. Soc.* **164** A1731–44

[59] Li X, Liang J, Yang X, Adair K R, Wang C, Zhao F and Sun X 2020 Progress and perspectives on halide lithium conductors for all-solid-state lithium batteries *Energy Environ. Sci.* **13** 1429–61

[60] Anantharamulu N, Koteswara Rao K, Rambabu G, Vijaya Kumar B, Radha V and Vithal M 2011 A wide-ranging review on Nasicon type materials *J. Mater. Sci.* **46** 2821–37

[61] Wang Y, Song S, Xu C, Hu N, Molenda J and Lu L 2019 Development of solid-state electrolytes for sodium-ion battery–a short review *Nano Mater. Sci.* **1** 91–100

[62] Wu J, Li J and Yao X 2025 Exploring the potential of halide electrolytes for next-generation all-solid-state lithium batteries *Adv. Funct. Mater.* **35** 2416671

[63] Fu J *et al* 2023 Superionic conducting halide frameworks enabled by interface-bonded halides *J. Am. Chem. Soc.* **145** 2183–94

[64] Li X *et al* 2019 Air-stable $Li_3InCl_6$ electrolyte with high voltage compatibility for all-solid-state batteries *Energy Environ. Sci.* **12** 2665–71

[65] Shi X, Zeng Z, Sun M, Huang B, Zhang H, Luo W, Huang Y, Du Y and Yan C 2021 Fast Li–ion conductor of $li_3hobr_6$ for stable all-solid-state lithium-sulfur battery *Nano Lett.* **21** 9325–31

[66] Li X *et al* 2019 Water-mediated synthesis of a superionic halide solid electrolyte *Angew. Chem., Int. Ed.* **58** 16427–32

[67] Liang J *et al* 2020 Site-occupation-tuned superionic $Li_xScCl_{3+x}$ halide solid electrolytes for all-solid-state batteries *J. Am. Chem. Soc.* **142** 7012–22

[68] Park K H, Kaup K, Assoud A, Zhang Q, Wu X and Nazar L F 2020 High-voltage superionic halide solid electrolytes for all-solid-state li–ion batteries *ACS Energy Lett.* **5** 533–9

[69] Helm B, Schlem R, Wankmiller B, Banik A, Gautam A, Ruhl J, Li C, Hansen M R and Zeier W G 2021 Exploring aliovalent substitutions in the lithium halide superionic

conductor $Li_{3-x}In_{1-x}Zr_xCl_6$ ($0 \leqslant x \leqslant 0.5$) *Chem. Mater.* **33** 4773–82
[70] Kim S Y, Kaup K, Park K-H, Assoud A, Zhou L, Liu J, Wu X and Nazar L F 2021 Lithium ytterbium-based halide solid electrolytes for high voltage all-solid-state batteries *ACS Mater. Lett.* **3** 930–8
[71] Asano T, Sakai A, Ouchi S, Sakaida M, Miyazaki A and Hasegawa S 2018 Solid halide electrolytes with high lithium–ion conductivity for application in 4 V class bulk-type all-solid-state batteries *Adv. Mater.* **30** 1803075
[72] Park J, Han D, Kwak H, Han Y, Choi Y J, Nam K-W and Jung Y S 2021 Heat treatment protocol for modulating ionic conductivity via structural evolution of $Li_{3-x}Yb_{1-x}M_xCl_6$ ($M = Hf^{4+}, Zr^{4+}$) new halide superionic conductors for all-solid-state batteries *Chem. Eng. J.* **425** 130630
[73] Combs S R, Todd P K, Gorai P and Maughan A E 2022 Editors' choice—review—designing defects and diffusion through substitutions in metal halide solid electrolytes *J. Electrochem. Soc.* **169** 040551
[74] Liu Z, Chien P-H, Wang S, Song S, Lu M, Chen S, Xia S, Liu J, Mo Y and Chen H 2024 Tuning collective anion motion enables superionic conductivity in solid-state halide electrolytes *Nat. Chem.* **16** 1584–91
[75] Schlem R, Banik A, Ohno S, Suard E and Zeier W G 2021 Insights into the lithium substructure of superionic conductors $Li_3YCl_6$ and $Li_3YBr_6$ *Chem. Mater.* **33** 327–37
[76] Schlem R, Muy S, Prinz N, Banik A, Shao-Horn Y, Zobel M and Zeier W G 2020 Mechanochemical synthesis: a tool to tune cation site disorder and ionic transport properties of $Li_3MCl_6$ (M = Y,Er) superionic conductors *Adv. Energy Mater.* **10** 1903719
[77] Park D, Kim K, Chun G H, Wood B C, Shim J H and Yu S 2021 Materials design of sodium chloride solid electrolytes $Na_3MCl_6$ for all-solid-state sodium-ion batteries *J. Mater. Chem. A* **9** 23037–45
[78] Qie Y, Wang S, Fu S, Xie H, Sun Q and Jena P 2020 Yttrium-sodium halides as promising solid-state electrolytes with high ionic conductivity and stability for Na–Ion batteries *J. Phys. Chem. Lett.* **11** 3376–83
[79] Kwak H, Lyoo J, Park J, Han Y, Asakura R, Remhof A, Battaglia C, Kim H, Hong S-T and Jung Y S 2021 $Na_2ZrCl_6$ enabling highly stable 3 V all-solid-state Na–ion batteries *Energy Storage Mater.* **37** 47–54
[80] Zhao T, Kraft M A and Zeier W G 2023 Synthesis-controlled polymorphism and anion solubility in the sodium-ion conductor $Na_3InCl_{6-x}Br_x$ ($0 \leqslant x \leqslant 2$) *Inorg. Chem.* **62** 11737–45
[81] Zhao T, Sobolev A N, Schlem R, Helm B, Kraft M A and Zeier W G 2023 Synthesis-controlled cation solubility in solid sodium ion conductors $Na_{2+x}Zr_{1-x}In_xCl_6$ *ACS Appl. Energy Mater.* **6** 4334–41
[82] Schlem R, Banik A, Eckardt M, Zobel M and Zeier W G 2020 $Na_{3-x}Er_{1-x}Zr_xCl_6$-A halide-based fast sodium-ion conductor with vacancy-driven ionic transport *ACS Appl. Energy Mater.* **3** 10164–73
[83] Zhao T, Sobolev A N, de Irujo Labalde X M, Kraft M A and Zeier W G 2024 On the influence of the coherence length on the ionic conductivity in mechanochemically synthesized sodium-conducting halides, $Na_{3-x}In_{1-x}Zr_xCl_6$ *J. Mater. Chem. A* **12** 7015–24
[84] Martinez de Irujo-labalde X *et al* 2024 How crystal structure and microstructure can influence the sodium-ion conductivity in halide perovskites *J. Mater. Chem. A* **12** 33707–22
[85] Okada Y, Kimura T, Motohashi K, Sakuda A and Hayashi A 2023 Mechanochemical synthesis and characterization of $Na_{3-x}In_{1-x}Zr_xCl_6$ solid electrolyte *Electrochemistry* **91** 077009
[86] Huang Z, Yoshida S, Akamatsu H, Hayashi K and Ohno S 2024 $NaMCl_6$ (M = Nb and Ta): a new class of sodium-conducting halide-based solid electrolytes *ACS Mater. Lett.* **6** 1732–8
[87] Hu Y *et al* 2024 Superionic amorphous $NaTaCl_6$ halide electrolyte for highly reversible all-solid-state Na–ion batteries *Matter* **7** 1018–34
[88] Motohashi K, Tsukasaki H, Sakuda A, Mori S and Hayashi A 2024 $NaTaCl_6$: chloride as the end-member of sodium-ion conductors *ACS Mater. Lett.* **6** 1178–83
[89] Tanaka Y, Ueno K, Mizuno K, Takeuchi K, Asano T and Sakai A 2023 New oxyhalide solid electrolytes with high lithium ionic conductivity >10 mS $cm^{-1}$ for all-solid-state batteries *Angew. Chem., Int. Ed.* **62** e202217581
[90] Newnham J A *et al* 2025 Correlation between the coherence length and ionic conductivity in $LiNbOCl_4$ via the anion stoichiometry *Chem. Mater.* **37** 4130–44
[91] Zhang S *et al* 2023 A family of oxychloride amorphous solid electrolytes for long-cycling all-solid-state lithium batteries *Nat. Commun.* **14** 3780
[92] Zhang S *et al* 2024 Amorphous oxyhalide matters for achieving lithium superionic conduction *J. Am. Chem. Soc.* **146** 2977–85
[93] Lin X *et al* 2024 A dual anion chemistry-based superionic glass enabling long-cycling all-solid-state sodium-ion batteries *Angew. Chem., Int. Ed.* **136** e202314181
[94] Zhao T, Samanta B, de Irujo-labalde X M, Whang G, Yadav N, Kraft M A, Adelhelm P, Hansen M R and Zeier W G 2024 Sodium metal oxyhalides $NaMOCl_4$ (M = Nb, Ta) with high ionic conductivities *ACS Mater. Lett.* **6** 3683–9
[95] Zhou L, Bazak J D, Li C and Nazar L F 2024 4 V Na solid state batteries enabled by a scalable sodium metal oxyhalide solid electrolyte *ACS Energy Lett.* **9** 4093–101
[96] Kageyama H, Hayashi K, Maeda K, Attfield J P, Hiroi Z, Rondinelli J M and Poeppelmeier K R 2018 Expanding frontiers in materials chemistry and physics with multiple anions *Nat. Commun.* **9** 772
[97] Riegger L M, Schlem R, Sann J, Zeier W G and Janek J 2021 Lithium-metal anode instability of the superionic halide solid electrolytes and the implications for solid-state batteries *Angew. Chem., Int. Ed.* **60** 6718–23
[98] Tao B, Zhong D, Li H, Wang G and Chang H 2023 Halide solid-state electrolytes for all-solid-state batteries: structural design, synthesis, environmental stability, interface optimization and challenges *Chem. Sci.* **14** 8693–722
[99] Goodwin L E, Ziegler M, Till P, Nazer N, Adelhelm P, Zeier W G, Richter F H and Janek J 2024 Halide and sulfide electrolytes in cathode composites for sodium all-solid-state batteries and their stability *ACS Appl. Mater. Interfaces* **16** 19792–805
[100] Cheng Z *et al* 2025 Beneficial redox activity of halide solid electrolytes empowering high-performance anodes in all-solid-state batteries *Nat. Mater.* **24** 1763–72
[101] Ridley P, Duong G, Ko S L, An Sam Oh J, Deysher G, Griffith K J and Meng Y S 2025 Tailoring chloride solid electrolytes for reversible redox *J. Am. Chem. Soc.* **147** 19508–19
[102] Kmiec S, Ruoff E and Manthiram A 2025 A new class of oxyhalide solid electrolytes $nanbcl_{6-2x}o_x$ for solid-state sodium batteries *Angew. Chem., Int. Ed.* **64** e20241697
[103] Ferrari S, Falco M, Muñoz-García A B, Bonomo M, Brutti S, Pavone M and Gerbaldi C 2021 Solid-state post li metal ion batteries: a sustainable forthcoming reality? *Adv. Energy Mater.* **11** 2100785
[104] Famprikis T, Canepa P, Dawson J A, Islam M A and Masquelier C 2019 Fundamentals of inorganic solid-state electrolytes for batteries *Nat. Mater.* **18** 1278–91

[105] Iton Z W B and See K Z 2022 Multivalent ion conduction in inorganic solids *Chem. Mater.* **34** 881–98

[106] Grill J, Steensen S K, Castro D L Q, Castelli I E and Popovic-Neuber J 2024 Solid-state inorganic electrolytes for next generation potassium batteries *Commun. Mater.* **5** 127

[107] Lu Z, Qiu P, Zhai H, Zhang G G, Chen X W, Lu Z, Wu Y and Chen X 2024 Facile synthesis of potassium decahydrido-monocarba-closo-decaborate imidazole complex electrolyte for all-solid-state potassium metal batteries *Angew. Chem., Int. Ed.* **63** e202412401

[108] Grill J and Popovic-Neuber J 2025 Bulk and interphase properties of W-doped $K_3SbS_4$ solid-state electrolyte *J. Energy Chem.* **111** 274–8

[109] Chen Y *et al* 2024 Superionic conduction in $K_3SbS_4$ enabled by Cl-modified anion lattice *Angew. Chem., Int. Ed.* **136** e202408574

[110] Jaschin P W, Gao Y, Li Y and Bo S H 2020 A materials perspective on magnesium-ion-based solid-state electrolytes *J. Mater. Chem.* **8** 2875–97

[111] Kisu K, Kim S, Inukai M, Oguchi H, Takagi H and Orimo S 2020 Magnesium borohydrate ammonia borane as a magnesium ionic conductor *ACS Appl. Energy Mater.* **3** 3174–9

[112] Amdisen M B, Grinderslev J B, Skov L N and Jensen T R 2023 Methylamine magnesium borohydrides as electrolytes for all-solid-state magnesium batteries *Chem. Mater.* **35** 1440–8

[113] Glaser C *et al* 2025 High room-temperature magnesium ion conductivity in spinel-type $MgYb_2Se_4$ solid electrolyte *Chem. Mater.* **37** 3353–62

[114] Shinohara T, Kisu K, Takagi S and Orimo S 2024 Investigating the ion conductivity and synthesis conditions of calcium monocarborane solid-state electrolytes *Energy Adv.* **3** 2758–63

[115] Amidsen M B and Jensen T 2025 Urea calcium borohydrides as $Ca^{2+}$ solid-state electrolytes *Chem. Mater.* **37** 1183–94

[116] Grinderslev J B, Skov L N, Kristensen L R and Jensen T R 2025 Advancing solid-state calcium batteries: achieving fast ionic conductivity at near ambient conditions in calcium hydridoborates *Angew. Chem., Int. Ed.* **64** e202510493

[117] Mercadier B, Coles S W, Duttine M, Legein M, Body M, Borkiewicz O J, Lebedev O, Morgan B J, Masquelier C and Dambournet D 2023 Dynamic lone pairs and fluoride-ion disorder in cubic-$BaSnF_4$ *J. Am. Chem. Soc.* **145** 23739–54

[118] Mori K, Sato S, Ogawa T, Kuwabara A, Song A, Saito T, Fukunaga T and Abe T 2024 Experimental visualization of F-ion diffusion pathways and geometric frustration-induced positional disorder in $CaF_2$-$BaF_2$ solid electrolytes *ACS Appl. Energy Mater.* **7** 7787–97

[119] Mohammad I, Witter R, Fichtner M and Reddy M A 2018 Room-temperature, rechargeable solid-state fluoride-ion batteries *ACS Appl. Energy Mater.* **1** 4766–75

[120] Hou T, Xu W, Pei X, Jiang L, Yaghi O M and Persson K A 2022 Ionic conduction mechanism and design of metal–organic framework based quasi-solid-state electrolytes *J. Am. Chem. Soc.* **144** 13446–50

[121] Paskevicius M, Pitt M P, Brown D H, Sheppard D A, Chumphongphan S and Buckley C E 2013 First-order phase transition in the $Li_2B_{12}H_{12}$ system *Phys. Chem. Chem. Phys.* **15** 15825–8

[122] Udovic T J, Matsuo M, Unemoto A, Verdal N, Stavila V, Skripov A V, Rush J J, Takamura H and Orimo S-I 2014 Sodium superionic conduction in $Na_2B_{12}H_{12}$ *Chem. Commun.* **50** 3750–2

[123] Duchêne L, Kühnel R-S, Rentsch D, Remhof A, Hagemann H and Battaglia C 2017 A highly stable sodium solid-state electrolyte based on a dodeca/deca-borate equimolar mixture *Chem. Commun.* **53** 4195–8

[124] Duchêne L, Lunghammer S, Burankova S, Liao W S, Embs J P, Copéret C, Wilkening H M R, Remhof A, Hagemann H and Battaglia C 2019 Ionic conduction mechanism in the $Na_2(B_{12}H_{12})_{0.5}(B_{10}H_{10})_{0.5}$ closo-borate solid-state electrolyte: interplay of disorder and ion–ion interactions *Chem. Mater.* **31** 3449–60

[125] Kweon K E, Varley J B, Shea P, Adelstein N, Mehta P, Heo T W, Udovic T J, Stavila V and Wood B C 2017 Structural, chemical, and dynamical frustration: origins of superionic conductivity in closo-borate solid electrolytes *Chem. Mater.* **29** 9142–53

[126] Tang W S, Yoshida K, Soloninin A V, Skoryunov R V, Babanova O A, Skripov A V, Dimitrievska M, Stavila V, Orimo S-I and Udovic T J 2016 Stabilizing superionic-conducting structures via mixed-anion solid solutions of monocarba-closo-borate salts *ACS Energy Lett.* **1** 659–64

[127] Payandeh S, Rentsch D, Łodziana Z, Asakura R, Bigler L, Černý R, Battaglia C and Remhof A 2021 Nido-hydroborate-based electrolytes for all-solid-state lithium batteries *Adv. Funct. Mater.* **31** 2010046

[128] Gulino V, Brighi M, Murgia F, Ngene P, de Jongh P, Černý R and Baricco M 2021 Room-temperature solid-state lithium–ion battery using a $LiBH_4$–MgO composite electrolyte *ACS Appl. Energy Mater.* **4** 1228–36

[129] Kim S, Kisu K, Takagi S, Oguchi H and Orimo S-I 2020 Complex hydride solid electrolytes of the $Li(CB_9H_{10})$–$Li(CB_{11}H_{12})$ quasi-binary system: relationship between the solid solution and phase transition, and the electrochemical properties *ACS Appl. Energy Mater.* **3** 4831–9

[130] Garcia A, Müller G, Černý R, Rentsch D, Asakura R, Battaglia C and Remhof A 2023 $Li_4B_{10}H_{10}B_{12}H_{12}$ as solid electrolyte for solid-state lithium batteries *J. Mater. Chem. A* **11** 18996–19003

[131] Duchêne L, Kühnel R S, Stilp E, Cuervo Reyes E, Remhof A, Hagemann H and Battaglia C 2017 A stable 3 V all-solid-state sodium–ion battery based on a closo-borate electrolyte *Energy Environ. Sci.* **10** 2609–15

[132] Braun H, Asakura R, Remhof A and Battaglia C 2024 Hydroborate solid-state lithium battery with high-voltage NMC811 Cathode *ACS Energy Lett.* **9** 707–14

[133] Asakura R, Reber D, Duchêne L, Payandeh S, Remhof A, Hagemann H and Battaglia C 2020 4 V room-temperature all-solid-state sodium battery enabled by a passivating cathode/hydroborate solid electrolyte interface *Energy Environ. Sci.* **13** 5048–58

[134] Duchêne L, Kim D H, Song Y B, Jun S, Moury R and Remhof A 2020 Crystallization of closo-borate electrolytes from solution enabling infiltration into slurry-casted porous electrodes for all-solid-state batteries *Energy Storage Mater.* **26** 543–9

[135] Muetterties E L, Balthis J H, Chia Y T, Knoth W H and Miller H C 1964 Chemistry of Boranes. VIII. Salts and Acids of $B_{10}H_{10}{}^{-2}$ and $B_{12}H_{12}{}^{-2}$ *Inorg. Chem.* **3** 444–51

[136] Asakura R, Łodziana Z, Grissa R, Rentsch D, Battaglia C and Remhof A 2025 Unveiling solid-state electrochemical oxidation of $LiBH_4$ and $Li_2B_{12}H_{12}$ for high-voltage all-solid-state batteries *ACS Appl. Energy Mater.* **8** 9637–45

[137] Bay M-C, Grissa R, Egorov K V, Asakura R and Battaglia C 2022 Low Na-$\beta''$-alumina electrolyte/cathode interfacial resistance enabled by a hydroborate electrolyte opening up new cell architecture designs for all-solid-state sodium batteries *Mater. Futures* **1** 031001

[138] Gigante A, Duchêne L, Moury R, Pupier M, Remhof A and Hagemann H 2019 Direct solution-based synthesis of $Na_4(B_{12}H_{12})(B_{10}H_{10})$ solid electrolyte *ChemSusChem* **12** 4832–7

[139] Berger A, Buckley C E and Paskevicius M 2021 Synthesis of closo-$CB_{11}H_{12}$–Salts using common laboratory reagents *Inorg. Chem.* **60** 14744–51

[140] Kulenkampff J, Armbruster C, Drolshagen J, Regnat C, Wienold T, Spari L, Fix J, Sterbak T, Scherer H and Krossing I 2024 Video documented upscaled synthesis of salts of the parent carbaborate ion $[CB_{11}H_{12}]^-$, its undecafluorinated form $[CHB_{11}F_{11}]^-$ and useful starting materials for its introduction *Chem. Methods* **4** e202400011

[141] Cheng D *et al* 2020 Unveiling the stable nature of the solid electrolyte interphase between lithium metal and LiPON via cryogenic electron microscopy *Joule* **4** 2484–500

[142] Turrell S J, Liang Y, Cai T, Jagger B and Pasta M 2025 Origin of stability in the solid electrolyte interphase formed between lithium and lithium phosphorus oxynitride *Chem. Mater.* **13** 3504–18

[143] Wenzel S, Sedlmaier S J, Dietrich C, Zeier W G and Janek J 2018 Interfacial reactivity and interphase growth of argyrodite solid electrolytes at lithium metal electrodes *Solid State Ion.* **318** 102–12

[144] Alpen U V, Rabenau A and Talat G H 1977 Ionic conductivity in $Li_3N$ single crystals *Appl. Phys. Lett.* **15** 621–3

[145] Li W *et al* 2025 Superionic conducting vacancy-rich $\beta$-$Li_3N$ electrolyte for stable cycling of all-solid-state lithium metal batteries *Nat. Nanotechnol.* **20** 265–75

[146] Nazri G 1989 Preparation, structure and ionic conductivity of lithium phosphide *Solid State Ion.* **34** 97–102

[147] Schmid M, Pielnhofer F and Pfitzner A 2025 The cubic structure of $Li_3As$ stabilized by pressure or configurational entropy via the solid solution $Li_3As$–$Li_2Se$ *RSC Mechanochem.* **2** 193–200

[148] Lorger S, Usiskin R and Maier J 1019 Transport and charge carrier chemistry in lithium oxide *J. Electrochem. Soc.* **166** A2215–20

[149] Landgraf V *et al* 2025 Disorder-mediated ionic conductivity in irreducible solid electrolytes *J. Am. Chem. Soc.* **147** 18840–52

[150] Lorger S, Usiskin R E and Maier J 2019 Transport and charge carrier chemistry in lithium sulfide *Adv. Funct. Mater.* **29** 1807688

[151] Geschwind G 1969 Anion reduced ionic conductivity in LiF *J. Phys. Chem. Solids* **30** 1631–5

[152] Sharon M and Pradhananga R R 1981 Ionic conductivity of MCI of pure and $Ca^{2+}$- and $Sr^{2+}$-doped single crystals *J. Solid State Chem.* **40** 20–27

[153] Schlaikjer C R and Liang C C 1971 Ionic conduction in calcium doped polycrystalline lithium iodide *J. Electrochem. Soc.* **118** 1447–50

[154] Wang Z, Xia J, Ji X, Liu Y, Zhang J, He X, Zhang W, Wan H and Wang C 2024 Lithium anode interlayer design for all-solid-state lithium-metal batteries *Nat. Energy* **9** 251–62

[155] Dawson J A, Famprikis T and Johnston K E 2021 Anti-perovskites for solid-state batteries: recent developments, current challenges and future prospects *J. Mater. Chem. A* **9** 18746–72

[156] Gao S *et al* 2021 Hydride-based antiperovskites with soft anionic sublattices as fast alkali ionic conductors *Nat. Commun.* **12** 201

[157] Li W *et al* 2023 Lithium-compatible and air-stable vacancy-rich $Li_9N_2Cl_3$ for high–areal capacity, long-cycling all–solid-state lithium metal batteries *Sci. Adv.* **9** eadh4626

[158] Landgraf V, Famprikis T, de Leeuw J, Bannenberg L J, Ganapathy S and Wagemaker M 2023 $Li_5NCl_2$: a fully-reduced, highly-disordered nitride-halide electrolyte for solid-state batteries with lithium-metal anodes *ACS Appl. Energy Mater.* **6** 1661–72

[159] Landgraf V, Tu M, Cheng Z, Vasileiadis A, Wagemaker M and Famprikis T 2025 Compositional flexibility in irreducible antifluorite electrolytes for next-generation battery anodes *J. Mater. Chem. A* **13** 3562–74

[160] Yu P *et al* 2024 Lithium metal-compatible antifluorite electrolytes for solid-state batteries *J. Am. Chem. Soc.* **146** 12681–90

[161] Szczuka C *et al* 2022 Forced disorder in the solid solution $Li_3P$–$Li_2S$: a new class of fully reduced solid electrolytes for lithium metal anodes *J. Am. Chem. Soc.* **144** 16350–65

[162] Tu M *et al* 2025 Highly Conductive Irreducible Electrolytes for Next-Generation Low-Potential Anodes *J. Am. Chem. Soc.* **148** 12576–86

[163] Richards W D, Miara L J, Wang Y, Kim J C and Ceder G 2016 Interface stability in solid-state batteries *Chem. Mater.* **28** 266–73

[164] Lavrinenko A K *et al* 2024 Optimizing ionic transport in argyrodites: a unified view on the role of sulfur/halide distribution and local environments *J. Mater. Chem. A* **12** 26596–611

[165] Simonov A and Goodwin A L 2020 Designing disorder into crystalline materials *Nat. Rev. Chem.* **4** 657–73

[166] Zhao Q, Stalin S, Zhao C-Z and Archer L A 2020 Designing solid-state electrolytes for safe, energy-dense batteries *Nat. Rev. Mater.* **5** 229–52

[167] Tian Y *et al* 2021 Promises and challenges of next-generation "Beyond Li–ion" batteries for electric vehicles and grid decarbonization *Chem. Rev.* **121** 1623–69

[168] Neudecker B J, Dudney N J and Bates J B 2000 "Lithium-Free" thin-film battery with *In Situ* plated li anode *J. Electrochem. Soc.* **147** 517–23

[169] Chi X *et al* 2022 An electrochemically stable homogeneous glassy electrolyte formed at room temperature for all-solid-state sodium batteries *Nat. Commun.* **13** 2854

[170] Mei A, Wang X-L, Lan J-L, Feng Y-C, Geng H-X, Lin Y-H and Nan C-W 2010 Role of amorphous boundary layer in enhancing ionic conductivity of lithium–lanthanum–titanate electrolyte *Electrochim. Acta* **55** 2958–63

[171] Di L *et al* 2023 Effect of grain boundary resistance on the ionic conductivity of amorphous $xLi_2S$-$(100-x)$LiI binary system *Front. Chem.* **11** 1230187

[172] Jung S-K, Gwon H, Yoon G, Miara L J, Lacivita V and Kim J-S 2021 Pliable lithium superionic conductor for all-solid-state batteries *ACS Energy Lett.* **6** 2006–15

[173] Yang X *et al* 2024 Fast room-temperature Mg–Ion conduction in clay-like halide glassy electrolytes *Adv. Energy Mater.* **14** 2400163

[174] Bates J B, Dudney N J, Gruzalski G R, Zuhr R A, Choudhury A and Luck C F 1992 Electrical properties of amorphous lithium electrolyte thin films *Solid State Ion.* **53** 647–54

[175] Yu X, Bates J B, Jellison J G E and Hart F X 1997 A stable thin-film lithium electrolyte: lithium phosphorus oxynitride *J. Electrochem. Soc.* **144** 524–32

[176] Senevirathne K, Day C S, Gross M D, Lachgar A and Holzwarth N A W 2013 A new crystalline LiPON electrolyte: synthesis, properties, and electronic structure *Solid State Ion.* **233** 95–101

[177] Zou Z, Xiao Z, Lin Z, Zhang B, Zhang C and Wei F 2024 Lithium phosphorous oxynitride as an advanced solid-state electrolyte to boost high-energy lithium metal battery *Adv. Funct. Mater.* **34** 2409330

[178] Atwal S, Bhasin V, Nayak C, Nagendra A, Karki V, Sahoo P K, Bhattacharyya K, Bhattacharyya D and Biswas A 2025 Spectroscopic ellipsometry study of $TiO_2$/LiPON and LNMC/LiPON solid electrode/electrolyte interfaces of solid-state batteries *ACS Appl. Energy Mater.* **8** 7730–43

[179] Kwon G *et al* 2025 Disorder-driven sintering-free garnet-type solid electrolytes *Nat. Commun.* **16** 3256

[180] Zhu Y *et al* 2024 Highly disordered amorphous Li-battery electrolytes *Matter* **7** 500–2

[181] Kuwata N, Lu X, Miyazaki T, Iwai Y, Tanabe T and Kawamura J 2016 Lithium diffusion coefficient in amorphous lithium phosphate thin films measured by secondary ion mass spectroscopy with isotope exchange methods *Solid State Ion.* **294** 59–66

[182] Kazyak E *et al* 2018 Atomic layer deposition and first principles modeling of glassy $Li_3BO_3$–$Li_2CO_3$ electrolytes for solid-state Li metal batteries *J. Mater. Chem. A* **6** 19425–37

[183] Hayashi A, Hama S, Morimoto H, Tatsumisago M and Minami T 2004 Preparation of $Li_2S$–$P_2S_5$ amorphous solid electrolytes by mechanical milling *J. Am. Ceram. Soc.* **84** 477–9

[184] Tsukasaki H, Mori S, Morimoto H, Hayashi A and Tatsumisago M 2017 Direct observation of a non-crystalline state of $Li_2S$-$P_2S_5$ solid electrolytes *Sci. Rep.* **7** 4142

[185] Lee B, Jun K, Ouyang B and Ceder G 2023 Weak correlation between the polyanion environment and ionic conductivity in amorphous Li–P–S superionic conductors *Chem. Mater.* **35** 891–9

[186] Chen Z, Du T, Krishnan N M A, Yue Y and Smedskjaer M M 2025 Disorder-induced enhancement of lithium-ion transport in solid-state electrolytes *Nat. Commun.* **16** 1057

[187] Xu R, Yao J, Zhang Z, Li L, Wang Z, Song D, Yan X, Yu C and Zhang L 2022 Room temperature halide-eutectic solid electrolytes with viscous feature and ultrahigh ionic conductivity *Adv. Sci.* **9** e2204633

[188] Spannenberger S *et al* 2029 Annealing-induced vacancy formation enables extraordinarily high $Li^+$ ion conductivity in the amorphous electrolyte $0.33LiI + 0.67Li_3PS_4$ *Solid State Ion.* **341** 115040

[189] Lin X *et al* 2025 A family of dual-anion-based sodium superionic conductors for all-solid-state sodium–ion batteries *Nat. Mater.* **24** 83–91

[190] Jang Y-J, Seo H, Lee Y-S, Kang S, Cho W, Cho Y and Kim J-H 2023 Lithium superionic conduction in $BH_4$-substituted thiophosphate solid electrolytes *Adv. Sci.* **10** e2204942

[191] Braga M H, Ferreira J A, Stockhausen V, Oliveira J E and El-Azab A 2014 Novel $Li_3ClO$ based glasses with superionic properties for lithium batteries *J. Mater. Chem. A* **2** 5470–80

[192] Seino Y, Ota T, Takada K, Hayashi A and Tatsumisago M 2014 A sulphide lithium super ion conductor is superior to liquid ion conductors for use in rechargeable batteries *Energy Environ. Sci.* **7** 627–31

[193] Ishiguro Y, Ueno K, Nishimura S, Iida G and Igarashib Y 2023 $TaCl_5$-glassified ultrafast lithium ion-conductive halide electrolytes for high-performance all-solid-state lithium batteries *Chem. Lett.* **52** 237–41

[194] Mizuno F, Hayashi A, Tadanaga K and Tatsumisago M 2006 High lithium ion conducting glass-ceramics in the system $Li_2S$–$P_2S_5$ *Solid State Ion.* **177** 2721–5

[195] Guo H, Wang Q, Urban A and Artrith N 2022 Artificial intelligence-aided mapping of the structure-composition-conductivity relationships of glass-ceramic lithium thiophosphate electrolytes *Chem. Mater.* **34** 6702–12

[196] Kam R L, Jun K, Barroso-Luque L, Yang J H, Xie F and Ceder G 2023 Crystal structures and phase stability of the $Li_2S$–$P_2S_5$ system from first principles *Chem. Mater.* **35** 9111–26

[197] Wang Y *et al* 2023 Self-organized hetero-nanodomains actuating super $Li^+$ conduction in glass ceramics *Nat. Commun.* **14** 669

[198] Ohtomo T, Mizuno F, Hayashi A, Tadanaga K and Tatsumisago M 2005 Mechanochemical synthesis of lithium ion conducting glasses and glass–ceramics in the system $Li_2S$–P–S *Solid State Ion.* **176** 2349–53

[199] Wu Z, Xie Z, Yoshida A, Wang Z, Hao X and Abudula A 2019 Utmost limits of various solid electrolytes in all-solid-state lithium batteries: a critical review *Renew. Sustain. Energy Rev.* **109** 367–85

[200] Schweiger L, Hogrefe K, Gadermaier B, Rupp J L M and Wilkening H M R 2022 Ionic conductivity of nanocrystalline and amorphous $Li_{10}GeP_2S_{12}$: the detrimental impact of local disorder on ion transport *J. Am. Chem. Soc.* **144** 9597–609

[201] Smith J G and Siegel D J 2020 Low-temperature paddlewheel effect in glassy solid electrolytes *Nat. Commun.* **11** 1483

[202] Qi J, Banerjee S, Zuo Y, Chen C, Zhu Z, Holekevi Chandrappa M L, Li X and Ong S P 2021 Bridging the gap between simulated and experimental ionic conductivities in lithium superionic conductors *Mater. Today Phys.* **21** 100463

[203] Sastre J, Futscher M H, Pompizi L, Aribia A, Priebe A, Overbeck J, Stiefel M, Tiwari A N and Romanyuk Y E 2021 Blocking lithium dendrite growth in solid-state batteries with an ultrathin amorphous Li–La–Zr–O solid electrolyte *Commun. Mater.* **2** 76

[204] Kalita D, Lee S, Lee K, Ko D and Yoon Y 2012 Ionic conductivity properties of amorphous Li–La–Zr–O solid electrolyte for thin film batteries *Solid State Ion.* **229** 14–19

[205] Zheng Z, Fang H, Yang F, Liu Z-K and Wang Y 2014 Amorphous $LiLaTiO_3$ as solid electrolyte material *J. Electrochem. Soc.* **161** A473–9

[206] Aguesse F, Roddatis V, Roqueta J, García P, Pergolesi D, Santiso J and Kilner J A 2015 Microstructure and ionic conductivity of LLTO thin films: influence of different substrates and excess lithium in the target *Solid State Ion.* **272** 1–8

[207] Lee T *et al* 2023 Atomic-scale origin of the low grain-boundary resistance in perovskite solid electrolyte $Li_{0.375}Sr_{0.4375}Ta_{0.75}Zr_{0.25}O_3$ *Nat. Commun.* **14** 1940

[208] Ling Q, Yu Z, Xu H, Zhu G, Zhang X, Zhao Y and Yu A 2016 Preparation and electrical properties of amorphous Li–Al–Ti–P–O thin film electrolyte *Mater. Lett.* **169** 42–45

[209] Luo C, Yi M, Cao Z, Hui W and Wang Y 2024 Review of ionic conductivity properties of NASICON type inorganic solid electrolyte LATP *ACS Appl. Electron. Mater.* **6** 641–57

[210] Wei B, Huang S, Wang X, Liu M, Huang C, Liu R and Jin H 2025 Intermediate phase induced *in situ* self-reconstruction of amorphous NASICON for long-life solid-state sodium metal batteries *Energy Environ. Sci.* **18** 831–40

[211] Ishiguro Y, Iida G, Ueno K, Nishimura S and Igarashib Y 2023 All-solid-state lithium batteries in cold environments of −20 °C enabled by amorphous halide-based electrolytes $LiNbCl_5X$ and $LiTaCl_5X$ (https://doi.org/10.21203/rs.3.rs-3072105/v1)

[212] Gupta S, Yang X and Ceder G 2023 What dictates soft clay-like lithium superionic conductor formation from rigid salts mixture *Nat. Commun.* **14** 6884

[213] Li R, Xu K, Wen S, Tang X, Lin Z, Guo X, Avdeev M, Zhang Z and Hu Y-S 2025 A sodium superionic chloride

electrolyte driven by paddle wheel mechanism for solid state batteries *Nat. Commun.* **16** 6633
[214] Choudhary S and Banerjee S 2025 Ion coordination and migration mechanisms in alkali metal complex borohydride-based solid electrolytes *Commun. Chem.* **8** 123
[215] Roy A, Sotoudeh M, Dinda S, Tang Y, Kübel C, Groß A, Zhao-Karger Z, Fichtner M and Li Z 2024 Improving rechargeable magnesium batteries through dual cation co-intercalation strategy *Nat. Commun.* **15** 492
[216] Dong Z L *et al* 2024 Structural insight and modulating of sulfide-based solid-state electrolyte for high-performance solid-state sodium sulfur batteries *Nano Energy* **128** 109871
[217] Cha G H and Jung S C 2022 Cation-assisted lithium ion diffusion in a lithium oxythioborate halide glass solid electrolyte *Electrochim. Acta* **426** 140806
[218] Qian L, Tu S, Wang Y, Yang X, Ye C and Qiao S Z 2025 Near-saturated coordinated cations in oxyhalide superionic conductors boost high-rate all-solid-state batteries *J. Am. Chem. Soc.* **147** 23170–9
[219] Dong Z L *et al* 2025 Novel sulfide-chloride solid-state electrolytes with tunable anion ratio for highly stable solid-state sodium–ion batteries *Adv. Mater.* **37** e2503107
[220] Lacivita V, Artrith N and Ceder G 2018 Structural and compositional factors that control the Li–Ion conductivity in LiPON electrolytes *Chem. Mater.* **30** 7077–90
[221] Baba T and Kawamura Y 2016 Structure and ionic conductivity of $Li_2S$–$P_2S_5$ glass electrolytes simulated with first-principles molecular dynamics *Front. Energy Res.* **4** 22
[222] Ohara K *et al* 2016 Structural and electronic features of binary $Li_2S$-$P_2S_5$ glasses *Sci. Rep.* **6** 21302
[223] Wang D, Jhang L J, Kou R, Liao M, Zheng S, Jiang H, Shi P, Li G-X, Meng K and Wang D 2023 Realizing high-capacity all-solid-state lithium-sulfur batteries using a low-density inorganic solid-state electrolyte *Nat. Commun.* **14** 1895
[224] Faka V, Agne M T, Till P, Bernges T, Sadowski M, Gautam A, Albe K and Zeier W G 2023 Pressure dependence of ionic conductivity in site disordered lithium superionic argyrodite $Li_6PS_5Br$ *Energy Adv.* **2** 1915–25
[225] Torres V, Philipp P, Kmiec S and Martin S W 2024 Ionic conductivity of and structure and property relationships in $Li_2S + SiS_2 + LiPO_3$ glassy solid electrolytes *Chem. Mater.* **36** 5521–33
[226] Kim Y and Martin S 2006 Ionic conductivities of various $GeS_2$-based oxy-sulfide amorphous materials prepared by melt-quenching and mechanical milling methods *Solid State Ion.* **177** 2881–7
[227] Tanibata N, Noi K, Hayashi A and Tatsumisago M 2018 Preparation and characterization of $Na_3PS_4$–$Na_4GeS_4$ glass and glass-ceramic electrolytes *Solid State Ion.* **320** 193–8
[228] Zhang Z, Li H, Kaup K, Zhou L, Roy P-N and Nazar L F 2020 Targeting superionic conductivity by turning on anion rotation at room temperature in fast ion conductors *Matter* **2** 1667–84
[229] Zhang Z, Roy P-N, Li H, Avdeev M and Nazar L F 2019 Coupled cation–anion dynamics enhances cation mobility in room-temperature superionic solid-state electrolytes *J. Am. Chem. Soc.* **141** 19360–72
[230] Jun K, Lee B, Kam R L and Ceder G 2024 The nonexistence of a paddlewheel effect in superionic conductors *Proc. Natl Acad. Sci.* **121** e2316493121
[231] Li F *et al* 2023 Amorphous chloride solid electrolytes with high Li–ion conductivity for stable cycling of all-solid-state high-nickel cathodes *J. Am. Chem. Soc.* **145** 27774–87
[232] Qian L, Singh B, Yu Z, Chen N, King G, Arthur Z and Nazar L F 2024 Unlocking lithium ion conduction in lithium metal fluorides *Matter* **7** 3587–607
[233] Sun Y, Ouyang B, Wang Y, Zhang Y, Sun S, Cai Z, Lacivita V, Guo Y and Ceder G 2022 Enhanced ionic conductivity and lack of paddle-wheel effect in pseudohalogen-substituted Li argyrodites *Matter* **5** 4379–95
[234] Zhang Z and Nazar L F 2022 Exploiting the paddle-wheel mechanism for the design of fast ion conductors *Nat. Rev. Mater.* **7** 389–405
[235] Jun K and Ceder G 2025 Reply to Smith and Siegel: most lithium hops in paddlewheel-claimed conductors occur without spatially and temporally correlated anion-group rotations *Proc. Natl Acad. Sci.* **122** e2423194122
[236] Smith J G and Siegel D J 2025 A proper definition of the paddlewheel effect affirms its existence *Proc. Natl. Acad. Sci.* **122** e2419892122
[237] Wang Y, Richards W D, Ong S P, Miara L J, Kim J C, Mo Y and Ceder G 2015 Design principles for solid-state lithium superionic conductors *Nat. Mater.* **14** 1026–31
[238] Yu S *et al* 2023 Design of a trigonal halide superionic conductor by regulating cation order-disorder *Science* **382** 573–9
[239] He Y, Scivally E, Shaji A, Ouyang B and Zeng Y 2025 Unraveling the fast ionic conduction in NASICON-type materials *Adv. Energy Mater.* **15** 2403877
[240] Liu Y, Wang S, Nolan A M, Ling C and Mo Y 2020 Tailoring the cation lattice for chloride lithium-ion conductors *Adv. Energy Mater.* **10** 2002356
[241] Dheerasinghe M J, Gan Y, Wang L, He Y, He Z, Xu G-L, Zhao Y and Ouyang B 2025 High throughput screening of high entropy spinel electrolytes for multivalent batteries *Chem. Commun.* **61** 11199–202
[242] Wang J, He T, Yang X, Cai Z, Wang Y, Lacivita V, Kim H, Ouyang B and Ceder G 2023 Design principles for NASICON super-ionic conductors *Nat. Commun.* **14** 5210
[243] Ouyang B, Wang J, He T, Bartel C J, Huo H, Wang Y, Lacivita V, Kim H and Ceder G 2021 Synthetic accessibility and stability rules of NASICONs *Nat. Commun.* **12** 5752
[244] Chen Y *et al* 2025 Coherent-precipitation-stabilized phase formation in over-stoichiometric rocksalt-type Li superionic conductors *Adv. Mater.* **37** e2416342
[245] Chen Y *et al* 2024 Unlocking Li superionic conductivity in face-centred cubic oxides via face-sharing configurations *Nat. Mater.* **23** 535–42
[246] Liu X, Ouyang B and Zeng Y 2025 Balancing autonomy and expertise in autonomous synthesis laboratories *Nat. Comput. Sci.* **5** 92–94
[247] Wang L, He Z and Ouyang B 2023 Data driven design of compositionally complex energy materials *Comput. Mater. Sci.* **230** 112513
[248] Bera P K, Medvedev G A, Caruthers J M and Ediger M D 2024 Structural relaxation time of a polymer glass during deformation *Phys. Rev. Lett.* **132** 208101
[249] Málek J 2023 Structural relaxation rate and aging in amorphous solids *J. Phys. Chem. C* **127** 6080–7
[250] Wang X, Wang J and Ruan H 2023 Ergodicity breaking of an inorganic glass aging near $T_g$ probed by elasticity relaxation *Phys. Rev. B* **107** 024205
[251] Höland W and Beall G H 2012 *Glass-ceramic Technology* (Wiley Online Library)
[252] Fu L, Engqvist H and Xia W 2020 Glass–ceramics in dentistry: a review *Materials* **13** 1049

[253] Minami T, Hayashi A and Tatsumisago M 2006 Recent progress of glass and glass-ceramics as solid electrolytes for lithium secondary batteries. *Solid State Ion.* **177** 2715−20

[254] Su H *et al* 2024 Deciphering the critical role of interstitial volume in glassy sulfide superionic conductors *Nat. Commun.* **15** 2552

[255] Krauskopf T, Richter F H, Zeier W G and Janek J 2020 Physicochemical concepts of the lithium metal anode in solid-state batteries *Chem. Rev.* **120** 7745–94

[256] Kwak H, Wang S, Park J, Liu Y, Kim K T, Choi Y, Mo Y and Jung Y S 2022 Emerging halide superionic conductors for all-solid-state batteries: design, synthesis, and practical applications *ACS Energy Lett.* **7** 1776–805

[257] Kwak H *et al* 2021 New cost-effective halide solid electrolytes for all-solid-state batteries: mechanochemically prepared $Fe^{3+}$-substituted $Li_2ZrCl_6$ *Adv. Energy Mater.* **11** 2003190

[258] Yang J, Lin J, Brezesinski T and Strauss F 2024 Emerging superionic sulfide and halide glass–ceramic solid electrolytes: recent progress and future perspectives *ACS Energy Lett.* **9** 5977–90

[259] Patel S V *et al* 2023 Charge-clustering induced fast ion conduction in 2LiX-$GaF_3$: a strategy for electrolyte design *Sci. Adv.* **9** eadj9930

[260] Dai T *et al* 2023 Inorganic glass electrolytes with polymer-like viscoelasticity *Nat. Energy* **8** 1221–8

[261] Kim W *et al* 2025 Oxygen-tuned aluminum-based halide solid electrolytes enabling low-voltage anode compatibility in all-solid-state batteries *Energy Environ. Sci.* **18** 2039–51

[262] Chaupatnaik A, Rousse G, Perez A J, Morozov A V, Elkaïm E, Avdeev M, Abakumov A M and Tarascon J-M 2024 Synthesis, structure, and electrochemistry of crystallized layered chlorides, $LiMCl_6$ (M= Ta/Nb) *Adv. Energy Mater.* **14** 2402555

[263] Kwak H *et al* 2023 Boosting the interfacial superionic conduction of halide solid electrolytes for all-solid-state batteries *Nat. Commun.* **14** 2459

[264] Wang G *et al* 2025 Oxychloride polyanion clustered solid-state electrolytes via hydrate-assisted synthesis for all-solid-state batteries *Adv. Mater.* **37** 2410402

[265] You I, Singh B, Cui M, Goward G, Qian L, Arthur Z, King G and Nazar L F 2025 A facile route to plastic inorganic electrolytes for all-solid state batteries based on molecular design *Energy Environ. Sci.* **18** 478–91

[266] Duan H *et al* 2024 Amorphous AlOCl compounds enabling nanocrystalline LiCl with abnormally high ionic conductivity *J. Am. Chem. Soc.* **146** 29335–43

[267] Yuan L *et al* 2025 Enhancing ion transport at primary interparticle boundaries of polycrystalline lithium-rich oxide in all-solid-state batteries *Angew. Chem., Int. Ed.* **64** e202508605

[268] Schlautmann E *et al* 2023 Impact of the solid electrolyte particle size distribution in sulfide-based solid-state battery composites *Adv. Energy Mater.* **13** 2302309

[269] Woo J *et al* 2023 Liquid-phase synthesis of highly deformable and air-stable Sn-substituted $Li_3PS_4$ for all-solid-state batteries fabricated and operated under low pressures *Adv. Energy Mater.* **13** 2203292

[270] Ohsaki S, Yano T, Hatada A, Nakamura H and Watano S 2021 Size control of sulfide-based solid electrolyte particles through liquid-phase synthesis *Powder Technol.* **387** 415–20

[271] Kim Y-S, Jeon S H, Cho W, Kim K, Yu J, Yi J, Jeong G and Park K-H 2022 Surficial sulfur loss of jet-milled $Li_6PS_5Cl$ powder under mild-temperature heat treatment *ACS Appl. Energy Mater.* **5** 15442–51

[272] Shannon R and Prewitt C 1970 Revised values of effective ionic radii *Struct. Sci.* **26** 1046–8

[273] Lei P, Wu G, Liu H, Qi X, Wu M, Li D, Li Y, Gao L, Nan C-W and Fan L-Z 2025 Boosting ion conduction and moisture stability through $Zn^{2+}$ substitution of chloride electrolytes for all-solid-state lithium batteries *Adv. Energy Mater.* **15** 2405760

[274] Kim K T, Woo J, Kim Y-S, Sung S, Park C, Lee C, Park Y J, Lee H-W, Park K and Jung Y S 2023 Ultrathin superhydrophobic coatings for air-stable inorganic solid electrolytes: toward dry room application for all-solid-state batteries *Adv. Energy Mater.* **13** 2301600

[275] Samanta S, Bera S, Biswas R K, Mondal S, Mandal L and Banerjee A 2024 Ionocovalency of the central metal halide bond-dependent chemical compatibility of halide solid electrolytes with $Li_6PS_5Cl$ *ACS Energy Lett.* **9** 3683–93

[276] Xia W, Zhao Y, Zhao F, Adair K, Zhao R, Li S, Zou R, Zhao Y and Sun X 2022 Antiperovskite electrolytes for solid-state batteries *Chem. Rev.* **122** 3763–819

[277] Li W, Li M, Ren H, Kim J T, Li R and Sham T-K 2025 Nitride solid-state electrolytes for all-solid-state lithium metal batteries *Energy Environ. Sci.* **18** 4521–54

[278] Shen L, Wang Z, Xu S, Law H M, Zhou Y and Ciucci F 2025 Harnessing database-supported high-throughput screening for the design of stable interlayers in halide-based all-solid-state batteries *Nat. Commun.* **16** 3687

[279] Xiao Y, Wang Y, Bo S H, Kim J C, Miara L J and Ceder G 2020 Understanding interface stability in solid-state batteries *Nat. Rev. Mater.* **5** 105–26

[280] Wang Y, Ye L, Fitzhugh W, Chen X and Li X 2023 Interface coating design for dynamic voltage stability of solid-state batteries *Adv. Energy Mater.* **13** 2302288

[281] Hwang T, Bae J H, Lee S R, Park H, Park J W, Ha Y C, Lee Y-J and Cho K 2024 Oxygen substitution to enhance chemo-mechanical stability at the cathode-sulfide electrolyte interface in all-solid-state batteries *ACS Nano* **18** 23320–30

[282] Zhang S *et al* 2021 Advanced high-voltage all-solid-state Li–ion batteries enabled by a dual-halogen solid electrolyte *Adv. Energy Mater.* **11** 2100836

[283] Strauss F, Stepien D, Maibach J, Pfaffmann L, Indris S, Hartmann P and Brezesinski T 2020 Influence of electronically conductive additives on the cycling performance of argyrodite-based all-solid-state batteries *RSC Adv.* **10** 1114–9

[284] Tan D H S, Wu E A, Nguyen H, Chen Z, Marple M A T, Doux J M, Wang X, Yang H, Banerjee A and Meng Y S 2019 Elucidating reversible electrochemical redox of $Li_6PS_5Cl$ solid electrolyte *ACS Energy Lett.* **4** 2418–27

[285] Suzuki K, Mashimo N, Ikeda Y, Yokoi T, Hirayama M and Kanno R 2018 High cycle capability of all-solid-state lithium–sulfur batteries using composite electrodes by liquid-phase and mechanical mixing *ACS Appl. Energy Mater.* **1** 2373–7

[286] Wang S, Zhang Y, Zhang X, Liu T, Lin Y-H, Shen Y, Li L and Nan C-W 2018 High-conductivity argyrodite $Li_6PS_5Cl$ solid electrolytes prepared via optimized sintering processes for all-solid-state lithium–sulfur batteries *ACS Appl. Mater. Interfaces* **10** 42279–85

[287] Song H *et al* 2025 All-solid-state Li–S batteries with fast solid–solid sulfur reaction *Nature* **637** 846–53

[288] Nikodimos Y, Su W-N and Hwang B J 2023 Halide solid-state electrolytes: stability and application for high voltage all-solid-state Li atteries *Adv. Energy Mater.* **13** 2202854

[289] Song Z, Dai Y, Wang T, Yu Q, Ye X, Wang L, Zhang Y, Wang S and Luo W 2024 An active halide catholyte boosts the extra capacity for all-solid-state batteries *Adv. Mater.* **36** 2405277

[290] Fu J *et al* 2025 A cost-effective all-in-one halide material for all-solid-state batteries *Nature* **643** 111–8

[291] Zhang G, Liu Z, Ma Y, Pepas J, Bai J, Zhong H, Tang Y and Chen H 2024 $Li_{2.9}Fe_{0.9}Zr_{0.1}Cl_6$ as redox-active catholyte for solid-state Li–ion batteries *Chem. Mater.* **36** 10104–12

[292] Wang K, Gu Z, Xi Z, Hu L and Ma C 2023 $Li_3TiCl_6$ as ionic conductive and compressible positive electrode active material for all-solid-state lithium-based batteries *Nat. Commun.* **14** 1396

[293] Ruoff E, Kmiec S and Manthiram A 2025 Redox-active halide catholytes for enhanced energy density in solid-state sodium batteries *ACS Appl. Mater. Interfaces* **17** 18420–9

[294] Schwietert T K *et al* 2020 Clarifying the relationship between redox activity and electrochemical stability in solid electrolytes *Nat. Mater.* **19** 428–35

[295] Zhang X, Wang S, Xue C, Xin C, Lin Y, Shen Y, Li L and Nan C-W 2019 Self-suppression of lithium dendrite in all-solid-state lithium metal batteries with poly(vinylidene difluoride)-based solid electrolytes *Adv. Mater.* **31** 1806082

[296] Piana G, Bella F, Geobaldo F, Meligrana G and Gerbaldi C 2019 PEO/LAGP hybrid solid polymer electrolytes for ambient temperature lithium batteries by solvent-free, "one pot" preparation *J. Energy Storage* **26** 100947

[297] Ren Y, Deng H, Chen R, Shen Y, Lin Y and Nan C-W 2015 Effects of Li source on microstructure and ionic conductivity of Al-contained $Li_{6.75}La_3Zr_{1.75}Ta_{0.25}O_{12}$ ceramics *J. Eur. Ceram. Soc.* **35** 561–72

[298] Zhou R, Gautam A, Suard E, Li S, Ganapathy S, Chen K, Zhang X, Nan C-W, Wang S and Wagemaker M 2025 Boosting ionic conductivity and air stability in bromide-rich thioarsenate argyrodite solid electrolytes *Adv. Funct. Mater.* **35** 2420971

[299] Zhang Z and Kennedy J H 1990 Synthesis and characterization of the $B_2S_3$-$Li_2S$, the $P_2S_5$-$Li_2S$ and the $B_2S_3$-$P_2S_5$-$Li_2S$ glass systems *Solid State Ion.* **38** 217–24

[300] Yu C, van Eijck L, Ganapathy S and Wagemaker M 2016 Synthesis, structure and electrochemical performance of the argyrodite $Li_6PS_5Cl$ solid electrolyte for Li–ion solid state batteries *Electrochim. Acta* **215** 93–9

[301] Mizuno F, Hayashi A, Tadanaga K and Tatsumisago M 2005 New, highly ion-conductive crystals precipitated from $Li_2S$–$P_2S_5$ glasses *Adv. Mater.* **17** 918–21

[302] Wang S, Gautam A, Wu X, Li S, Zhang X, He H, Lin Y, Shen Y and Nan C-W 2024 Effect of processing on structure and ionic conductivity of chlorine-rich lithium argyrodites *Adv. Energy Sustain. Res.* **5** 2200197

[303] Zhou L, Zuo T-T, Kwok C Y, Kim S Y, Assoud A, Zhang Q, Janek J and Nazar L F 2022 High areal capacity, long cycle life 4 V ceramic all-solid-state Li–ion batteries enabled by chloride solid electrolytes *Nat. Energy* **7** 83–93

[304] Miura A, Rosero-Navarro N C, Sakuda A, Tadanaga K, Phuc N H H, Matsuda A, Machida N, Hayashi A and Tatsumisago M 2019 Liquid-phase syntheses of sulfide electrolytes for all-solid-state lithium battery *Nat. Rev. Chem.* **3** 189–98

[305] Li G, Wang S, Fu J, Liu Y and Chen Z 2023 Manufacturing high-energy-density sulfidic solid-state batteries *Batteries* **9** 347

[306] Wang C *et al* 2021 A universal wet-chemistry synthesis of solid-state halide electrolytes for all-solid-state lithium-metal batteries *Sci. Adv.* **7** eabh1896

[307] Liu Y, Xu B, Zhang W, Li L, Lin Y and Nan C 2020 Composition modulation and structure design of inorganic-in-polymer composite solid electrolytes for advanced lithium batteries *Small* **16** 1902813

[308] Li S, Yang Z, Wang S-B, Ye M, He H, Zhang X, Nan C-W and Wang S 2024 Sulfide-based composite solid electrolyte films for all-solid-state batteries *Commun. Mater.* **5** 44

[309] Zhang Z, Wu L, Zhou D, Weng W and Yao X 2021 Flexible sulfide electrolyte thin membrane with ultrahigh ionic conductivity for all-solid-state lithium batteries *Nano Lett.* **21** 5233–9

[310] Wang C, Yu R, Duan H, Lu Q, Li Q and Adair K R 2022 Solvent-free approach for interweaving freestanding and ultrathin inorganic solid electrolyte membranes *ACS Energy Lett.* **7** 410–6

[311] Fleischauer M D, Hatchard T D, Rockwell G P, Topple J M, Trussler S, Jericho S K, Jericho M H and Dahn J R 2003 Design and testing of a 64-channel combinatorial electrochemical cell *J. Electrochem. Soc.* **150** A1465–9

[312] Al-Maghrabi M A, van der Bosch N, Sanderson R J, Stevens D A, Dunlap R A and Dahn J R 2011 A new design for a combinatorial electrochemical cell plate and the inherent irreversible capacity of lithiated silicon *Electrochem. Solid-State Lett.* **14** A42–4

[313] Beal M S *et al* 2011 High throughput methodology for synthesis, screening, and optimization of solid state lithium ion electrolytes *ACS Comb. Sci.* **13** 375–81

[314] Yada C, Lee C E, Laughman D, Hannah L, Iba H and Hayden B E 2015 A high-throughput approach developing lithium-niobium-tantalum oxides as electrolyte/cathode interlayers for high-voltage all-solid-state lithium batteries *J. Electrochem. Soc.* **162** A722–6

[315] Szymanski N J *et al* 2023 An autonomous laboratory for the accelerated synthesis of novel materials *Nature* **624** 86–91

[316] Jonderian A, Anderson E, Peng R, Xu P, Jia S, Cozea V and McCalla E 2022 Suite of high-throughput experiments for screening solid electrolytes for Li batteries *J. Electrochem. Soc.* **169** 050504

[317] Jonderian A, Rehman S, Card Gormley M, Jia S, Ma S B, Kwon G and McCalla E 2024 Pioneering combinatorial investigation to unlock the potential of lithium borosilicate glasses as solid electrolytes *ACS Appl. Energy Mater.* **7** 11278–87

[318] Anderson E, Zolfaghar E, Jonderian A, Khaliullin R and McCalla E 2024 Comprehensive dopant screening in $Li_7La_3Zr_2O_{12}$ garnet solid electrolyte *Adv. Energy Mater.* **14** 230425

[319] Johari N S M, Jonderian A, Jia S, Cozea V, Yao E, Adnan S B R S, Ahmad N and McCalla E 2022 High-throughput development of $Na_2ZnSiO_4$-based hybrid electrolytes for sodium-ion batteries *J. Power Sources* **541** 231706

[320] McCalla E 2023 Semiautomated experiments to accelerate the design of advanced battery materials: combining speed, low cost, and adaptability *ACS Eng. Au.* **3** 391–402

[321] Manna S, Paul P, Manna S S, Das S and Pathak B 2025 Utilizing machine learning to advance battery materials design: challenges and prospects *Chem. Mater.* **37** 1759–87

[322] McCalla E 2024 Braving the elements: learning from 60+ dopants in battery materials *J. Phys. Chem. C* **128** 16831–43

[323] Shukla S, Anand G and Agarwal S 2025 Advancements in solid-state batteries for electric vehicles: a comprehensive review *Int. J. Smart Sustain. Intell. Comput.* **2** 1–14

[324] Zeinali Galabi N, Liu C, Jain M, Kamel M, Jia S and Bengio J 2025 Navigating ternary doping in Li–ion cathodes with closed-loop multi-objective Bayesian optimization *Adv. Mater.* e19790

[325] Vahdatkhah P, Zolfaghar Y and McCalla E 2025 Adapting high-throughput synthesis for aggressively air-sensitive halide solid electrolytes *247th ECS conf.* (available at:

https://ecs.confex.com/ecs/247/meetingapp.cgi/Paper/200609) pp A03–0197
[326] Zolfaghar E, Vahdatkhah P and McCalla E 2025 Development of high-throughput solid-state synthesis and screening of halide solid electrolytes *247th ECS conf.* (available at: https://ecs.confex.com/ecs/247/meetingapp.cgi/Paper/202568) pp A03–0404
[327] Projects for graduate students in CEDER group (available at: https://ceder.berkeley.edu/wp-content/uploads/2024/02/Projects-for-Graduate-Students-in-CEDER-group-UC-Berkeley.pdf) (Accessed 22 July 2025)
[328] Gendron D M, Torabi A, Wanees M, Dsouza M S, Feddersen B and Holme T 2025 Method—a high-throughput technique for unidirectional critical current density testing of solid electrolyte materials *J. Electrochem. Soc.* **172** 020511
[329] Atkins D *et al* 2022 Accelerating battery characterization using neutron and synchrotron techniques: toward a multi-modal and multi-scale standardized experimental workflow *Adv. Energy Mater.* **12** 2102694
[330] Strauss F, Kitsche D, Ma Y, Teo J H, Goonetilleke D, Janek J, Bianchini M and Brezesinski T 2021 Operando characterization techniques for all-solid-state lithium–ion batteries *Adv. Energy Sustain. Res.* **2** 2100004
[331] Huang Y, Perlmutter D, Fei-Huei Su A, Quenum J, Shevchenko P, Parkinson D Y, Zenyuk I V and Ushizima D 2023 Detecting lithium plating dynamics in a solid-state battery with operando x-ray computed tomography using machine learning *npj Comput. Mater.* **9** 93
[332] Ning Z *et al* 2021 Visualizing plating-induced cracking in lithium-anode solid-electrolyte cells *Nat. Mater.* **20** 1121–9
[333] Ji T *et al* 2025 Operando neutron imaging-guided gradient design of Li–ion solid conductor for high-mass-loading cathodes *Nat. Commun.* **16** 7667
[334] Bradbury R, Kardjilov N, Dewald G F, Tengattini A, Helfen L, Zeier W G and Manke I 2023 Visualizing lithium ion transport in solid-state Li–S batteries using $^{6}$Li contrast enhanced neutron imaging *Adv. Funct. Mater.* **33** 2302619
[335] Perrenot P, Bayle-Guillemaud P, Jouneau P-H, Boulineau A and Villevieille C 2024 Operando focused ion beam–scanning electron microscope (FIB-SEM) revealing microstructural and morphological evolution in a solid-state battery *ACS Energy Lett.* **9** 3835–40
[336] Yadav N G, Folastre N, Bolmont M, Jamali A, Morcrette M and Davoisne C 2022 Study of failure modes in two sulphide-based solid electrolyte all-solid-state batteries via *in situ* SEM *J. Mater. Chem. A* **10** 17142–55
[337] Zhao L *et al* 2025 Imaging the evolution of lithium-solid electrolyte interface using operando scanning electron microscopy *Nat. Commun.* **16** 4283
[338] Basak S *et al* 2020 Operando transmission electron microscopy study of all-solid-state battery interface: redistribution of lithium among interconnected particles *ACS Appl. Energy Mater.* **3** 5101–6
[339] Brant W R, Li D, Gu Q and Schmid S 2016 Comparative analysis of ex-situ and operando x-ray diffraction experiments for lithium insertion materials *J. Power Sources* **302** 126–34
[340] Korjus O, Anil Kumar S, Gendrin L, Vial S, Villevieille C and Suard E 2025 Enabling operando neutron diffraction for solid-state battery studies *ACS Mater. Lett.* **7** 2725–31
[341] Choudhary K, Santos M I O, Nadeina A, Becker D, Lombard T, Seznec V and Chotard J-N 2023 Operando x-ray diffraction in transmission geometry « at home » from tape casted electrodes to all-solid-state battery *J. Power Sources* **553** 232270
[342] Boulet-Roblin L, Borel P, Sheptyakov D, Tessier C, Novák P and Villevieille C 2016 Operando neutron powder diffraction using cylindrical cell design: the case of $LiNi_{0.5}Mn_{1.5}O_4$ vs graphite *J. Phys. Chem. C* **120** 17268–73
[343] Bianchini M, Leriche J B, Laborier J-L, Gendrin L, Suard E, Croguennec L and Masquelier C 2013 A new null matrix electrochemical cell for rietveld refinements of *in-situ* or operando neutron powder diffraction data *J. Electrochem. Soc.* **160** A2176–83
[344] Roberts M, Biendicho J J, Hull S, Beran P, Gustafsson T, Svensson G and Edström K 2013 Design of a new lithium ion battery test cell for *in-situ* neutron diffraction measurements *J. Power Sources* **226** 249–55
[345] Stavola A M, Sun X, Guida D P, Bruck A M, Cao D, Okasinski J S, Chuang A C, Zhu H and Gallaway J W 2023 Lithiation gradients and tortuosity factors in thick NMC111-Argyrodite solid-state cathodes *ACS Energy Lett.* **8** 1273–80
[346] Sottmann J, Di Michiel M, Fjellvåg H, Malavasi L, Margadonna S, Vajeeston P, Vaughan G B M and Wragg D S 2017 Chemical structures of specific sodium ion battery components determined by operando pair distribution function and x-ray diffraction computed tomography *Angew. Chem., Int. Ed.* **56** 11385–9
[347] Li Z *et al* 2020 Synchrotron operando depth profiling studies of state-of-charge gradients in thick $Li(Ni_{0.8}Mn_{0.1}Co_{0.1})O_2$ cathode films *Chem. Mater.* **32** 6358–64
[348] Hu J, Young R S, Lukic B, Broche L, Jervis R, Shearing P R, Di Michiel M, Withers P J, Rettie A and Paul P P 2025 Quantifying heterogeneous degradation pathways and deformation fields in solid-state batteries *Adv. Energy Mater.* **15** 2404231
[349] Finegan D P *et al* 2020 Spatial quantification of dynamic inter and intra particle crystallographic heterogeneities within lithium ion electrodes *Nat. Commun.* **11** 631
[350] Ulvestad A, Singer A, Clark J N, Cho H M, Kim J W, Harder R, Maser J, Meng Y S and Shpyrko O G 2015 Topological defect dynamics in operando battery nanoparticles *Science* **348** 1344–7
[351] Jacquet Q, Cele J, Casiez L, Tardif S, Medjahed A, Pouget S, Burghammer M, Lyonnard S and Oukassi S 2025 Operando microimaging of crystal structure and orientation in all components of all-solid-state-batteries *Nat. Commun.* **16** 11524
[352] Villevieille C, Thompson O and Vaughan G 2024 Revealing the spatial distribution of decomposition products upon ageing on $Li_6PS_5Cl$ solid electrolyte via x-ray diffraction computed tomography (Research Square) (https://doi.org/10.21203/rs.3.rs-5191594/v1)
[353] Villevieille C 2025 The challenge of studying interfaces in battery materials *Nat. Nanotechnol.* **20** 2–5
[354] Chen Y T *et al* 2024 Enabling uniform and accurate control of cycling pressure for all-solid-state batteries *Adv. Energy Mater.* **14** 2304327
[355] Lee C, Kim J Y, Bae K Y, Kim T, Jung S-J, Son S and Lee H-W 2024 Enhancing electrochemomechanics: how stack pressure regulation affects all-solid-state batteries *Energy Storage Mater.* **66** 103196
[356] Reif B, Ashbrook S E, Emsley L and Hong M 2021 Solid-state NMR spectroscopy *Nat. Rev. Meth. Primers* **1** 2
[357] Chandran C V and Heitjans P 2016 Solid-state NMR studies of lithium ion dynamics across materials classes *Ann. Rep. NMR Spectr.* **89** 1–102
[358] Harm S, Hatz A-K, Moudrakovski I, Eger R, Kuhn A, Hoch C and Lotsch B V 2019 Lesson learned from NMR: characterization and ionic conductivity of LGPS-like $Li_7SiPS_8$ *Chem. Mater.* **31** 1280–8
[359] Hogrefe K, Minafra N, Hanghofer I, Banik A, Zeier W G and Wilkening H M R 2022 Opening diffusion pathways

through site disorder: the interplay of local structure and ion dynamics in the solid electrolyte $Li_{6+x}P_{1-x}Ge_xS_5I$ as probed by neutron diffraction and NMR *J. Am. Chem. Soc.* **144** 1795–812
[360] Böhmer R, Jeffrey K R and Vogel M 2007 Solid-state Li NMR with applications to the translational dynamics in ion conductors *Prog. Nucl. Magn. Reson. Spectrosc.* **50** 87–174
[361] Hogrefe K, Minafra N, Zeier W G and Wilkening H M R 2021 Tracking ions the direct way: long-range $Li^+$ dynamics in the thio-LISICON family $Li_4MCh_4$ (M = Sn,Ge;Ch = S, Se) as probed by $^7$Li NMR relaxometry and $^7$Li spin-alignment echo NMR *J. Phys. Chem. C* **125** 2306–17
[362] Hogrefe K, Stainer F, Minafra N, Zeier W G and Wilkening H M R 2024 NMR down to cryogenic temperatures: accessing the rate-limiting step of Li transport in argyrodite electrolytes *Chem. Mater.* **36** 6527–34
[363] Wilkening M and Heitjans P 2006 Extremely slow cation exchange processes in $Li_4SiO_4$ probed directly by two-time $^7$Li stimulated-echo nuclear magnetic resonance spectroscopy *J. Phys.: Condens. Matter* **18** 9849–62
[364] Gamon J *et al* 2019 Computationally guided discovery of the sulfide $Li_3AlS_3$ in the Li–Al–S phase field: structure and lithium conductivity *Chem. Mater.* **31** 9699–714
[365] Marko A, Hogrefe K, Schweiger L, Stainer F, Königsreiter J, Spychala J, Schwaiger J, Heitjans P, Gadermaier B and Wilkening H M R 2025 Mapping the various $Li^+$ jump pathways in $Li_{10}GeP_2S_{12}$: from ultraslow exchange to high-temperature diffusion *J. Am. Chem. Soc.* **147** 38215–24
[366] Patel S V, Banerjee S, Liu H, Wang P, Chien P-H, Feng X, Liu J, Ong S P and Hu Y-Y 2021 Tunable lithium-ion transport in mixed-halide argyrodites $Li_{6-x}PS_{5-x}ClBr_x$: an unusual compositional space *Chem. Mater.* **33** 1435–43
[367] Hanghofer I, Brinek M, Eisbacher S, Bitschnau B, Volck M, Hennige V, Hanzu I, Rettenwander D and Wilkening H M R 2019 Substitutional disorder: structure and ion dynamics of the argyrodites $Li_6PS_5Cl$, $Li_6PS_5Br$ and $Li_6PS_5I$ *Phys. Chem. Chem. Phys.* **21** 8489–507
[368] Tapler D, Gadermaier B, Spychala J, Stainer F, Marko A, Königsreiter J, Hogrefe K, Heitjans P and Wilkening H M R 2025 Unraveling ultrafast Li–ion dynamics in the solid electrolyte $LiTi_2(PS_4)_3$ by NMR down to cryogenic temperatures *J. Am. Chem. Soc.* **147** 20023–32
[369] Banik A, Famprikis T, Ghidiu M, Ohno S, Kraft M A and Zeier W G 2021 On the underestimated influence of synthetic conditions in solid ionic conductors *Chem. Sci.* **12** 6238–63
[370] Stainer F, Gadermaier B and Wilkening H M R 2025 Local and long-range diffusion in $Li_3InCl_6$: impact of preparation method on ion dynamics *Chem. Mater.* **37** 2650–63
[371] Lunghammer S and Wilkening H M R 2025 $Na^+$ self-diffusion and ionic transport in sodium $\beta''$-alumina *Solid State Ion.* **422** 116809
[372] Bottke P, Freude D and Wilkening M 2013 Ultraslow Li exchange processes in diamagnetic $Li_2ZrO_3$ as monitored by EXSY NMR *J. Phys. Chem. C* **117** 8114–9
[373] Bottke P, Hogrefe K, Kohl J, Nakhal S, Wilkening A, Heitjans P, Lerch M and Wilkening H M R 2023 Energetically preferred $Li^+$ ion jump processes in crystalline solids: site-specific hopping in $\beta$-$Li_3VF_6$ as revealed by high-resolution $^6$Li 2D EXSY NMR *Mater. Res. Bull.* **162** 112193
[374] Gombotz M, Hogrefe K, Zettl R, Gadermaier B and Wilkening H M R 2021 Fuzzy logic: about the origins of fast ion dynamics in crystalline solids *Phil. Trans. A* **379** 20200434
[375] Jiang Y, Zhao M, Peng Z and Zhong G 2024 Progress in *in-situ* electrochemical nuclear magnetic resonance for battery research *Magn. Res. Lett.* **4** 200099
[376] Heitjans P 1986 Use of beta radiation-detected NMR to study ionic motion in solids *Solid State Ion.* **18–19** 50–64
[377] MacFarlane W A 2015 Implanted-ion $\beta$NMR: a new probe for nanoscience *Solid State Nucl. Magn. Reson.* **68–69** 1–12
[378] MacFarlane W A 2022 Status and progress of ion-implanted $\beta$NMR at TRIUMF *Z. Phys. Chem.* **236** 757–98
[379] Zhang X and Huo H 2021 Nuclear magnetic resonance studies of organic-inorganic composite solid electrolytes *Magn. Res. Lett.* **1** 142–52
[380] Zagórski J, López Del Amo J M, Cordill M J, Aguesse F, Buannic L and Llordés A 2019 Garnet-polymer composite electrolytes: new insights on local Li-ion dynamics and electrodeposition stability with Li metal anodes *ACS Appl. Energy Mater.* **2** 1734–46
[381] Heitjans P and Indris S 2003 Diffusion and ionic conduction in nanocrystalline ceramics *J. Phys.: Condens. Matter* **15** R1257–89
[382] Breuer S, Uitz M and Wilkening H M R 2018 Rapid Li ion dynamics in the interfacial regions of nanocrystalline solids *J. Phys. Chem. Lett.* **9** 2093–7
[383] Gombotz M, Pree K P, Pregartner V, Hanzu I, Gadermaier B, Hogrefe K and Wilkening H M R 2021 Insulator:conductor interfacial regions—Li ion dynamics in the nanocrystalline dispersed ionic conductor LiF:$TiO_2$ *Solid State Ion.* **369** 115726
[384] Breuer S, Pregartner V, Lunghammer S and Wilkening H M R 2019 Dispersed solid conductors: fast interfacial Li–ion dynamics in nanostructured LiF and LiF:g–$Al_2O_3$ composites *J. Phys. Chem. C* **123** 5222–30
[385] Marko A, Scheiber T, Gadermaier B and Wilkening H M R 2025 Interfacial lithiation of lithium aluminum titanium phosphate explored by $^7$Li NMR *Commun. Chem.* **8** 102
[386] Huang Y, Wu X, Nie L, Chen S, Sun Z, He Y and Liu W 2020 Mechanism of lithium electrodeposition in a magnetic field *Solid State Ion.* **345** 115171
[387] Hanghofer I, Gadermaier B and Wilkening H M R 2019 Fast rotational dynamics in argyrodite-type $Li_6PS_5X$ (X: cl, Br, I) as seen by $^{31}$P nuclear magnetic relaxation—on cation–anion coupled transport in thiophosphates *Chem. Mater.* **31** 4591–7
[388] Hogrefe K, Gadermaier B, Schneider C, Bette S, Lotsch B V and Wilkening H M R 2025 A dynamically induced phase transition in $Na_4P_2S_6$: ultrafast $Na^+$ mobility triggering rotor phase formation *J. Am. Chem. Soc.* **147** 28799–809
[389] Blanc F, Leskes M and Grey C P 2013 In situ solid-state NMR spectroscopy of electrochemical cells: batteries, supercapacitors, and fuel cells *Acc. Chem. Res.* **46** 1952–63
[390] Maity A, Svirinovsky-Arbeli A, Buganim Y, Oppenheim C and Leskes M 2024 Tracking dendrites and solid electrolyte interphase formation with dynamic nuclear polarization NMR spectroscopy *Nat. Commun.* **15** 9956
[391] Freytag A I, Pauric A D, Krachkovskiy S A and Goward G R 2019 In situ magic-angle spinning $^7$Li NMR analysis of a full electrochemical lithium-ion battery using a jelly roll cell design *J. Am. Chem. Soc.* **141** 13758–61
[392] Marbella L E, Zekoll S, Kasemchainan J, Emge S P, Bruce P G and Grey C P 2019 $^7$Li NMR chemical shift imaging to detect microstructural growth of lithium in all-solid-state batteries *Chem. Mater.* **31** 2762–9
[393] Liu H *et al* 2025 Dendrite formation in solid-state batteries arising from lithium plating and electrolyte reduction *Nat. Mater.* **24** 581–8

[394] Hope M A, Rinkel B L D, Gunnarsdóttir A B, Märker K, Menkin S, Paul S, Sergeyev I V and Grey C P 2020 Selective NMR observation of the SEI–metal interface by dynamic nuclear polarisation from lithium metal *Nat. Commun.* **11** 2224

[395] Fan E, Li L, Wang Z, Lin J, Huang Y, Yao Y, Chen R and Wu F 2020 Sustainable recycling technology for li–ion batteries and beyond: challenges and future prospects *Chem. Rev.* **120** 7020–63

[396] Rasoulnia P, Chen Q, Yang X and He C 2025 Recovery of valuable metals from end-of-life Li–ion batteries: technologies, progress, and perspectives *Resour. Conserv. Recycl.* **223** 108497

[397] Xu P, Tan D H S, Jiao B, Gao H, Yu X and Chen Z 2023 A materials perspective on direct recycling of lithium–ion batteries: principles, challenges and opportunities *Adv. Funct. Mater.* **33** 2213168

[398] Schirmer T, Qiu H, Goldmann D, Stallmeister C and Friedrich B 2022 Influence of P and Ti on phase formation at solidification of synthetic slag containing Li, Zr, La, and Ta *Minerals* **12** 310

[399] Schwich L, Küpers M, Finsterbusch M, Schreiber A, Fattakhova-Rohlfing D, Guillon O and Friedrich B 2020 Recycling strategies for ceramic all-solid-state batteries—part I: study on possible treatments in contrast to li–ion battery recycling *Metals* **10** 1523

[400] Waidha A I *et al* 2023 Recycling of all-solid-state li–ion batteries: a case study of the separation of individual components within a system composed of LTO, LLZTO, and NMC *ChemSusChem* **16** e202202361

[401] Bertau M and Martin G 2019 Integrated direct carbonation process for lithium recovery from primary and secondary resources *Mater. Sci. Forum* **959** 69–73

[402] Ihrig M *et al* 2023 Thermal recovery of the electrochemically degraded $LiCoO_2$/$Li_7La_3Zr_2O_{12}$:Al,Ta interface in an all-solid-state lithium battery *ACS Appl. Mater. Interfaces* **15** 4101–12

[403] Tan D H S, Xu P, Yang H, Kim M-C, Nguyen H, Wu E A, Doux J-M, Banerjee A, Meng Y S and Chen Z 2020 Sustainable design of fully recyclable all solid-state batteries *MRS Energy Sustain.* **7** E23

[404] Wissel K, Hu Z, Wu X, Jacob M, Küster K, Starke U and Clemens O 2025 Towards recycling of all-solid-state batteries with argyrodite sulfide electrolytes: insights into electrolyte and electrode degradation in dissolution-based separation processes *ChemSusChem* **18** e202402128

[405] Wissel K, Haben A, Küster K, Starke U, Kautenburger R, Ensinger W and Clemens O 2024 Direct recycling of $\beta$-$Li_3PS_4$-based all-solid-state li–ion batteries: interactions of electrode materials and electrolyte in a dissolution-based separation process *Adv. Energy Sustain. Res.* **5** 2300280

[406] Ghidiu M, Ruhl J, Culver S P and Zeier W G 2019 Solution-based synthesis of lithium thiophosphate superionic conductors for solid-state batteries: a chemistry perspective *J. Mater. Chem. A* **7** 17735–53

[407] Jacob M, Moreno Fernandez H, Haben A, Waidha A I, Özel S, Hofmann J P, Kautenburger R, Clemens O and Wissel K 2025 Direct recycling of all-solid-state batteries with a halide solid electrolyte via water-based separation: interactions of electrode materials in aqueous $Li_3InCl_6$ solutions *Batter. Supercaps* **8** e202500189

[408] Azhari L, Bong S, Ma X and Wang Y 2020 Recycling for all solid-state lithium–ion batteries *Matter* **3** 1845–61

[409] Jacob M, Wissel K and Clemens O 2024 Recycling of solid-state batteries—challenge and opportunity for a circular economy? *Mater. Futures* **3** 012101

[410] Pehlivan İ B, Marsal R, Niklasson G A, Granqvist C G and Georén P 2010 PEI–LiTFSI electrolytes for electrochromic devices: characterization by differential scanning calorimetry and viscosity measurements *Sol. Energy Mater. Sol. Cells* **94** 2399–404